63-4-2

408346

SUMMARY REPORT 2
~~Final Report~~

Contract AF 61 (052) - 506

Research on Electrically Small Antennas

Prof. Dr. H. H. Meinke

Institut für Hochfrequenztechnik
der Technischen Hochschule München

Contract AF 61(052)-506

~~Final Report~~
SUMMARY REPORT 2

Research on electrically small antennas

Prof.Dr.H.H.Meinke, Institut für Hochfrequenztechnik
Technische Hochschule München, Germany
30. April 1963

"The research reported in this document has been sponsored by the Aeromautical Systems Division, AFSC through the European Office, Aerospace Research, United States Air Force

Table of contents

Part 1: Electrically small antennas embedded in a dielectric or magnetic medium

Part I: Electrically small antennas embedded in a dielectric or magnetic medium.

Abstract

This research project is primarily concerned with the improvement of the impedance relationships of dipoles whose actual length is small as compared to the wave length in free space. This improvement should be obtained as a result of directly surrounding the dipole with dielectric or magnetic medium. The surrounding shape should not have too large a volume since the resulting increase of antenna size should be kept small. Fig. 1 shows the arrangement which we are studying.

Sect. I states exactly those characteristics of impedance behaviour which should be improved, especially efficiency and bandwidth of the dipole. The value of the radiation resistance itself is not very important.

Sect. II gives a summary of the physical effects introduced by a surrounding dielectric. Two different effects exists:

1. An altered impedance transformation since the wave impedance in the region of the radiator has been changed.
2. A stronger formation of space waves since the wave length in the dielectric is smaller than in air causing a larger ratio of radiator length to wavelength within the dielectric.

Sect. III, IV and V contain the fundamental theory.

In Sect. III the problem is presented in exact mathematical form A non-uniform, rectangular coordinate system is introduced which has already been untilized for Contract AF 61 (052)-41 for solving the problem of wide-band radiators.

Sect. IV shows the derivation of the wave equations for a radiator of very general shape in a dielectric medium of various size.

Sect. V treats equations for the impedance transformation caused by the dielectric.

Sect. VI shows how the theory is specially used for very short antennas. In this case only the transforming effect is working. The theory is checked by measuring the impedance of a radiator in air and in differently shaped dielectric mediums of Polystyrol.

It is shown, that this simplified theory of transformation can explain the measured influence of the dielectric to the input impedance for lower frequencies (short radiators). At higher frequencies additional resistive components of the input impedance are measured. These resistive components cannot be explained by dielectric losses alone and demonstrate additional radiation caused by the dielectric.

Sect. VII treats the bandwidth of several dielectric or magnetic shapes surrounding the antenna. Theoretical considerations lead to an improvement of the surrounding shape. The dielectric in the immediate vicinity of the feeding point causes an undesirable increase in the reactive power of the transmission line wave. Therefore an increase in the antenna bandwidth can not be obtained by inserting dielectric material in the immediate vicinity of the feeding point. The improvement can be obtained at some distance away from the feeding point. There is also shown in this section the usefulness of ferrites with very large μ_r.

In Sect. VIII the polystyrol body of improved shape according to Fig. 21 is discussed. The corresponding feeding point impedance and bandwidth is calculated and compared with measured values. An improvement in the bandwidth as compared to that of the antenna of Sect. VI was obtained. However the bandwidth of the antenna surrounded with the improved polystyrol shape is still smaller than the bandwidth of an antenna in air.

In Sect. IX ferrite bodies according to Fig. 21 of two different material types were used and investigated. The corresponding feeding point impedance and antenna bandwidth were calculated and compared with the measured values. The results show that compared to the radiator in air no improvement of the bandwidth of very small antennas (λ_0 larger than 1/20 antenna height) is obtained by surrounding the antenna with either a ferrite or polystyrol shell. If the height of the antenna is larger than $\lambda_0/20$ some improvement of the antenna bandwidth can be obtained by surrounding the antenna with a dielectric medium especially ferrite.

I. Exact Definition of the Problem

The impedance of a short radiator shall be improved by imbedding the radiator into a dielectric medium of finite size.

Very short antennas are only used when the antenna height is limited due to technical reasons, for example: in high-speed aircraft. Therefore the case of special interest is that the height of the total structure (including dielectric) may not exceed that of a radiator without dielectric since the total antenna height must be kept small.

Before we trat specific problems, we should first present an exact explanation to the question: "What should be accomplished by using a dielectric medium?" Even though the radiation resistance of a short antenna is small, this characteristic is not a disadvantage in itself since it is always possible to match a given antenna impedance to that of a transmitter or receiver by using an appropriate transformation arrangement. Therefore it will not be necessary to apply complicated dielectric forms for the only purpose to have a higher resistive part of the impedance. A simple inductance parallel to the input will transform the radiation resistance to very high values without any change in radiator arrangement.

Examples:

	Radiator impedance for 200 Mc/sec	1,38 - j 130	Ohm
1.	Inductove shunt	j 450	Ohm
	Resulting impedance	2,76 - j 184	Ohm
	Increase in resistive component		1:2
2.	Inductive shunt	j 192	Ohm
	Resulting impedance	13,8 - j 410	Ohm
	Increase in resistive component		1:10
3.	Inductive shunt	j 153	Ohm
	Resulting impedance	69 - j 920	Ohm
	Increase in resistive component		1:50

Especially very small radiation resistance can be transformed into very high resistive components.

Only the following two view points can be taken into consideration, if an improvement of the radiator is wanted.

1. Poor Efficiency

The resistance of small antennas consists of the sum of the radiation resistance R_s and an attenuation resistance R_v due to losses. An improvement of antenna behaviour by inserting into a dielectric medium can only be obtained if this results with an increase in the ratio.

$$\frac{R_s}{R_v}$$

It should be remembered that the increase of R_s alone does not necessarily bring an improvement since the insertion into a dielectric medium may also increase R_v. In this respect the ferrite materials available to-day, may be too inferior to give an improvement of R_s/R_v when used as a dielectric medium for a small antenna [1] . This certainly is an important item to take into consideration. However the present state-of-the-art in the ferrite industry certainly should not prevent us from making a theoretical study to determine the effect of a magnetic medium since the possibility exists that suitable dielectrics and ferrites having small losses

will be available in the future. The resulting theoretical analysis indicates that a lossless dielectric having magnetic properties can improve the radiation properties then there always is the possibility that the use of such a medium can be realized at some future date. Therefore the development of a theory for a lossless dielectric would certainly prove to be a worthwhile and beneficial task for possible future application.

However, other problems of efficiency exist even for lossless dielectric. The losses of a radiator without dielectric is due to the resistance of the conductor, silver being the best conductor. The losses of a silver plated conductor can not be surpassed. If dielectric and magnetic losses are neglected for the moment then for a radiator imbedded in dielectric the following question must be evaluated; is it possible that a radiator imbedded in a dielectric has a larger current flow, thus causing larger losses due to the resistance of the conductor, as compared to a radiator without dielectric even when a lossless dielectric is used? Therefore the ratio R_s/R_v should be evaluated to see if it changes after a radiator is inserted into dielectric when the dielectric is considered to be lossless and only the silver plated radiator is considered.

2. Antenna Bandwidth beeing too small

A bandwidth beeing too small limits the amount of communication flow, prevents the use of higher modulation frequencies and makes it impossible to transmit or receive short-time signals. The optimum circuit design can be influenced by the behaviour of the antenna impedance. This is especially true for very short dipoles and is a well known effect of long wave radio communication. Therefore The question arises: What will be the maximum bandwidth of the complete input circuit of such a short radiator when fed by a transmitter, or: What will be the maximum bandwidth of the complete input circuit of a receiver in com-

bination with a short radiator as receiving antenna. The best general answer will be, that for short radiators the maximum bandwidth of each transmitter or receiver arrangement is dependent upon the ratios

$$\frac{R_s}{X} \qquad \text{and} \qquad \frac{R_s}{\omega \frac{dX}{d\omega}}$$

where R_s is the radiation resistance, X is the antenna reactance and $\frac{dX}{d\omega}$ is the frequency dependency of the reactance which describes the antenna. [2]

An improvement of the maximum bandwidth is only obtained when these ratios are increased. Thus if it is possible to increase h_s and prevent a simultaneous increase of X and $dX/d\omega$ this improvement can be achieved. Therefore the question of whether an increase in R_s by a dielectric surrounding is worthwhile can first be answered when the behaviour of X and $dX/d\omega$ is known.

II. Physical Principles

The radiator according to Fig. 1 is located above a conducting surface. It is cylinder-symmetrical and imbedded in dielectric material in the vicinity of the feeding point ($\varepsilon_r > 1$). The dielectric material may also have magnetic properties ($\mu_r > 1$). The heigth of the radiator should be small as compared to the wavelength.

It is assumed that the antenna is fed by a coaxial line for the theoretical evaluation and for the impedance measurements. Thus a defined field relationship is established in the vicinity of the feeding point of the antenna. Since the input impedance is measured by using a slotted coaxial line, the measured values can be directly compared with those calculated. It will be assumed that the feeding line is also filled with dielectric, when the radiator is surrounded by a dielectric, and filled with air, when the radiator is surrounded by air. This simplifies the theory but is not

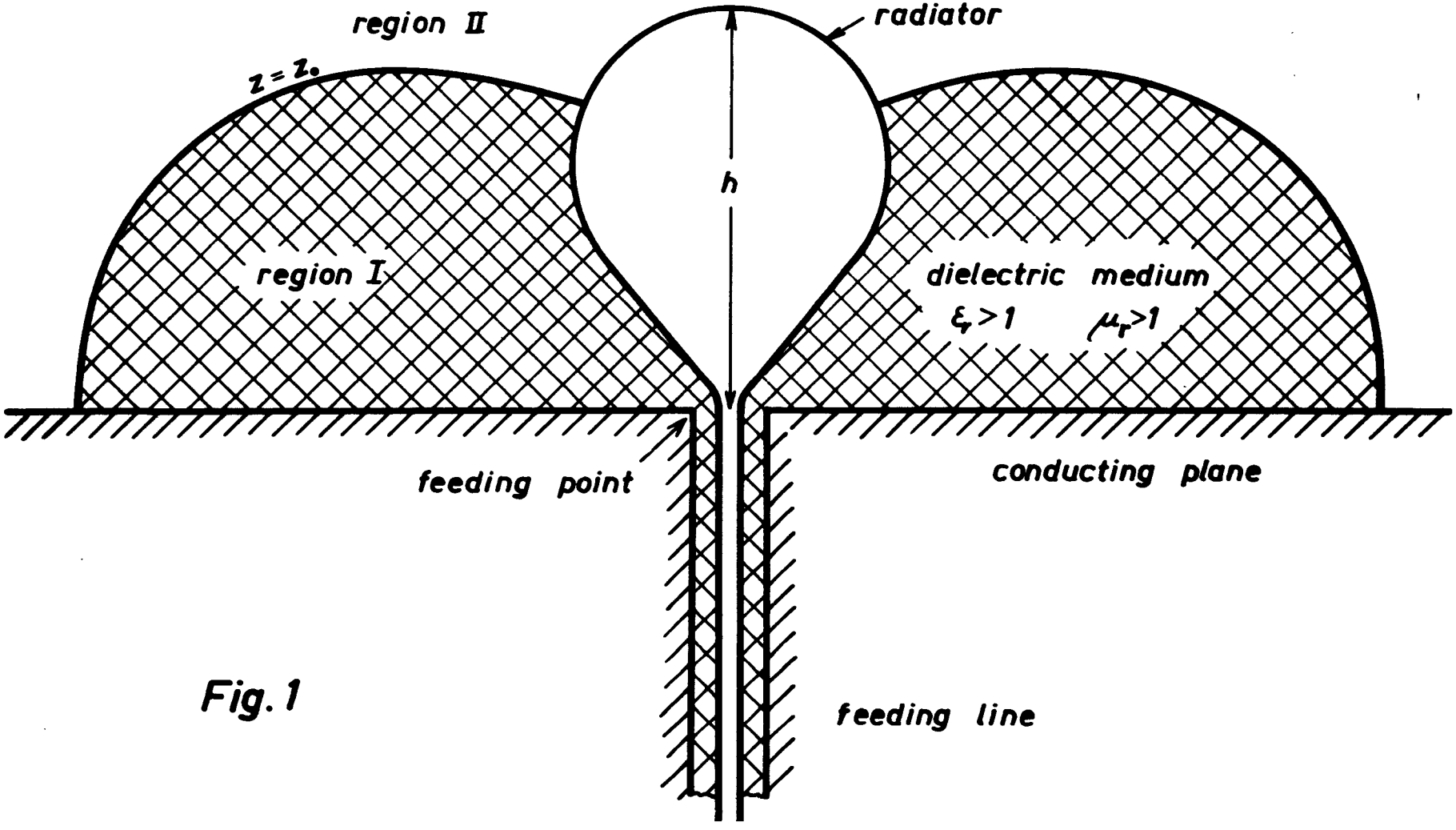
region II
radiator
z = z₀
h
region I
dielectric medium
ξ > 1
μ_r > 1
feeding point
conducting plane
feeding line

Fig. 1

essential for technical application.

The physical processes are clarified by the same reasoning which has already been established in the Technical Reports for Contract AF 61 (052)-41, [3].

A wave of the TEM type having electric field lines E, between the inner and outer conductor propagates through the coaxial feeding line. This wave continues with field lines existing between the radiator and the ground plane. The field lines of the TEM wave are identical to the field lines of a static electrical field between radiator and ground plane.

The TEM wave slowly converts over to the TM type in the inhomogeneous field outside of the coaxial feeding point as the distance from the feeding point increasases. Thus a continuous transition and building up of the TM space wave occurs. These TM space waves have electric fields leaving and returning to the ground plane. The field of these space waves is a sum of various TM modes. However in the case of very short radiators they are almost completly dominated by the TM, type as long as the radiation pattern is the one familiar to short antennas. The field lines of the TM_1 wave wedge themselves between the field lines of the TEM wave. The TEM field decreases rapidly with increasing distance from the radiator and at larger distances only the TM waves remain. For the TEM wave the space between the radiator and the ground plane acts like a coaxial line. The coaxial feeding line directly passes over to this coaxial radiator line.

Fig. 3a is a schematical representation of this occurrance for a radiator without dielectric. The wave impedance increases with increasing distance from the feeding point since the spacing between radiator and ground plane increases accordingly.

The coaxial radiator line has a finite length corresponding to the finite height of radiator. The antenna is open at the end and there the antenna current is zero. The

formation of the TM waves occurs in such a manner that the radiator line seems to be coupled inductively to another line causing a continuous energy transition of most of the TEM input wave to that of the TM wave with the remainder of TEM energy being reflected at the radiator end back into feeding line.

Fig. 3b shows the waves for a radiator with dielectric. Here essentially new is the fact that all wave impedances in the dielectric have decreased by the factor $\sqrt{\mu_r/\varepsilon_r}$ and an abrupt wave impedance change occurs at the transition to air. This wave impedance jump exists for TEM waves as well as for TM waves and causes an additional reflection at the boundary of the dielectric. This causes additional reflected waves in the feeding cable, which would have a different magnitude if no dielectric were used. If these events are described by using the conception of impedance then it can be said that the first effect of the dielectric is an altered impedance transformation. This is theoretically evaluated in detail in Part VI.

However the dielectric has a second effect. Referring to the theory developed earlier for Contract AF 61 (052)-41 an expansion of this theory is contained in Part III. The steady transition of the TEM mode to a TM wave is in every point of the field essentially dependent upon the length of field lines in this point as compared to the wavelength λ_o.

The following rule exists for the case of air:
In the region where the field lines are shorter than $\lambda_o/2$ the conversion of TEM to TM waves is quite small; this region behaves like a waveguide below the critical frequency with an evanescent TM mode; the TM modes which were coupled out of the TEM mode can not propagate as waves, rather the TM fields decrease exponentially from the point of origin. The longer the field lines are, the slower is the rate of exponential decrease, thus causing a stronger TM mode. The transition from TEM to TM is very strong where the field lines are longer than $\lambda_o/2$; This region behaves like a waveguide operating above its critical frequency and the TM field being coupled in propagates in this space as a wave. Those field lines of Fig. 4a which have the

length $\lambda_0/2$, separate the region of the evanescent TM modes from that region in which TM waves can exist.

Instead of λ_0 in free space, the wave length is $\lambda_\varepsilon = \lambda_0/\sqrt{\mu_r \varepsilon_r}$ in the dielectric. Thus the TM fields do not propagate as waves as long as the length of the field lines is smaller then $\lambda_\varepsilon/2$. Therefore the conversion rate improves continuously as the field line length approaches the value $\lambda_\varepsilon/2$ and becomes extremely strong as soon as the field line length exeeds $\lambda_\varepsilon/2$. The boundary field line in the dielectric has the length $\lambda_\varepsilon/2$ as shown in Fig. 4b.

The formation of the evanescent modes has a certain effect upon the formation of space waves since these fields partially protrude through the boundary field line and thus project into the adjacent space in which space waves are possible. Large amplitudes of the protruding evanescent modes prepare to some degree the formation of space waves in the adjacent wave region.

For radiators of small height in air, the field lines in the immediate vicinity of the radiator are smaller than $\lambda_0/2$; Thus the formation of space waves in the region is rather minute. If the field lines of length $\lambda_0/2$ for a given frequency are drawn in Fig. 4a, it is readily realized that these lie far away from the feeding point of short radiators. Only evanescent TM modes exist in the region between the feeding point and the boundary field line. On the other side of the boundary field line space waves are formed. The small radiation capability of a short antenna is explained by the lack of space wave formation in the immediate vicinity of the radiator. The higher the frequency, the closer the boundary field line shifts toward the feeding point, thus the wave region becomes correspondingly larger and the radiation improves accordingly.

Fig. 4b shows a radiator having an infinite dielectric medium for the same frequency as was used for Fig. 4a. The dielectric causes a wavelength λ_ε at the location where λ_0 was previously. The boundary field line of length $\lambda_\varepsilon/2$ for the same frequency shifts closer to the feeding point and the radiation of space waves improves. Since $\lambda_\varepsilon = \lambda_0/\sqrt{\mu_r \varepsilon_r}$ the radiation improves due to ε_r as well as to μ_r.

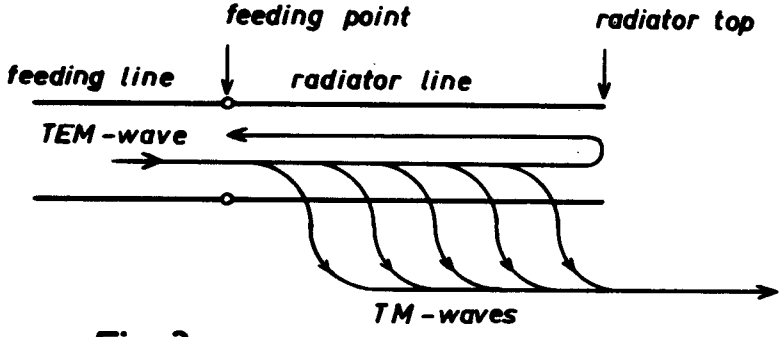

Fig. 3a

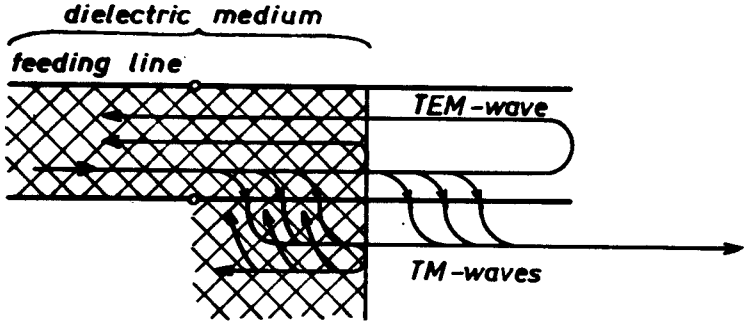

Fig. 3b

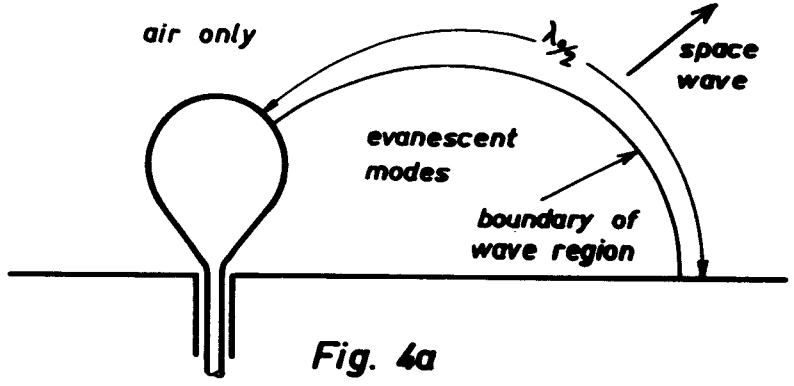

Fig. 4a

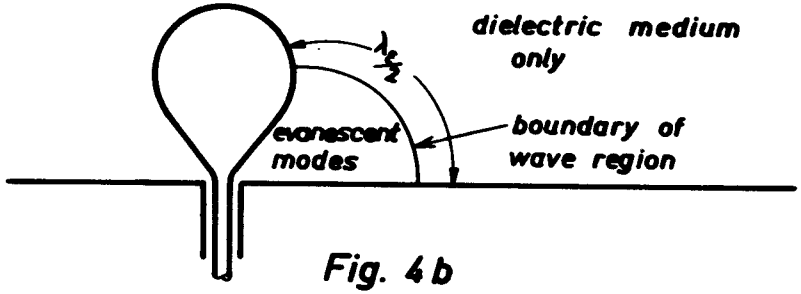

Fig. 4b

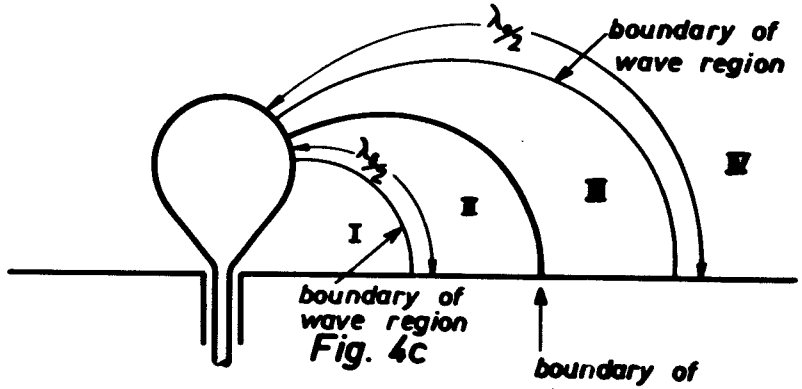

Fig. 4c

If the dielectric medium has a finite size as shown in Fig. 1, Then three cases exist:

a) The boundary of the dielectric lies outside of the boundary drawn in Fig. 4a of length $\lambda_0/2$. Then the wave transformation already begins within the dielectric and the waves coming out of the dielectric into air are immediately in that region which supports space propagation. This is a case in which the dielectric will cause a desirable effect since the wave region is enlarged by the dielectric and the boundary of the wave supporting region is shifted back to the field line of length $\lambda_\varepsilon/2$. However this case does not apply to very short radiators, which are of special interest here; rather this effect becomes usable for antennas whose height approximates $\lambda_0/4$.

b) The boundary of the dielectric medium as shown in Fig. 4c lies between the field lines $\lambda_0/2$ and $\lambda_\varepsilon/2$. The the wave of the feeding line moves first into Region I where the evanescent modes are formed and only a small degree of wave transformation occurs. Thereafter the TEM wave moves into Region II in which the TM wave can exist and a high degree of wave transformation occurs here. However the resulting TM waves are strongly reflected at the dielectric boundary since the TM fields can only exist as evanescent modes on the outer side of the boundary in Region III. The wave impedance of the TM mode in Region III is imaginary and thus the reflection factor of the dielectric boundary surface is considerably higher for the TM mode as compared to the TEM mode. In Region II the dielectric acts like an attenuated waveguide resonator for the TM wave.

The smaller the extension of Region III in the direction of wave propagation, the more the already formed TM fields of Region II can get through Region III to Region IV and support the formation of TM waves in IV. Therefore it is possible that the use of this dielectric can improve the excitation of space waves in IV! This would be an interesting case as far as our problem is concerned, since the radiator is already short and the dielectric could bring an improvement of the real components.

c) The boundary of the dielectric lies within the boundary line $\lambda_\varepsilon/2$ of Fig.4b. Then only evanescent modes exist within the dielectric medium and this is also true for the immediate surrounding region of air. The boundary line $\lambda_o/2$ of Fig. 4a is then far distant from the dielectric boundary surface. Therefore the dielectric can hardly bring a radiation improvement and actually only performs the already mentioned transformation of the TEM wave. This is the case of very short radiators.

III. The Curvilinear Coordinate System

In order to evaluate a radiator of general shape a curvilinear, right angle, coordinate system whose coordinates are the field lines of a static electric field between radiator and ground plane is introduced. This coordinate system is the same as the one which was used in Contract AF 61 (052)-41 for solving the broadband antenna problems.

Since a comparison of radiator performance with and without dielectric is to be made, the coordinate lines are drawn for a field without dielectric. In addition the boundary between air and dielectric should be a field line of this static field since then the static field lines with and without dielectric are the same and all the evaluations have a very simplified form. By this procedure all the information concerning the effect of other dielectric shapes is naturally lost. However as long as the dimensions of the radiator and the dielectric medium are small compared to a wavelength, it is not to be expected that other dielectric shapes will give considerably different results.

Fig. 5 shows the static field lines and equipotential lines between radiator and ground plane. They are drawn in accordance with the familiar rule that everywhere between adjacent equipotential lines the same voltage difference exists and the region between adjacent field lines without dielectric has the same capacitance throughout the regions. The drawn section of Fig.5 contains the coordinates x and z. The field lines are the curves

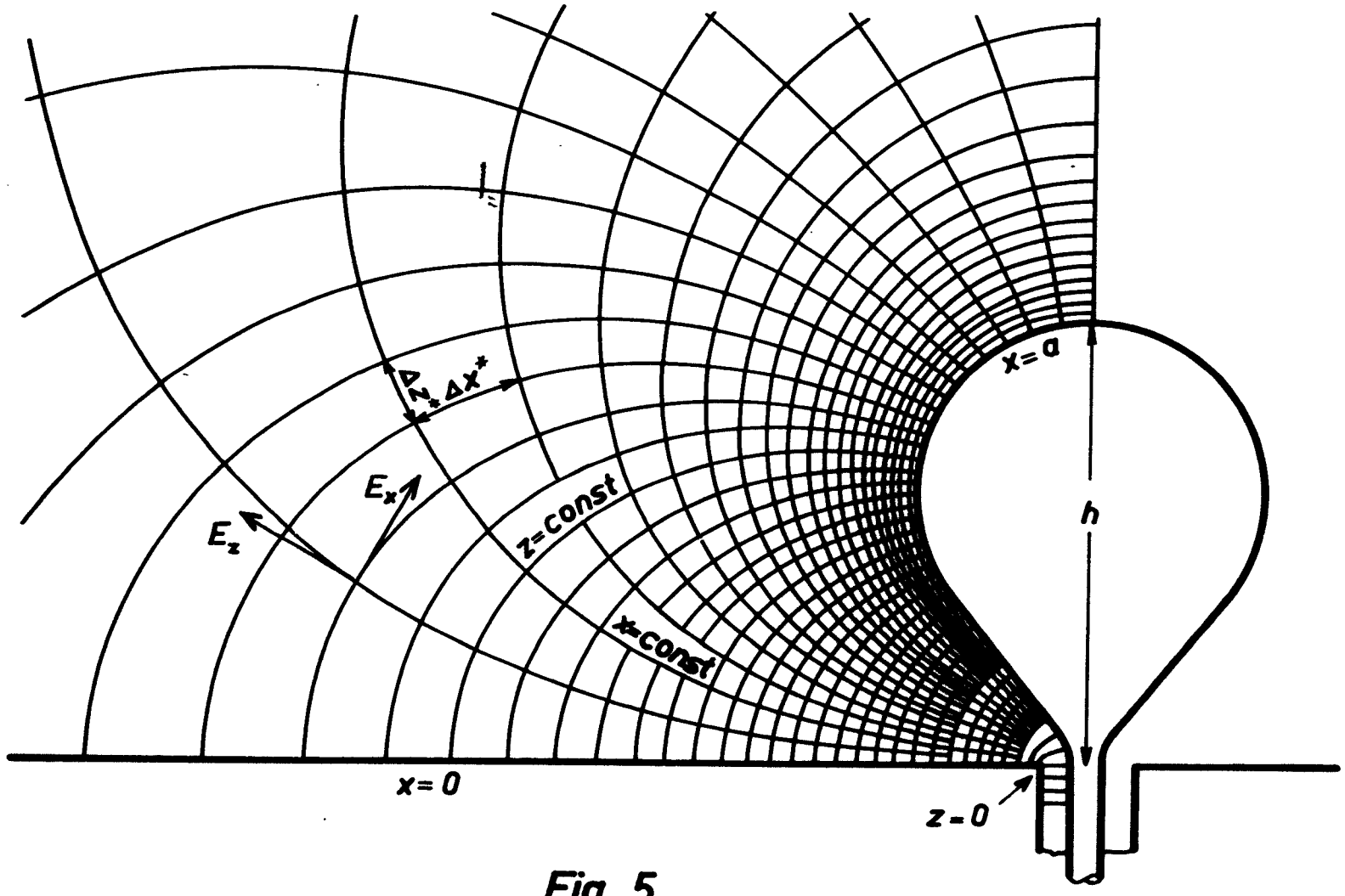

Fig. 5

z = constant. The ground plane contains the coordinate x = 0; the radiator the coordinate x = a, where a may be freely chosen. The same coordinate difference Δx exists everywhere between two adjacent equipotential lines. Therefore x of a special equipotential line is the static voltage between that special equipotential line and the ground plane if the voltage "a" exists between the radiator and the ground plane. The coordinate z begins with z = 0 at the base of the radiator where the impedance is to be calculated and measured. The same coordinate difference Δz exists everywhere between adjacent field lines of Fig. 5. The capacitance ΔC of a region between two field lines is therefore proportional to the corresponding coordinate difference Δz and

$$C = C_o^* \cdot \Delta z; \qquad C_o^* = \frac{\Delta C}{\Delta z} \tag{1}$$

C_o^* is constant along the radiator.

Δx^* is the true distance between equipotential lines.

Δz^* is the true distance between the field lines, see Fig.5. Then relationships between the coordinate differences and the corresponding actual distances can be found in accordance with the theory of the cylinder-symmetrical static fields [4] .

$$\Delta z^* = A(x,z) \cdot \Delta z; \qquad A(x,z) = \frac{\Delta z^*}{\Delta z} \tag{2}$$

$$\Delta x^* = B(x,z) \cdot \Delta x; \qquad B(x,z) = \frac{\Delta x^*}{\Delta x} \tag{3}$$

According to the general rules for cylinder-symmetrical potential fields, the following is true for the edges of an element ΔF

$$\frac{A}{B} = \frac{r_o}{r} \tag{4}$$

where r is the distance of ΔF from the radiator axis of rotation and r_o is a length which may be freely chosen. Experience has shown that the field has its most suitable form for numerical

evaluation when r_o is approximately equal to the radiator height. The reports for Contract AF 61 (052)-41 contain several examples showing the static field for such radiators. After the static field has been plotted, Δx^*, Δz^* and r can be obtained directly from the field plot. Also A,B and r_o/r can be calculated for each ΔF by using equations (2) to (4).

IV. The Wave Equations

Detailed information of the following procedures can be found in references [5] and [6] . The cylinder-symmetrical field has circular magnetic field lines with their center at the axis of rotation and the magnetic field intensity H_y (x,z) is constant along each magnetic field line.

In the cylinder-symmetrical field, the electrical field lines always lie in a plane which intersects the axis of rotation. Therefore in accordance with Fig. 7 an electrical field component E_x in the direction of the lines z = constant, and an electrical field component E_z in the direction of the lines x = constant, exist. Their equations and their solutions are different depending upon whether the evaluation is for Region I with dielectric or for Region II without dielectric. Therefore a separate solution must be sought for these two regions and the boundary conditions of the bounding surface between these regions must be satisfied.

Wave Equations for Region I:

$\varepsilon_r > 1$ and $\mu_r \geq 1$ are constants. All field components of this region are marked by the index 1.

For this cylinder-symmetrical region having the line elements dx^* and dz^* in accordance with (2) to (5) the following field equations are valid:

$$j\omega \varepsilon_o \varepsilon_r (E_{x1} \cdot \frac{r}{r_o} \cdot A) = - \frac{\partial}{\partial z} (H_1 \cdot \frac{r}{r_o}) \qquad (6)$$

$$j\omega \varepsilon_o \varepsilon_r (E_{z1} \cdot A) = (\frac{r_o}{r})^2 \frac{\partial}{\partial x} (H_1 \cdot \frac{r}{r_o}) \qquad 7)$$

$$j\omega/u_o/u_r(H_1 \cdot \frac{r}{r_o}) \cdot A^2 = \frac{\partial}{\partial x}(E_{z1} \cdot A) - \frac{\partial}{\partial z}(E_{x1} \cdot \frac{r}{r_o} \cdot A) \qquad (8)$$

The boundary condition which does not allow tangential electrical fields on the bounding conductor surfaces is in this coordinate system

$$E_{z1} = 0 \quad \text{for } x = 0 \quad \text{and } x = a \qquad (9)$$

If (6) and (7) are substituted into (8) then the wave equation for $(H_1 \frac{r}{r_o})$ is:

$$-\omega^2/u_o \varepsilon_o/u_r \varepsilon_r (H_1 \cdot \frac{r}{r_o}) \cdot A^2$$
$$= \frac{\partial}{\partial x}\left[(\frac{r_o}{r})^2 \frac{\partial}{\partial x}(H_1 \cdot \frac{r}{r_o})\right] + \frac{\partial^2}{\partial z^2}(H_1 \cdot \frac{r}{r_o}) \qquad (10)$$

Where:

$$\omega^2/u_o \varepsilon_o = (\frac{2\pi}{\lambda_o})^2 \qquad (11)$$

λ_o = wavelength in free space

$$\omega^2/u_o \varepsilon_o u_r \varepsilon_r = (\frac{2\pi}{\lambda_o})^2 \cdot /u_r \varepsilon_r = (\frac{2\pi}{\lambda_\varepsilon})^2 \qquad (12)$$

λ_ε = wavelength in dielectric

The boundary condition (9) and equations (6) and (7) are satisfied by theseries expansions:

$$H_1 = -\frac{r_o}{r} \cdot j\omega \varepsilon_o \varepsilon_r \left[W_{01}(z) + W_{11}(z)\cos\frac{\pi x}{a} + \right.$$
$$\left. + W_{21}(z)\cos\frac{2\pi x}{a} + \ldots\right] \qquad (13)$$

$$E_{x1} = \frac{v_0}{v} \cdot \frac{1}{A} \left[W_{10}'(z) + W_{11}'(z) \cos \frac{\pi x}{a} + W_{12}'(z) \cos \frac{2\pi x}{a} + \cdots \right] \tag{14}$$

$$E_{z1} = \left(\frac{v_0}{v} \right)^2 \cdot \frac{1}{A} \cdot \frac{\pi}{a} \left[W_{10}(z) \sin \frac{\pi x}{a} + 2 W_{11}(z) \sin \frac{2\pi x}{a} + \cdots \right] \tag{15}$$

Before (13) is substituted into (10) A^2 must be changed to the following form:

$$A^2 = F_0(z) + F_1(z) \cos \frac{\pi x}{a} + F_2(z) \cos \frac{2\pi x}{a} + \cdots \tag{16}$$

In order to obtain suitable equations for the functions W_{n1}. The functions $F_n(z)$ are obtained by a Fourier analysis of the function $A^2(x,z)$ obtained from the static field pattern.

$$F_0(z) = \frac{1}{a} \int_0^a A^2(x,z)\, dx \tag{17}$$

$$F_n(z) = \frac{2}{a} \int_0^a A^2(x,z) \cos \frac{n\pi x}{a}\, dx \tag{18}$$

Such an analysis of the function A^2 has been carried out in detail for an example in Cantract AF 61 (052)41.

In order to bring equation (10) into a suitable form, a corresponding analysis of the function $(r_0/r)^2$ is required:

$$\left(\frac{v_0}{v} \right)^2 = G_0(z) + G_1(z) \cos \frac{\pi x}{a} + G_2(z) \cos \frac{2\pi x}{a} + \cdots \tag{19}$$

The functions $G_n(z)$ are obtained by a Fourier analysis of the function $(r_0/r)^2$. The function $(r_0/r)^2$ is given by the static field pattern. Thus

$$G_0(k) = \frac{1}{a}\int_0^a \left(\frac{v_0}{v}\right)^2 dx \qquad (20)$$

$$G_n(k) = \frac{2}{a}\int_0^a \left(\frac{v_0}{v}\right)^2 \cos\frac{n\pi x}{a}\, dx \qquad (21)$$

Such an analysis is also contained in detail in an example in Contract AF 61 (052)-41.

Then equations (13), (16) are substituted into (10) and the resulting products are simplified by using the following trigonometric formulas:

$$\sin\alpha\cdot\cos\beta = \frac{1}{2}\sin(\alpha+\beta) + \frac{1}{2}\sin(\alpha-\beta) \qquad (22)$$

$$\cos\alpha\cdot\cos\beta = \frac{1}{2}\cos(\alpha+\beta) + \frac{1}{2}\cos(\alpha-\beta) \qquad (23)$$

The resulting cos $\frac{n\pi x}{a}$ terms are then collected on both sides of the equation. Equation (10) is satisfied when same cos $\frac{n\pi x}{a}$ terms on both sides of the equation are equal. This gives a system having an infinite number of differential equations for the functions W_{n1}.

$$\left(\frac{\lambda_g}{2\pi}\right)^2 W_{01}'' + F_0 W_{01} = -\left(\frac{1}{2}F_1 W_{11} + \frac{1}{2}F_2 W_{21} + \frac{1}{2}F_3 W_{31} + \cdots\cdots\right) \qquad (24)$$

$$\left(\frac{\lambda_g}{2\pi}\right)^2 W_{11}'' + \left[\left(F_0 + \frac{1}{2}F_2\right) - \left(\frac{\lambda_g}{2a}\right)^2 \left(G_0 - \frac{1}{2}G_2\right)\right] W_{11} = \qquad (25)$$

$$= -\left\{F_1 W_{01} + \left[\frac{1}{2}\left(F_1 + F_3\right) - \left(\frac{\lambda_g}{2a}\right)^2 \left(G_1 - G_3\right)\right] W_{31} + \cdots\cdots\right\}$$

$$\left(\frac{\lambda_g}{2\pi}\right)^2 W_{21}'' + \left[\left(F_0 + \frac{1}{2}F_4\right) - \left(\frac{\lambda_g}{2a}\right)^2 \left(G_0 - \frac{1}{2}G_4\right)\right] W_{21} = \qquad (26)$$

$$= -\left\{F_2 W_{01} + \left[\frac{1}{2}\left(F_1 + F_3\right) - \left(\frac{\lambda_g}{2a}\right)^2 \left(G_1 - G_3\right)\right] W_{11} + \cdots\right\}$$

$$\left(\frac{\lambda_s}{2\pi}\right)^2 W_{n1}'' + \left[\left(1 - \frac{1}{2}F_{2n}\right) - \left(\frac{n\lambda_s}{2a}\right)^2\left(G_0 - \frac{1}{2}G_{2n}\right)\right] W_{n1} = -\left\{F_n W_{01} + \sum_{n \neq k} K_{nk} W_{k1}\right\} \tag{27}$$

The coupling factors K_{nk} are symmetrical.

$$K_{nk} = K_{kn} \tag{28}$$

Explanation of Physics Involved in the Equations (24) to (27)

Each W_{n1} is a wave of definite mode. W_{01} is a TEM mode in accordance with Fig. 8a having electrical field lines along the static field lines z = constant because E_{z1} in equation (15) has no W_{01} terms. Therefore $E_{z1} = 0$ for this partial mode type. The other modes are of the TM type. The behaviour of their components E_{x1} and E_{z1} is in accordance with equations (14) and (15) respectively. W_{11} is a mode whose E_z-component distribution follows the function $\sin \frac{2\pi x}{a}$. The corresponding electrical fields can be found in Fig. 8c. All partial modes are coupled to the TEM mode W_{01} by the $F_n W_{01}$ terms. They are also coupled with each of the other TM modes by the $K_{nk} W_{k1}$ terms.

Wave Equations for Region II

$\varepsilon_r = 1$; $\mu_r = 1$. All field components of this region have the index 2. The way to obtain them is the same as for the wave equations of region I. (See [10])

Boundary Conditions at the Dielectric Boundary $z = z_o$ (Fig.1)

The boundary is a static field line z = constant. The tangential components continuously pass through the boundary surface.

$$E_{x1}(z_o) = E_{x2}(z_o) \tag{41}$$

$$H_1(z_o) = H_2(z_o) \tag{42}$$

From this follows

$$W_{h1}'(z_0) = W_{h2}'(z_0) \tag{44}$$

And

$$\varepsilon_r W_{h1}(z_0) = W_{h2}(z_0) \tag{45}$$

V. The Impedance in the Radiator Field

An impedance can only be defined in a region where a TEM mode exists. That portion of the TEM mode field within the dielectric medium is given in accordance with equations (13) and (14) by:

$$H_1 = -j\omega\varepsilon_0\varepsilon_r \frac{r_0}{r} W_{01}(z) \tag{46}$$

$$E_{x1} = \frac{r_0}{r} \cdot \frac{1}{A} \cdot W_{01}'(z) \tag{47}$$

For this mode current voltage and impedance can be defined by using Fig. 9.

Between the end points P_1 and P_2 of a line z = constant, the voltage on the conductor for the W_{01} wave is given by:

$$U_{01}(z) = \int_0^a E_{x1}\, dx = \int_0^a E_{x1} \cdot B \cdot dx = \int_0^a W_{01}'(z)\, dx = W_{01}'(z) \cdot a \tag{48}$$

A circle z = constant on the radiator and intersecting P_1 belongs to the coordinate z on the cylinder-symmetrical radiator of Fig. 9. The surface current density existing on and perpendicular to this circle is:

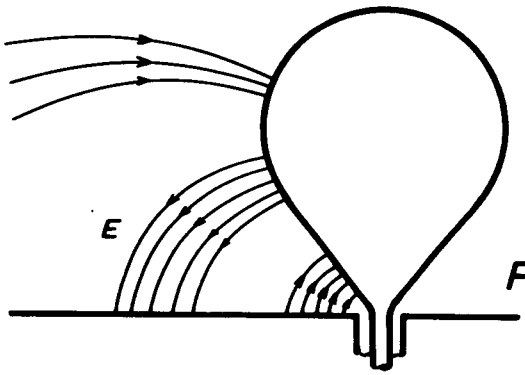

Fig. 8a

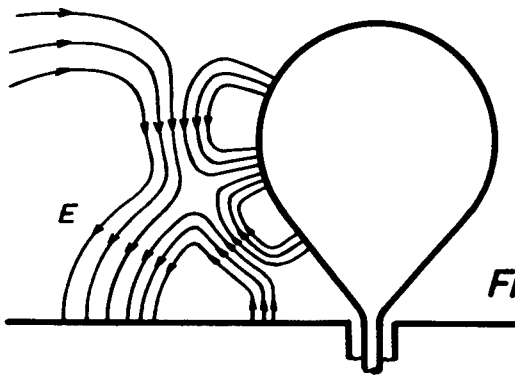

Fig. 8b

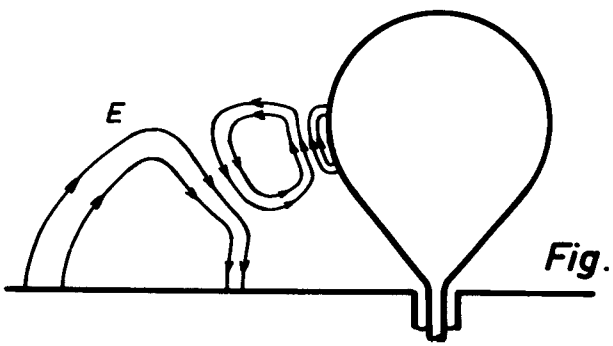

Fig. 8c

Fig. 9

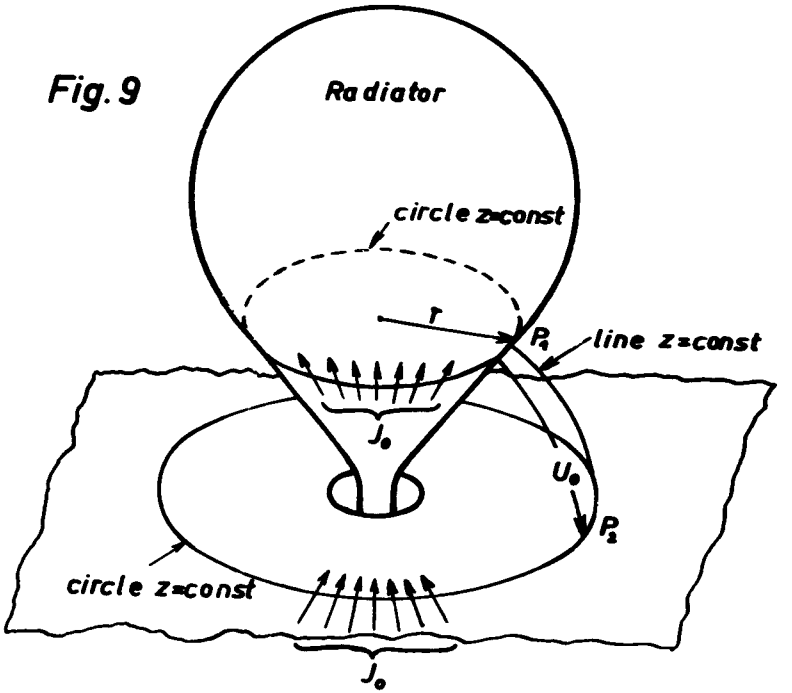

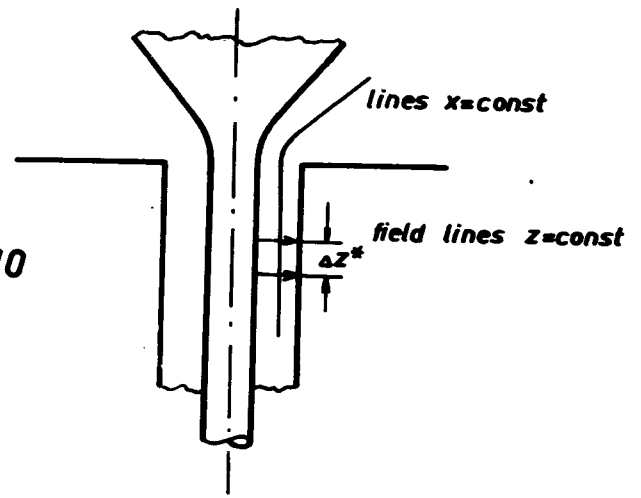

Fig. 10

$$J^* = H_1(z) = -j\omega\varepsilon_0\varepsilon_r \frac{r_y}{r} \cdot W_{01}(z) \qquad (49)$$

Therefore the total current flowing through this circle is:

$$J_{01}(z) = 2\pi r J^* = -j\omega\varepsilon_0\varepsilon_r 2\pi r_0 W_{01}(z) \qquad (50)$$

The same current flows in Fig. 9 on the ground plane above the circle z = constant and through P_2 having the same z as P_1. Therefore the impedance of the W_0 wave belonging to the coordinate z within the dielectric, is defined by

$$Z_1(z) = \frac{U_{01}(z)}{J_{01}(z)} = j \frac{1}{\omega\varepsilon_0\varepsilon_r} \cdot \frac{a}{2\pi r_0} \cdot \frac{W_{01}'}{W_{01}} \qquad (51)$$

This definition is also valid for the feeding line. Since only the TEM mode exists here, the definition of Z in the feeding line is identical to the usual impedance conception. For Z_2 outside the dielectric in Region II there exists a formula analog to (51) with $\varepsilon_I = 1$.

Final Determination of the Coordinate z

The electrical field lines are parallel straight lines within the feeding line; thus Δz^* is independent of x and according to (2) A is also independent of x. As a result $F_0 = A^2$ in the feeding line according to equation (16). Since the feeding line is homogeneous and sections of equivalent length also have the same capacitance, the same Δz belongs to the same separation Δz^* everywhere within the feeding line as shown by equation (1). Therefore $A^2 = F_0$ is also independent of z and constant. It is advisable to choose $F_0 = 1$ for the region within the feeding point. Then for this region (according to Fig. 10):

$$\Delta z^* = \Delta z \; ; \; A = 1 \; ; \; F_0 = 1 \qquad (55)$$

It is also very practical to insert the beginning z = 0 in that cross sectional plane of the feeding line at which the radiator input impedance is to be measured. In this manner and by using equation (55) the coordinate z becomes well defined since the capacitance C_0^* along the system must remain constant according to equation (1).

Final Determination of the Coordinate x

The wave impedance of the feeding line of Fig. 1 has a definite value for Z_1 when dielectric is used. If a travelling wave exists within the line, then $Z = U/I = Z_1$. Under this condition the W_{01} wave has a constant amplitude and a linear increasing phase shift in respect to z in the feeding line

$$W_{01}(z) = W_{01}(0) \cdot e^{-j\frac{2\pi z}{\lambda_\varepsilon}} \tag{56}$$

$$W_{01}'(z) = W_{01}(0) \cdot \left(-j\frac{2\pi}{\lambda_\varepsilon}\right) e^{-j\frac{2\pi z}{\lambda_\varepsilon}} \tag{57}$$

If these equations are now inserted into equation (51) and by using equation (12) the following is obtained:

$$Z_L = \frac{a}{2\pi r_0}\sqrt{\frac{\mu_0}{\varepsilon_0}} \cdot \sqrt{\frac{\mu_r}{\varepsilon_r}} \tag{58}$$

If the characteristic impedance Z_1 of the feeding line is given, then the following relationship exists between a and r_0:

$$a = 2\pi r_0 \frac{Z_L}{Z_F} \tag{59}$$

Where

$$Z_F = \sqrt{\frac{\mu_0}{\varepsilon_0}}\sqrt{\frac{\mu_r}{\varepsilon_r}} \tag{59a}$$

is the wave impedance of the dielectric.

If r_0 is chosen freely, a is fixed by equation (59). If in accordance with Fig. 5, the ground plane has the coordinate x = 0 and the radiator the coordinate x = a, then the coordinate x is well defined once r_0 has been chosen.

The boundary Condition in the Form of an Impedance Equation:

If equation (44) is divided by (45) then for n = 0

$$\frac{W_{01}'(z_0)}{\varepsilon_r W_{01}(z_0)} : \frac{W_{02}'(z_0)}{W_{02}(z_0)} \tag{59b}$$

This means in accordance with equation (51)

$$Z_1(z_0) = Z_2(z_0) \tag{60}$$

as a substitute for the boundary condition (44) in the case of n = 0.

The TM wave travelling from the boundary surface $z = z_0$ into the outer region yields an impedance $Z_2(z)$ at any arbitrary location z and especially the value $Z_2(z_0)$ at the surface of the dielectric which appears as an unchanged termination impedance for the TEM W_{01} wave inside the dielectric, according to equation (60). This $Z_1(z_0)$ is then the value $Z_1(o)$. Since the input surface z = 0 is so chosen that all space waves W_n are negligibly small there, this $Z_1(o)$ is an actual and measurable impedance which acts as a termination for the feeding line. This same impedance is designated the input impedance of the radiator.

The transformation through the dielectric from $Z_1(z_0)$ to $Z_1(o)$ is given by a differential equation. If equation (15) is differentiated in respect to z, the following is obtained:

$$\frac{dZ_1}{dz} = j\frac{1}{\omega\varepsilon_0\varepsilon_r}\cdot\frac{a}{2\pi r_0}\left[\frac{W_{01}''}{W_{01}} - \left(\frac{W_{01}'}{W_{01}}\right)^2\right] \qquad (61)$$

Then W_{01}'' and W_{01}'/W_{01} from equations (24) and (51) respectively are substituted into equation (61). The following equation results in conjunction with (58)

$$\frac{d\zeta_1}{dz} = j\frac{2\pi}{\lambda_z}\left[\zeta_r^2 - \zeta_L\left(F_0 + \frac{1}{2}F_1\frac{W_{11}}{W_{01}} + \frac{1}{2}F_2\frac{W_{12}}{W_{01}} + \cdots\right)\right] \qquad (62)$$

This is the transformation equation for the impedance within the dielectric medium.

VI. Application of the Theory for very short Antennas in a finite Dielectric Medium.

It is required that all the radiator dimensions as well as all the dielectric dimensions, be essentially smaller than a wavelength. Since no higher order TM modes other than the W_{01} and W_{12} have an appreciable magnitude in the surrounding space,

all the equations take on a more simplified form. This is readily realized since all short radiators have the same radiation pattern and the field intensity distribution corresponds to that of W_{12} mode. As long as the measurement of the radiation pattern shows no essential deviation from that of a short radiator, all W_{n2} with $n > 1$ may be studied here, not only the impedance but also the radiation pattern is measured at high frequencies in order to be sure that only the W_{12} wave exists in this region thus allowing for the use of a simplified theory. The measured radiation patterns show, that indeed all W_{n2} with $n > 1$ may be neglected. (see [10])

The above problem can be solved by using a two step method:

a) For very low frequencies (radiator length very small compared to wavelength) W_{11} may also be neglected within the dielectric. Then only the TEM mode exists within the dielectric. The dielectric medium acts only as a transforming inhomogeneous line for the W_{01} wave.

b) At somewhat higher frequencies an evanescent W_{11} mode whose magnitude increases with the square of frequency, also forms in the dielectric. The boundary conditions at the dielectric boundary surface causes this W_{11} mode to excite an additional formation of the W_{12} mode. As a result, an increased radiation of the W_{12} space wave as compared to a radiator without dielectric occurs to a certain extent.

Impedance Transformation for very short Radiators without consideration of the TM fields in the Dielectric.

It is assumed that in Region I between the feeding point and the surface $z = z_0$, only the W_{10} wave becomes effective. Then equation (62) has the form

$$\frac{dZ_0}{dz} = j \frac{\pi}{\lambda_\varepsilon} \cdot \frac{1}{Z_L} \left[Z_L^2 - \Gamma_0 Z_L^2 \right] \qquad (67)$$

This is the familiar equation for the impedance transformation of an inhomogeneous line with dielectric. This line has the wavelength λ_L and the position-dependent characteristic impedance $Z_L \cdot \sqrt{F_0}$. The outer region of Fig. 1 produces an impedance $Z_2(z_0)$ in the boundary surface $z = z_0$ of the dielectric which is also the termination impedance $Z_1(z_0)$ of the dielectric according to (60). This $Z_1(z_0)$ is transformed into the desired input impedance $Z_1(o)$ at $z = o$ in Fig. 1 by the use of dielectric and with the aid of equation (67). As long as no W_{11} fields of appreciable magnitude exist in the dielectric, then the W_{12} space wave is only formed outside of the dielectric. Then the same fields are produced outside the dielectric as those of a radiator without dielectric. The impedance $Z_2(z_0)$ caused by the outer region is then independent of the existence of a dielectric and is also valid for the location z_0 of a radiator with and without dielectric.

To be able to compare radiators with and without dielectric also the theory of a radiator without dielectric must be established. Then the wave equations (30) to (40) are valid up to the base point $z = 0$. Due to the larger λ_{c1} the TM modes are still smaller as compared to the case with dielectric and can then always be neglected if they are negligible for the same frequency in the dielectric. If Z_2 is the impedance in the air region, then in analogy to (67) with $\varepsilon_r = 1$, the following is valid for Z_2:

$$\frac{d\,\underline{z}_i}{dz} = j\,\frac{2\pi}{\lambda_0}\,\frac{1}{\underline{z}_{L0}}\left[\underline{z}_i^{\,2} - F_0\,\underline{z}_{L0}^{\,2}\right] \tag{68}$$

where according to (58) for $\varepsilon_r = 1$

$$\underline{z}_{L0} = \frac{o}{2\pi r_0}\sqrt{\frac{\mu_0}{\varepsilon_0}} \tag{69}$$

The difference between (67) and (68) is that this antennaline with dielectric has a larger capacitance according to the factor $\varepsilon_r > 1$ or for the case of $\mu_r > 1$, a larger inductance according to the factor $_0/\mu_r$. As a result the wavelength and the characteristic impedance Z_L are different in both cases.

Experimental Testing of the Theory of Impedance Transformation for very short Radiators

For the radiator without dielectric, the input impedance $Z_2(o)$ at the base point $z = 0$ is measured as a function of frequency. For this measurement we are using the same arrangement as used for Contract AF 61 (052)-41 [3].

Fig. 13 shows the working plane, Fig. 14 the radiator without dielectric, Fig. 15a and 15b the radiator surrounded with dielectric.

Curve I of the Smith chart of Fig. 16 shows the input impedance $Z_2(0)$ of the radiator drawn in Fig. 5 without dielectric for the frequency range of 200 to 1000 mc/s. From this $Z_2(0)$ The impedance $Z_2(z_0)$ in the sketched surface $z = z_0$ is calculated with the aid of equation (68) for the condition that the region from $z = 0$ to $z = z_0$ is filled with air. As an example, Fig. 17 shows the migration of $Z_2(0)$ to $Z_2(z_0)$ along this inhomogeneous line at 200 mc/s, in accordance with equation (68), if the losses due to the silver-plated conductor surface are neglected. Curve II of Fig. 16 shows a plot of the calculated results for $Z_2(z_0)$ obtained in this manner for the frequency range of 200 to 1000 mc/s. This $Z_2(z_0)$ is simultaneously the $Z_1(z_0)$ by which the dielectric is terminated in the surface $z = z_0$. From $Z_1(z_0)$ and by using equation (67) the input impedance $Z_1(0)$ for the radiator with dielectric is calculated. Fig. 17 shows the transformation at 200 mc/s from $Z_1(z_0)$ to $Z_1(0)$ along this inhomogeneous line which is assumed to be filled with a lossless dielectric ($\varepsilon_r = 2.5$). Curve III of Fig. 16 shows the $Z_1(0)$ which were calculated in this manner for the frequency range of 200 to 1000 mc/s and curve IV shows the

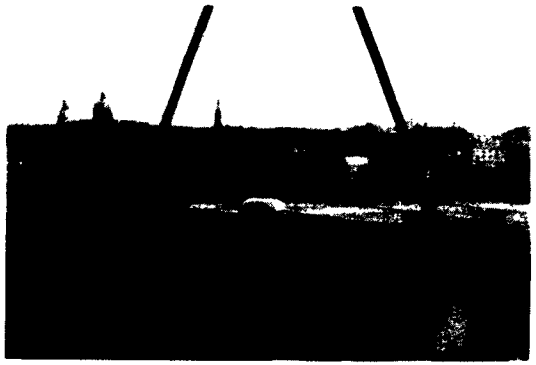

Fig. 13

Fig. 15a

Fig. 14

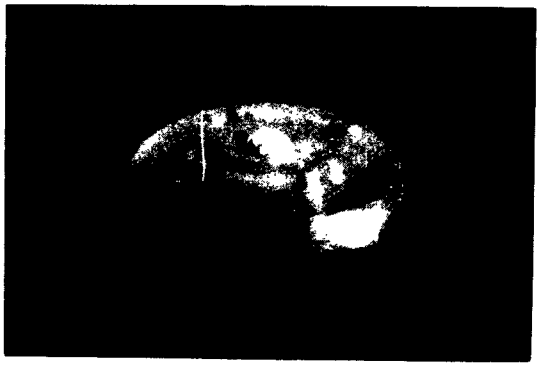

Fig. 15b

measured values $Z_1(0)$ of the radiator with dielectric.

If this measured $Z_1(0)$ at 200 mc/s is inserted in Fig. 17 then it can be seen that the measured $Z_1(0)$ lies close to the calculated $Z_1(0)$. Thus the theory has been confirmed at the frequency of 200 mc/s. The small deviation at 200 mc/s between the measred and calculated values has a magnitude which can readily be explained by the losses of the radiator.

The deviations between the calculated values and the measured values of $Z_1(0)$ become larger with increasing frequency. These deviations could have the following two causes:

a) Dielectric and radiator losses

b) Additional radiation where the W_{11} is no longer negligible. The line $z = z_0$ which is drawn in Fig. 1 has a length of 18.3 cm which is approximately $\lambda_0/2$ at 900 mc/s such certainly new radiation effects due to the dielectric occur at this frequency. This line has approximately the engths $\lambda\varepsilon/2$ at 600 mc/ s such that the W_{11} in the dielectric could be appreciable and cause a considerable part of the deviation. An approximative calculation in [10] shows, that the dielectric and resistive losses are negligible in the Frequency range between 200 and 1000 mc/s.

The deviations between the calculated impedance $Z_1(0)$ and the measured values $Z_1(0)$ can only be explained by an additional radiation caused by the dielectric. As the impedance measure - ments show, this additional radiation becomes consistantly stronger with increasing frequency.

VII. Theoretical Results especially for a Dielectric having $\mu_r > \varepsilon_r$

As was shown in Section VI, the very short radiator which is sur ounded ith dielectric has no additional radiation effects as compared to the radiator in air. The only effect the dielectric is a different impedance transformation from $Z_1(z_0)$ to $Z_1(0)$. This is also valid for a dielectric of $\mu_r > \varepsilon_r$. Sin e the theory for the impedance transformation (neglecting losses) of very short radiators has been confirmed experimen-

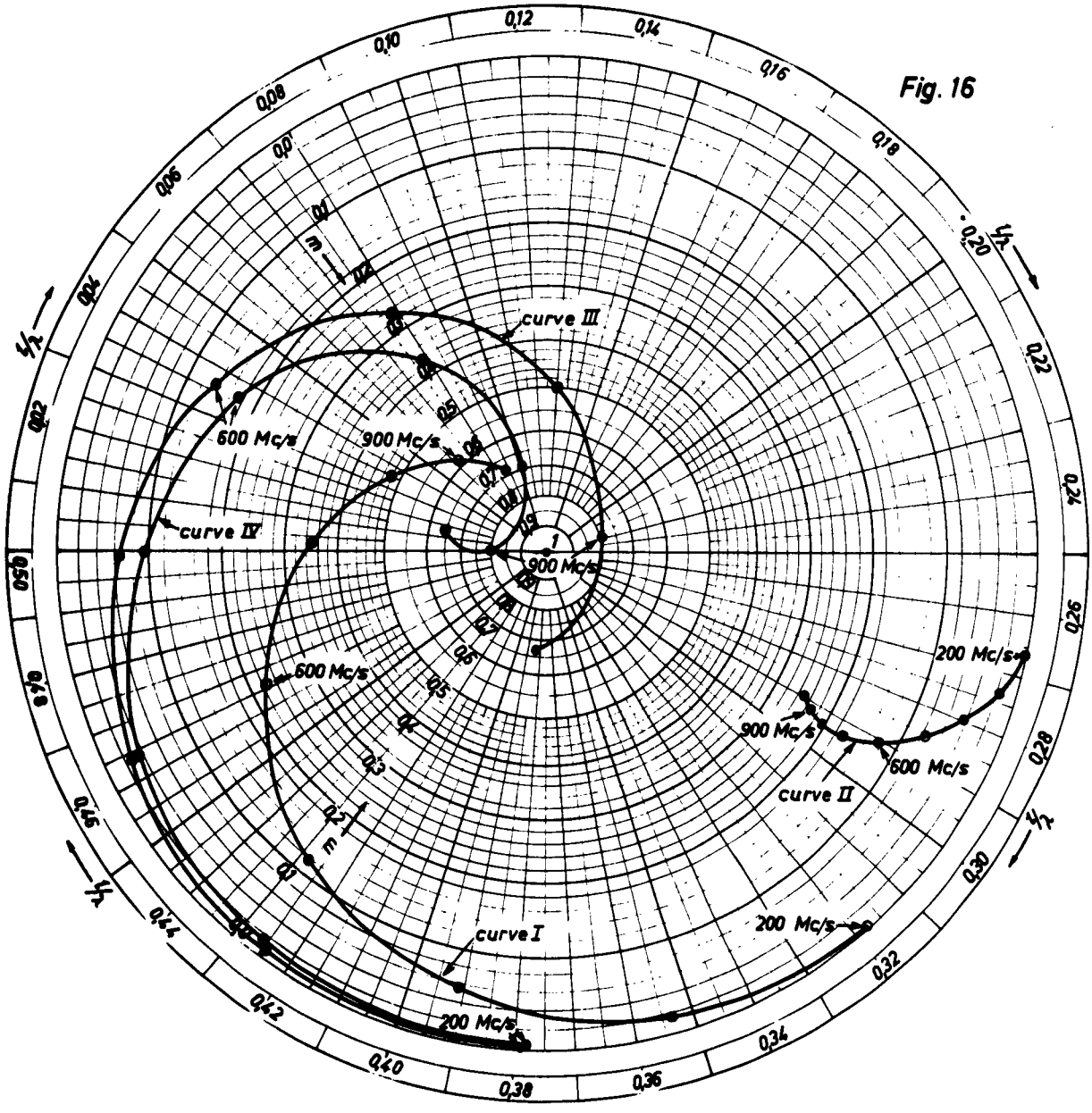
curve III
curve IV
curve II
curve I
600 Mc/s
900 Mc/s
200 Mc/s
900 Mc/s
600 Mc/s
200 Mc/s
900 Mc/s
600 Mc/s
200 Mc/s
1
0,12
0,14
0,16
0,18
0,20
0,22
0,24
0,26
0,28
0,30
0,32
0,34
0,36
0,38
0,40
0,42
0,44
0,46
0,48
0,50
0,10
0,08
0,06
0,04
0,02

Fig. 16

tally, it suffices to calculate the transformation of various dielectrics without conducting measurement. The transformation occurs according to the equation:

$$\frac{d Z_1}{d \ell} = j \frac{2\pi}{\lambda^*} \cdot \frac{1}{\ell_L} \left[Z_1^2 - F_0 Z_L^2 \right] \qquad (70)$$

with

$$\lambda^* = \frac{\lambda_0}{\sqrt{\varepsilon_r \mu_r}}$$

This equation is analogous to equation (67) for the impedance transformation along an inhomogneous line with dielectric with the addition that equation (70) accounts for an ε_r as well as a μ_r.

The position of the impedance $Z_1(0)$ in the complex impedance plane is not important. A suitable transformation arrangement always allows for the transformation of an arbitrary impedance $Z_1(0)$ at the base of the radiator to a different arbitrary impedance at each freely chosen frequency.

Bandwidth of very short Antennas with $\frac{h}{\lambda_0} < \frac{1}{20}$.

The transformation in the dielectric causes a different frequency-dependent impedance at the base of the radiator as compared to that of a radiator in air. As was shown above, the value of the impedance at the antenna base has no influence upon the antenna performance; however the frequency-dependency of the impedance at the antenna base plays a very important part. A very small frequency-dependency of the impedance is desired.

The question, can the relative bandwidth b_r of a very short antenna be improved by using dielectric, will be considered in the following.

The relative bandwidth b_r of the antenna is defined by:

$$b_r = \frac{R}{\omega \left| \frac{dZ}{d\omega} \right|} \qquad (71)$$

R is the real part of the impedance Z at the base of the antenna. According to [2] the expression

$$\frac{R}{\omega \left| \frac{dX}{d\omega} \right|}$$

is a measure for determining the frequency interval Δf in which a frequency-dependent impedance $Z(f) = R + jX(f)$ may be transformed into a arbitrary frequency-independent impedance. This definition is more generalized in that $|dZ/d\omega|$ instead of $|dX/d\omega|$ is inserted. For an electrically short radiator, $|dX/d\omega|$ is approximately equal to $|dZ/d\omega|$. The ratio of the bandwidth b_{rD} of a radiator with dielectric to the bandwidth b_{rA} of a radiator in air is according to equation (71):

$$\frac{b_{rD}}{b_{rA}} = \frac{R_{sD}}{R_{sA}} \cdot \left| \frac{dZ_A}{dZ_D} \right| \qquad (72)$$

R_{sD} is the real part of the impedance Z_D at the base of a radiator in dielectric. R_{sA} is the real part of the impedance Z_A at the base of a radiator in air.

Now the ratio b_{rD}/b_{rA} of equation (72) will be obtained at 200 mc/s for various dielectrics for the radiator in question. The measured impedance $Z_2(0)$ of the radiator in air which is transformed into $Z_2(z_0) = Z_1(z_0)$ according to equation (68) and from $Z_1(z_0)$ into $Z_1(0)$ according to equation (70) is used here. The transformation according to equation (70) is exact since this radiator is very short at 200 mc/s and does not show any additional radiation.

For a dielectric with $\varepsilon_r = 2.5$ $\mu_r = 1$ the ratio

$$\frac{R_{sD}}{R_{sA}} = 0.236 \qquad \frac{dZ_A}{dZ_D} = 2.07$$

is obtained and from equation (72)

$$\frac{b_{rD}}{b_{rA}} = 0.47$$

Therefore the bandwidth of a radiator with dielectric ($\varepsilon_r = 2.5$ / $u_r = 1$) is smaller than the bandwidth of a radiator in air.

For a dielectric with $\varepsilon_r = /u_r = 2.5$ the ratio

$$\frac{R_{sD}}{R_{sA}} = 0.3 \quad \frac{dZ_A}{dZ_D} = 1.82$$

is obtained and

$$\frac{b_{rD}}{b_{rA}} = 0.55$$

For a dielectric with $/u_r > \varepsilon_r$: $\varepsilon_r = 1$, $/u_r = 2,5$ the ratio

$$\frac{R_{sD}}{R_{sA}} = 1.15 \qquad \frac{dZ_A}{dZ_D} = 0.95$$

is obtained and

$$\frac{b_{rD}}{b_{rA}} = 1.09$$

This is larger than 1, but is very close to 1. Therefore the bandwidth enlarging effect with $/u_r > \varepsilon_r$ is very small.

Thus it can readily be seen that the bandwidth of an antenna with dielectric with $/u_r < \varepsilon_r$ becomes poorer when the dielectric only has a transformation effect. By using a dielectric

with $\mu_r > \varepsilon_r$ a small inprovement of the bandwidth as compared to the radiator in air can be obatained. However, since no dielectric with $\mu_r > \varepsilon_r$ is known of to-date in the frequency range considered, the transformation obtained by using dielectric will always cause a decrease in the bandwidth. Therefore the performance of very short antennas having $\frac{h}{\lambda_o} < \frac{1}{20}$ will be deteriorated by the dielectric.

Bandwidth of a very short Antenna with $\frac{1}{20} < \frac{h}{\lambda_o} < \frac{1}{10}$

With a somewhat longer radiator having $\frac{h}{\lambda_o} > \frac{1}{20}$, the dielectric causes an additional radiation as has been experimentally confirmed in Section VI. Then R_{sD} in equation (72) becomes larger than the R_{sD} calculated from the transformation according to equation (68) and (70). The ratio b_{rD}/b_{rA} also becomes larger than the calculated value obtained from the transformation equation (68) and (70). The ratio b_{rD}/b_{rA} as calculated from equation (68), (70) and (72) will be compared to the measured value obtained in accordance with equation (72) for a radiator surrounded with Polystyrol ($\varepsilon_r = 2.5$ for the frequency range between 200 and 600 mc/s. Curve I of Fig. 20 shows the calculated values for b_{rD}/b_{rA} and Curve II of the same figure shows the measured values as a function of frequency. It can be seen that the values obtained from measurements are always larger than the calculated ones, since the measured data contain the additional radiation effect of the dielectric which was neglected in the transformation calculation. However the magnitude of b_{rD}/b_{rA} which was obtained from measured data was also less than 1. This means that the somewhat larger antenna in dielectric ($\varepsilon_r = 2.5$ $\mu_r = 1$) is not better than the antenna in air. This is caused by the fact that the bandwidth decreasing transformation effect of the dielectric whose bandwidth decreasing transformation effect is as small as possible should be chosen. In this respect the calculated examples have shown that a dielectric having the highest possible μ_r and smallest ε_r would be most suitable for this purpose.

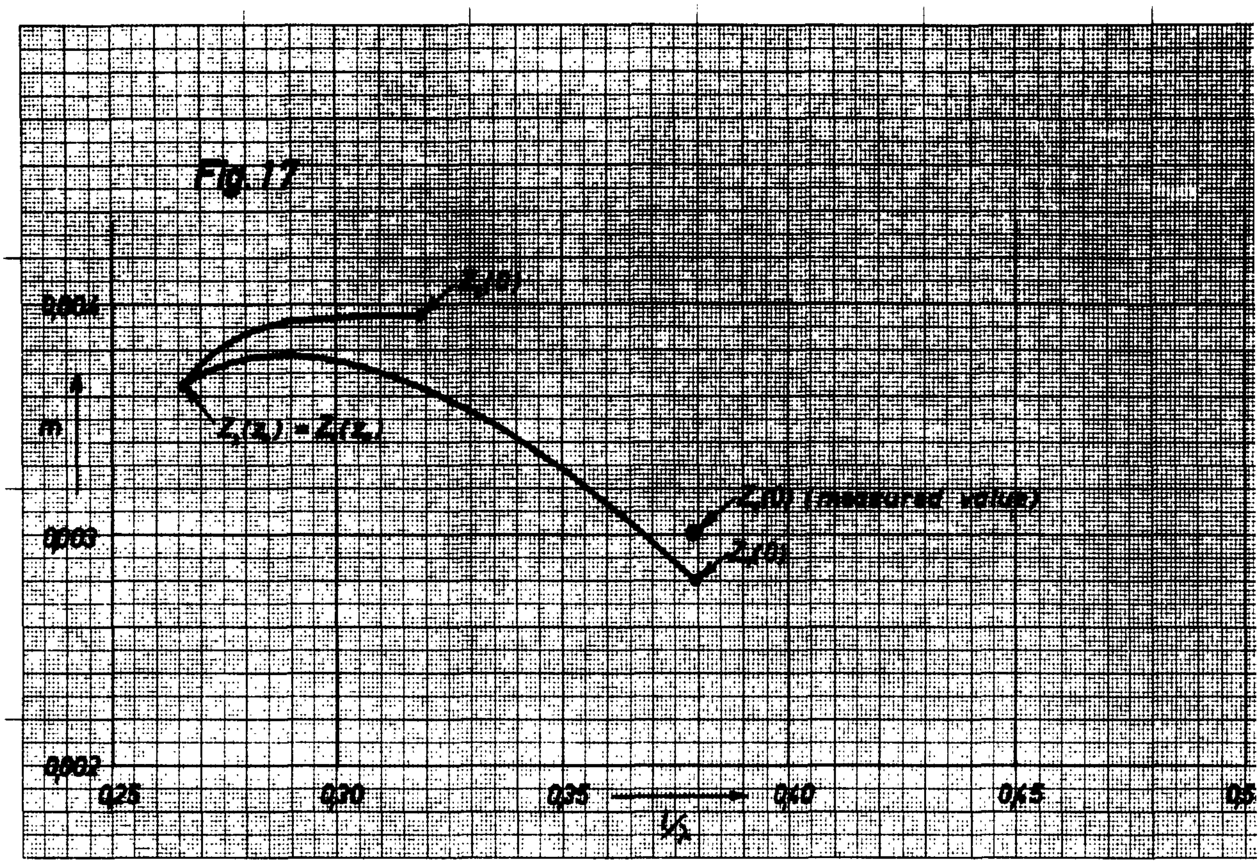
Fig.17
0,004
0,003
0,002
m
0,25
0,30
0,35
0,40
0,45
0,5

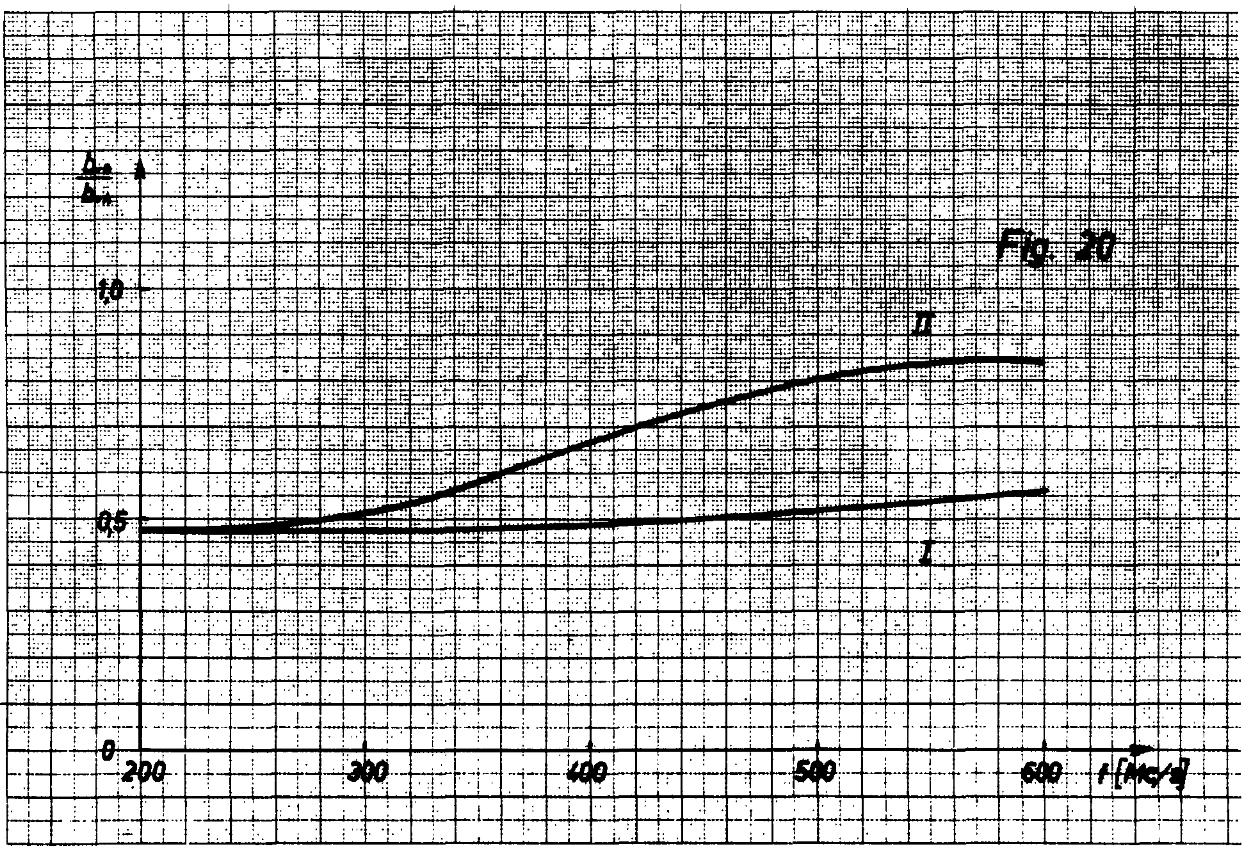
Fig. 20
1,0
0,5
0
200
300
400
500
600
II
I

Improvement of the Frequency-dependency of a Radiator with Dielectric

It will now be attempted to find a suitable geometric shape for the dielectric which will tend to prevent as much as possible the bandwidth decreasing transformation effect of the dielectric, butdoes not effect the additional radiation. This could be achieved by placing the dielectric only in those regions of the inhomogeneous line where it could aid the effect of additional radiation.

The region of the inhomogeneous line which is important for radiation is the location where the transition of the W_0 wave to the W_1 wave is most pronouced. In examining equations (25) and (13) it can be recognized that the transition of W_0 to W_1 is approximately proportional to $I_0 \cdot F_1$. I_0 is the current of the W_0 wave on the radiator and F_1 is defined by equation (16). It can be readily realized that it is not advantageous to insert dielectric within the field line $z/h = 0.5$ since the line is homogeneous here and no mode transition from W_0 to W_1 occurs. Therefore the dielectric should first be inserted outside the field line $z/h = 0.5$.

A second point of view which should be considered for a radiator surrounded with a dielectric medium is the following: The length of boundary field line is determined by the magnitude of $\mu_r \cdot \varepsilon_r$. By means of a siutable choice of dielectric it can be accomplished that the boundary field line of the W_1 wave lies within the boundary of the dielectric. Then the W_1 mode is capable of existing in wave form within the dielectric. For this case the dielectric should extend outwards as close as possible to the boundary field line of the W_1 wave in air, so that the W_1 which was formed in the dielectric can also exist in the outer air region in wave form.

Such a dielectric arrangement would allow the bandwidth - enlargening additional radiation effect to exceed the bandwidth-decreasing transformation effect, even for the case $\mu_r < \varepsilon_r$. Therefore the expectation exists that the use of a dielectric

having suitable chosen geometric dimensions in conjunction with antennas with $h/\lambda_0 > 1/20$ will give $b_{rD}/b_{rA} > 1$ even for the case of $\mu_r < \varepsilon_r$. However the desirable effect will not be very large.

Effect of a dielectric with very large μ_r

The use of a dielectric with very large μ_r causes a considerable enlargement of the electrical length of the antenna with $h/\lambda_0 < 1/20$ if it is regarded as a line, but no enlargement of the electrical length if it is regarded as a radiator. It is a familiar fact that on the average, long lines have a smaller bandwidth. In specific cases the bandwidth can also be enlarged somewhat. Since the entire procedure is concerned with transformations, the improvement of the bandwidth can also be achieved by inserting a properly chosen four-pole transformation arrangement in the feeding line. Therefore the transformation effect of a dielectric with very large μ_r does not bring a direct improvement of antenna performance.

For a radiator with dielectric, a considerable enlargement of the bandwidth can only be obtained as a result of a large additional radiation. However the additional radiation caused by the dielectric is very small for the case of very small radiators. Since the size of the dielectric should not extend beyond the geometric height h of the very short radiatior, the boundary field line of the W_1 wave in air is far distant from the boundary of the dielectric. The air filled region III of Fig. 4c within the boundary field line possesses an imaginary wave impedance for the W_1 mode. Due to the large μ_r, the W_1 fields that are formed within the dielectric are capable of existing in the form of waves. However they decrease exponentially in the air region III of Fig. 4c surrounding the dielectric since this region shows an imaginary wave impedance up to the boundary field line of the W_1 wave in air. The very short radiator with very large μ_r and $h/\lambda_0 < 1/20$ has a very large region III of Fig. 4c. Therefore the fields of W_1 decrease very much until arriving at the boundary field line in air. As a re-

sult they can hardly cause an additional radiation in this region.

Therefore the use of dielectric with very large μ_r can not bring an improvement for very short antennas.

VIII. Very short Radiator in a Polystyrol Shell of improved Shape

Between the field line z/h = 0.5 and the feeding point of the radiator, the dielectric medium only causes a bandwidth decreasing transformation effect. Therefore the dielectric material should only be placed in those regions of the antenna where it could aid the effect of additional radiation. Fig. 21 shows the improved geometric shape of the dielectric material. This improved shape is constructed of the same polystyrol material as that of the shape in sect. VI ($\varepsilon_r = 2.5$).

The impedance caused by the outer space at the coordinate $z = z_o$ which is the border of the dielectric medium is always the same for very short antennas, independent of the dielectric medium. Curve II of Fig. 16 shows this impedance Z_1 at $z = z_o$ which has been calculated from the impedance measurements of the antenna in air. The transformation of this known impedance Z_1 at the field line $z = z_o$ inwards towards the field line $z = z_d$ of Fig. 21 is obtained by using a computer in conjunction with the Runge-Kutta method for solving eq. (101)

$$\frac{dZ_1}{dz} = j \frac{2\pi}{\lambda_\varepsilon} \cdot \frac{1}{Z_{Lo}\sqrt{\frac{1}{\varepsilon_r}}} \left(Z_1^2 - F_o Z_{Lo}^2 \frac{1}{\varepsilon_r} \right) \qquad (101)$$

this corresponds to equation (67)
Z_1 is the impedance to be transformed.
Z_{Lo} is the characteristic impedance of the feeding line.

$$\lambda_\varepsilon = \frac{\lambda_o}{\sqrt{\varepsilon_r}} \qquad (102)$$

The transformation of the impedance from $z = z_d$ inwards towards $z = 0$ occurs according to

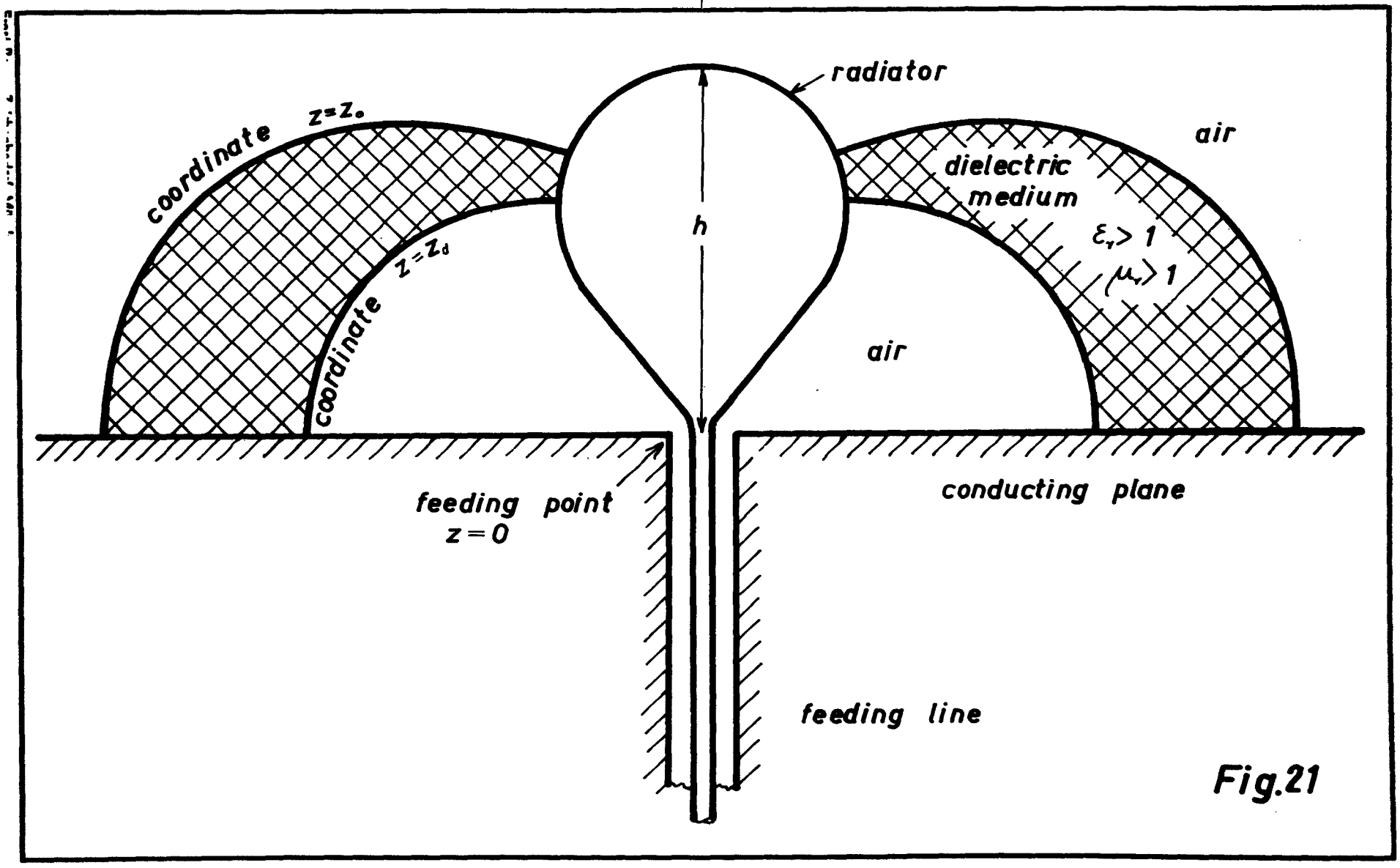
radiator
coordinate $z=z_0$
coordinate $z=z_d$
h
air
dielectric medium
$\varepsilon_r > 1$
$(\mu_r > 1)$
air
feeding point
$z=0$
conducting plane
feeding line

Fig.21

$$\frac{d\underline{z}_e}{dz} = j\,\frac{2\pi}{\lambda_0}\cdot\frac{1}{\underline{z}_{L0}}\left(\underline{z}_e^2 - F_0\,\underline{z}_{L0}^2\right) \qquad (103)$$

This corresponds to equation (68)

The dielectric and resistive losses are so small that they can be neglected in the calculation procedure as was done with the antenna in sect. VI.

Curve I in the Smith-chart of Fig. 22 shows the plot of the calculated feeding point impedance for the frequency range 200 - 1000 mc/s. Curve II gives the measured values.

If the antenna height h is smaller than $\lambda_0/20$ then the measured and calculated impedance values are in good agreement. If h is larger than $\lambda_0/20$ then the measured impedance values lie closer to the SWR = 1 point than the calculated values. This was also observed with the antenna described sect. VI and is caused by the additional radiation effect of the dielectric.

Fig. 23 gives a plot of b_{rD}/b_{rA} according to equation (72). Curve I of Fig. 23 is a plot for this ratio using the calculated impedance values; Curve II gives a plot for the same ratio using the measured impedance values. As a result of the additional radiation, the values for b_{rD}/b_{rA} obtained by using the calculated impedance data.

If the curves of Fig. 23 are compared with the corresponding curves of Fig. 20 then it is readily realized that the new form of the dielectric medium yields a noticeable improvement of the bandwidth. However the bandwidth of the antenna surrounded with the improved polystyrol shape is still smaller than the bandwidth of an antenna in air.

IX. Very short Radiator in Ferrite Shells of improved Shape

The medium which surrounds the spherical antenna shall now be constructed of Ferrite material. Ferrite powder mixed with

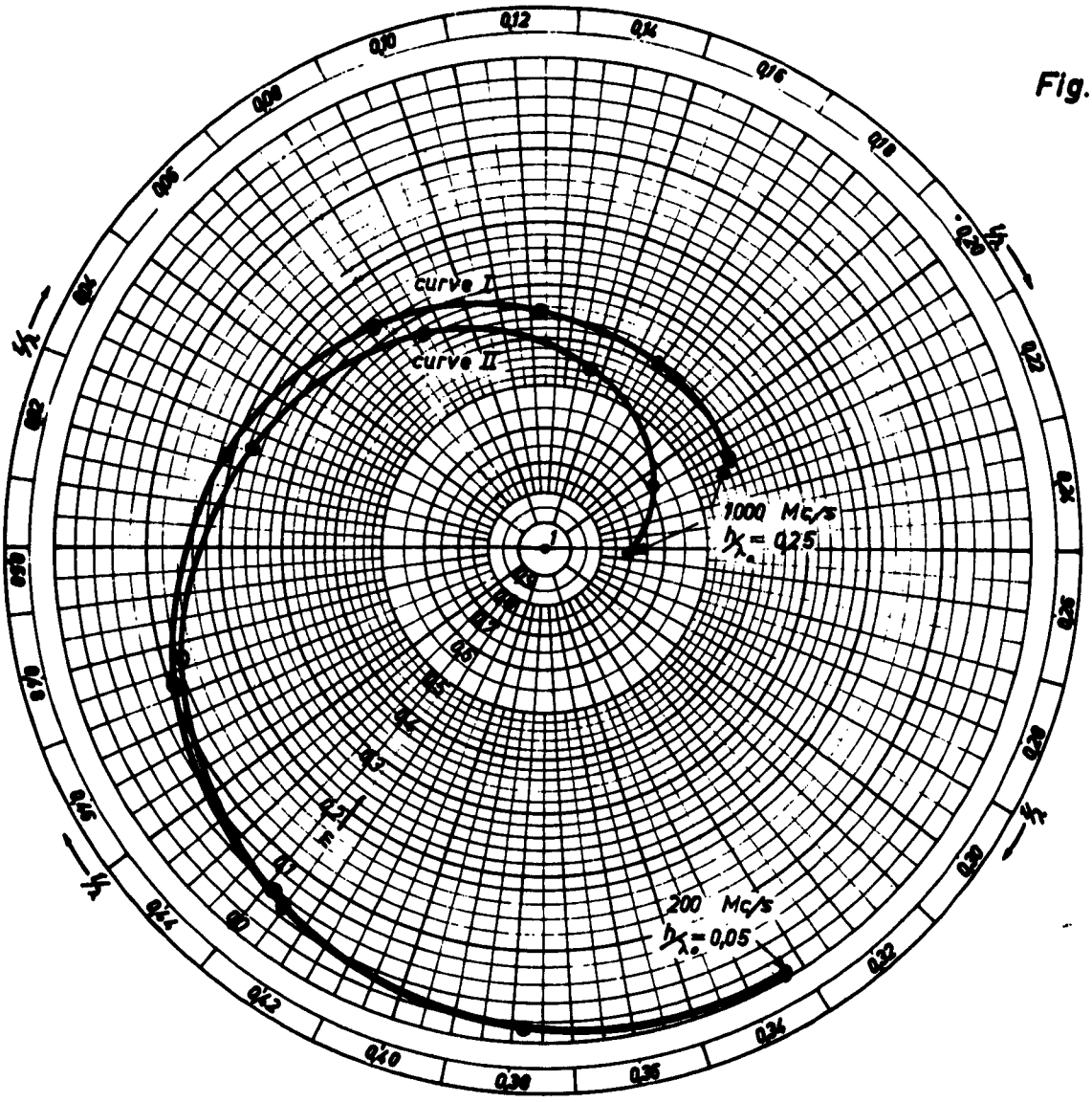

Fig. 22

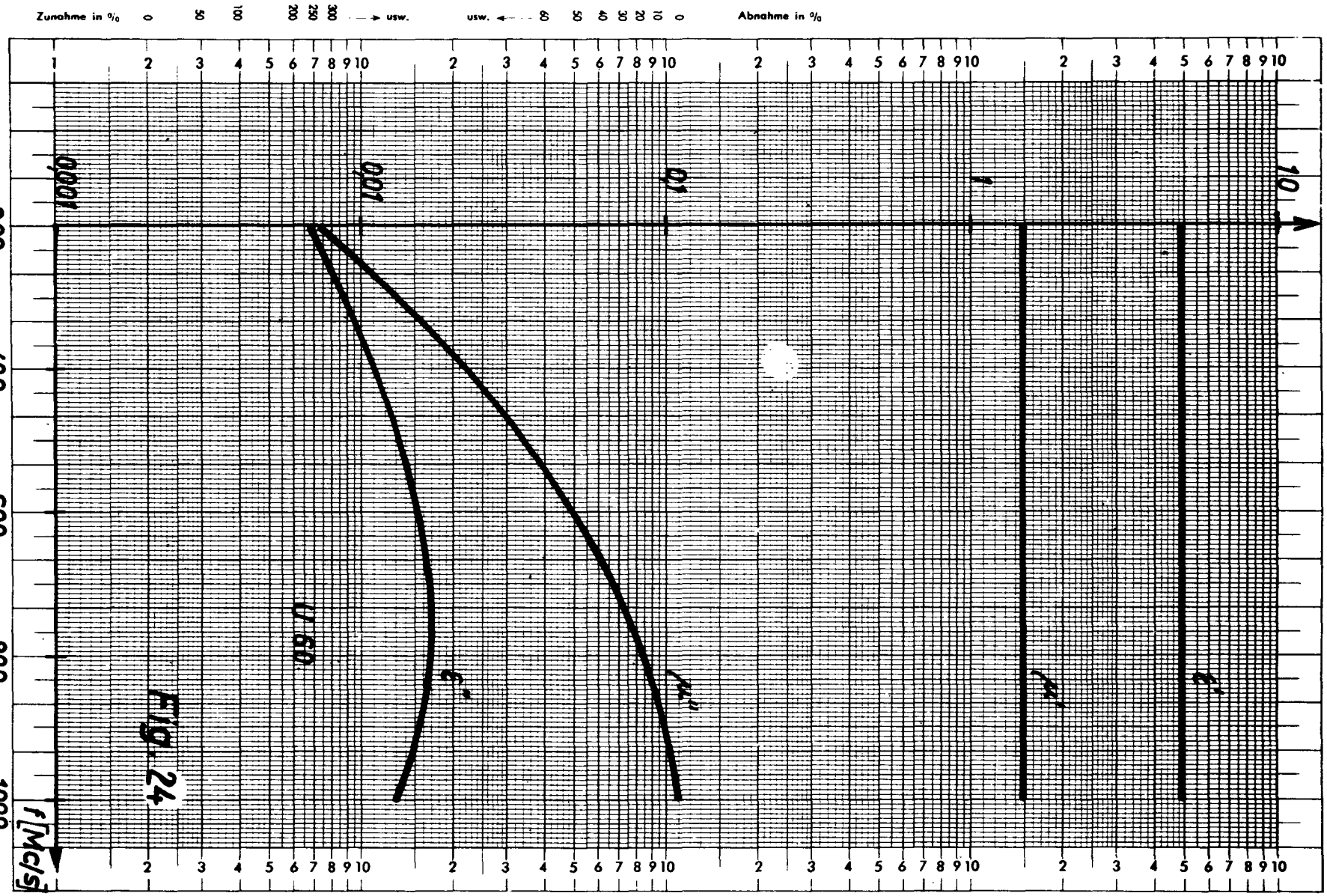

 Nr. 369½:6 P

Eine Achse logar. geteilt von 1 bis 10000, Einheit 62,5 mm, die andere in mm

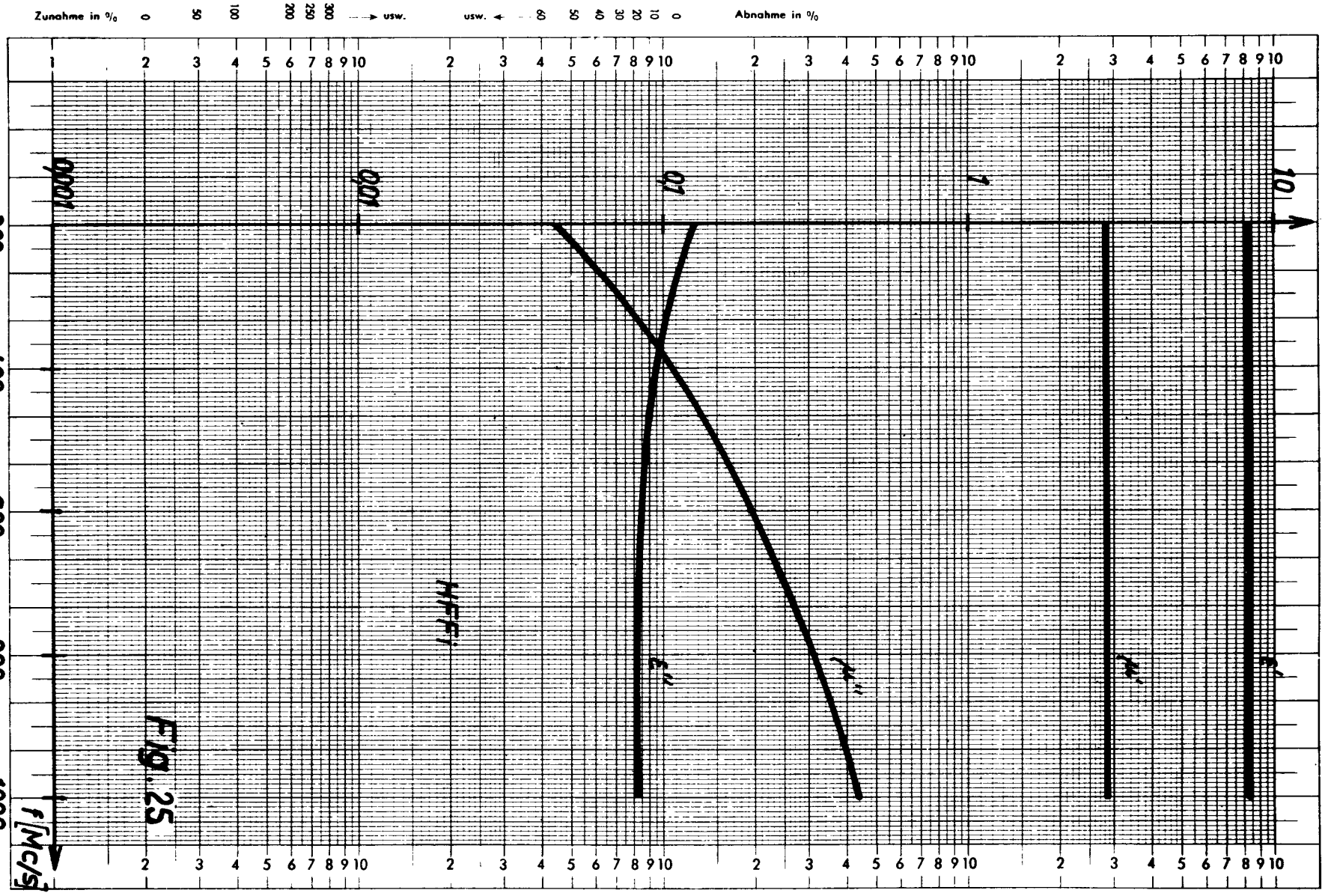

 Nr. 369½:6 P

Eine Achse logar. geteilt von 1 bis 10000, Einheit 62,5 mm, die andere in mm

melted paraffin (binding medium) was used. At warm temperatures this mixture could be formed to the desired shapes. Upon cooling the mixture has approximately the same rigidity as paraffin.

A test set-up was constructed for measuring the electric and magnetic characteristics of this material. The latter consists of a variable short circuit tuning stub, a test-sample line and a slotted line arrangement. The measuring equipment serves as a means of determining the following material constants:

$$\varepsilon_v', \varepsilon_v'' \qquad \text{with} \quad \tan\delta_\varepsilon = \frac{\varepsilon_v''}{\varepsilon_v'}$$

and (105)

$$\mu_v', \mu_v'' \qquad \text{with} \quad \tan\delta_\mu = \frac{\mu_v''}{\mu_v'}$$

Fig. 24 and 25 give the measured material constants of ferrite of type U 60 (Fig. 24) and HFFi (Fig. 25) from Siemens & Halske Company which were used in the construction of the improved shapes (Fig. 21). For measured data of other ferrite materials see [11] . The constants ε_r' and μ_r' remain approximately constant in the frequency range between 200 and 1000 mc/s. Whereas ε_r'' increases slightly with increasing frequency and μ_r'' increases rapidly with increasing frequency.

Fig. 26 shows the plaster molds used for forming the ferrite shapes.

Fig. 27 shows two finished ferrite shapes and one shape made out of polystyrol.

Fig. 28 shows a bottom view of a ferrite shape and Fig. 29 shows the latter with a spherical radiator in its center on the measuring plane.

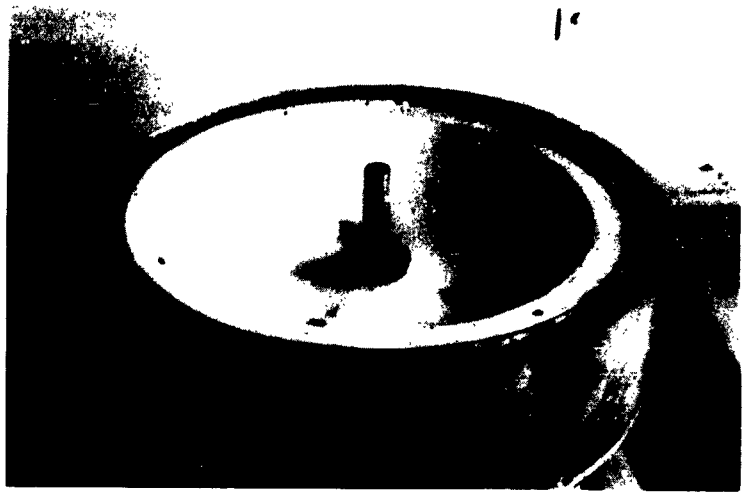

Fig. 26 a

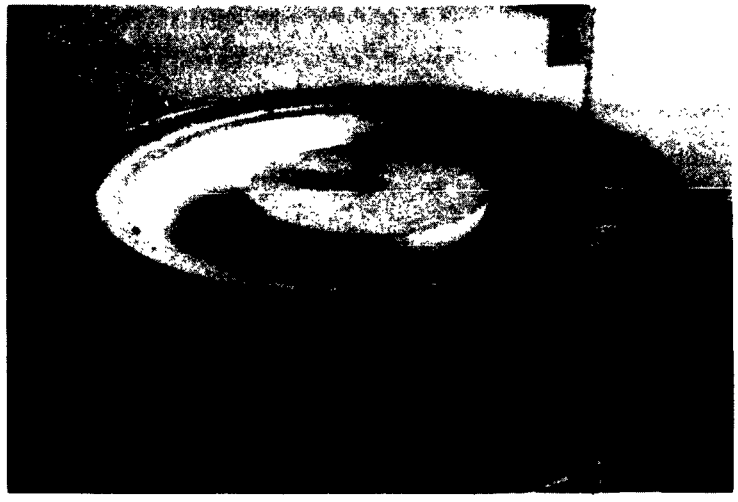

Fig. 26 b

Fig. 27

Fig. 28

Fig. 29

Calculation of the Feeding Point Impedance taking into consideration the electric and magnetic field losses.

The transformation of the known impedance at the field line $z = z_0$ (see Fig. 16 curve II) inwards towards the field line $z = z_d$ occurs according to:

$$\frac{d\underline{z}_1}{dz} = j\,\frac{2\pi}{\lambda^*}\cdot\frac{1}{\underline{z}_{L0}\sqrt{\frac{\mu_r}{\varepsilon_r}}}\left(\underline{z}_1^2 - \underline{r}_0\,\underline{z}_{L0}^2\,\frac{\mu_r}{\varepsilon_r}\right) \qquad (106)$$

with

$$\lambda^* = \frac{\lambda_0}{\sqrt{\varepsilon_r \mu_r}}$$

this corresponds to equation (70).

As was the case with the antenna in sect. VI, the resistive losses can be neglected since the outer surface of the radiator is silver plated. However the electric and magnetic field losses of the ferrite body itself are so large in the frequency range between 200 and 1000 mc/s that these must be included in the impedance calculation. Therefore a complex material constant is actually used.

$$\underline{\varepsilon}_r = \varepsilon_r' - j\,\varepsilon_r''$$
$$\underline{\mu}_r = \mu_r' - j\,\mu_r'' \qquad (107)$$

$\varepsilon_r', \varepsilon_r'', \mu_r', \mu_r''$ are obtained from Fig. 24 and 25. If equation (107) is inserted into equation (106) then a transformation equation for the inhomogeneous line with consideration of the electric and magnetic field losses is obtained. The impedance which is obtained in this manner is now transferred from the field line $z = z_1$ inward towards the feeding point $z = 0$ by using equation (103).

Curve I of Fig. 30 shows the calculated feeding point impedance of the antenna with ferrite U 60 ($\varepsilon' = 4.9$, $\mu' = 1.48$).

The latter is plotted on a Smith-chart for the frequency range between 200 and 1.00 mc/s. Curve II shows the measured values of the feeding point impedance of this antenna.

If the antenna height h is larger than $\lambda_0/20$ then the measured impedance values once again lie nearer the SWR = 1 circle than the calculated values, and can again be explained as being caused by the additional radiation due to the ferrite. However a second effect exists here:

The measured impedance of curve II in Fig. 30 shows an indentation with a small loop in the frequency range about 600 mc/s. Here the impedance lies very close to the SWR = 1 point. This loop is caused by a cavity-resonance of the W_1-wave within the ferrite body. The wavelength λ_{w1} of the W_1 wave within the ferrite body is smaller than its equivalent in air by the factor:

$$\frac{1}{\sqrt{\varepsilon_r \mu_r}}$$

The first resonance of the W_1-wave occurs in the frequency range about 600 mc/s where the electrical wavelength between z_1 and z_0 has the values $\lambda_{w1}/2$. The next resonance occurs at twice this frequency namely: 1.200 mc/s. In the impedance plot of curve II in Fig. 30 one can already notice the beginning of the second loop at 1.000 mc/s.

The exact transformation of the impedance Z from the outer field line $z = z_0$ inwards towards the field line z_d occurs according to the equation:

$$\frac{dZ}{dz} = j \frac{2\pi}{\lambda^*} \left[Z_{L0} \sqrt{\frac{\mu_r}{\varepsilon_r}} - Z_{L0} \sqrt{\frac{\mu_r}{\varepsilon_r}} \left(F_0 + \frac{1}{2} F_1 \frac{\omega_1}{\omega_0} + \dots \right) \right] \quad (108)$$

with

$$\lambda^* = \frac{\lambda_0}{\sqrt{\varepsilon_r \mu_r}}$$

This corresponds to equation (62).

In the vicinity of the cavity resonance of the W_1-wave, W_1/W_0 becomes very large and via the factor F_1 of equation(108) influences the impedance transformation dZ/dz of the W_0-wave. In the calculation of the impedance in accordance with equation (106) the factor $\frac{1}{2} \cdot F_1 \cdot \frac{W_1}{W_0}$ of equation (108) was not taken into consideration.

Therefore the calculated impedance depicted by curve I of Fig. 30 does not contain a loop.

In the impedance calculation a consideration of the W_1-wave is not possible since the magnitude of W_1/W_0 is not known. Whereas the impedance Z of the W_0 wave of a radiator in air can be determined via measurement and used for the impedance calculation of the W_0-wave of the ferrite antenna, this is not possible for the W_1 cavity resonance since the antenna surrounded with air does not possess such a cavity resonance.

The resonance behaviour of the W_1-wave in ferrite does not cause a change in the cosine shape of the directional pattern of the antenna as long as the geometric antenna height h is small compared to the wavelenght. If a different antenna pattern is desired then the geometrical height h must be in the order of λ_0 [12].

The cavity resonance can be considered as a transforming network in the inhomogeneous antenna line. Therefore it can be replaced by a suitably chosen four pole network which is inserted at the feeding point of the small antenna. As a result it can be realized that this phenomenon does not bring a real improvement of the antenna characteristics.

Figure 31 shows the ratio b_{rF}/b_{rA} of the relative bandwidth of an antenna imbedded in Ferrite U 60 to the relative bandwidth of the antenna in air. Curve I of Fig. 31 is that of the calculated impedance; curve II is a plot of the measured values. As a result of the additional radiation and the additional transformation effect of the cavity resonance at 600 mc/s, curve I lies above curve I.

The definition of the bandwidth is only plausible when the impedance plot does not contain loops. Therefore curve II is shown in broken line form above 450 mc/s.

Fig. 32 gives a plot of the feeding point impedance of an antenna with ferrite HFFi ($\varepsilon_r' = 8.25$, $\mu_r' = 2.82$) in the frequency range 200 to 1000 mc/s. Curve I shows the calculated values, curve II the measured values of the feeding point impedance of this antenna.

Curve II once again lies closer to the point SWR = 1 of the Smith-chart than does curve I. As a result of the large values of ε_r' and μ_r' the loop in the measured impedance plot already occurs at 350 mc/s. Curve I of Fig. 33 shows the ratio b_{rF}/b_{rA} using the calculated impedance values and curve II for the measured impedance values. Since the first loop already occurs at 350 mc/s, curve II is drawn in broken line form above 250 mc/s.

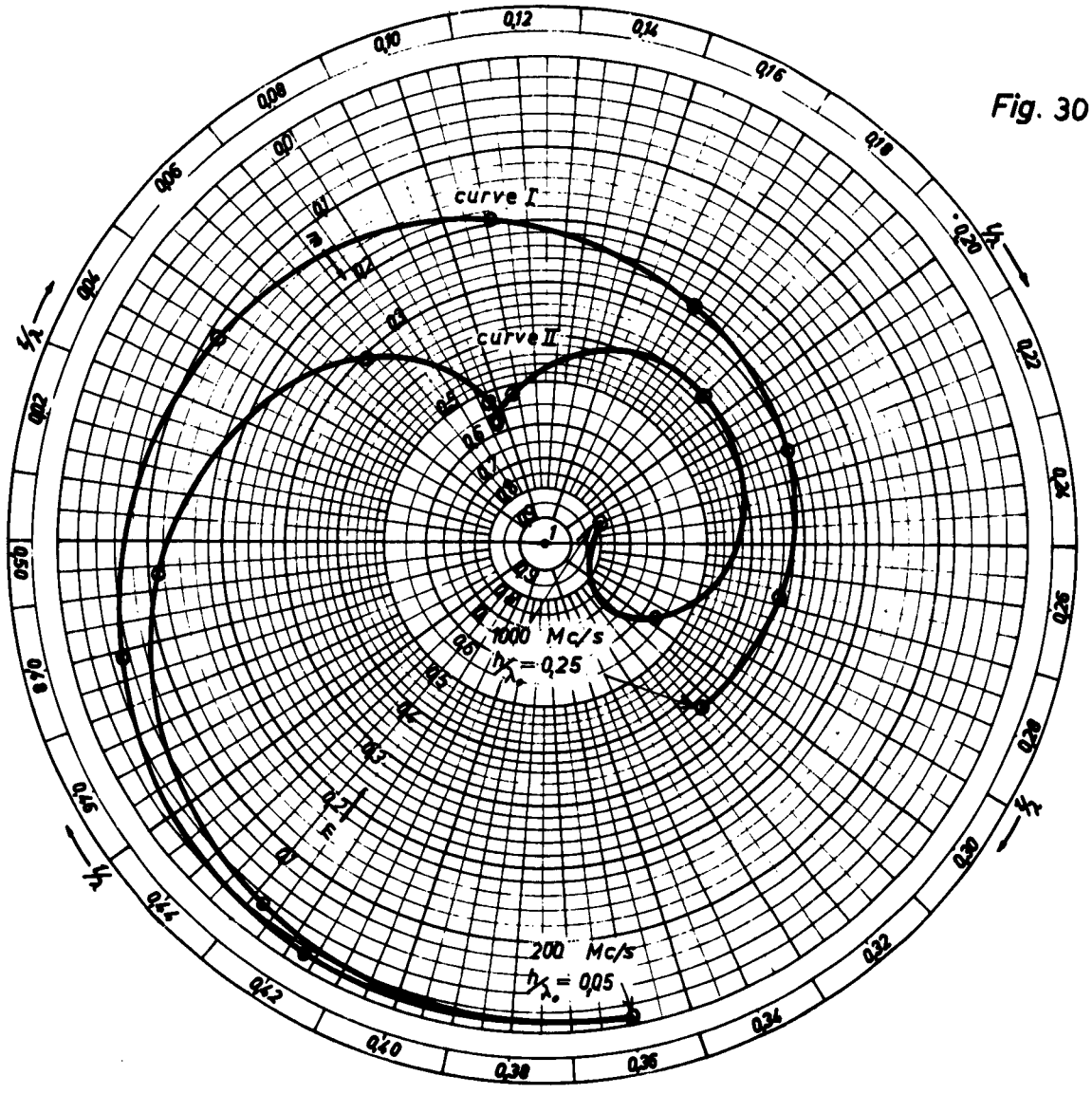

Fig. 30

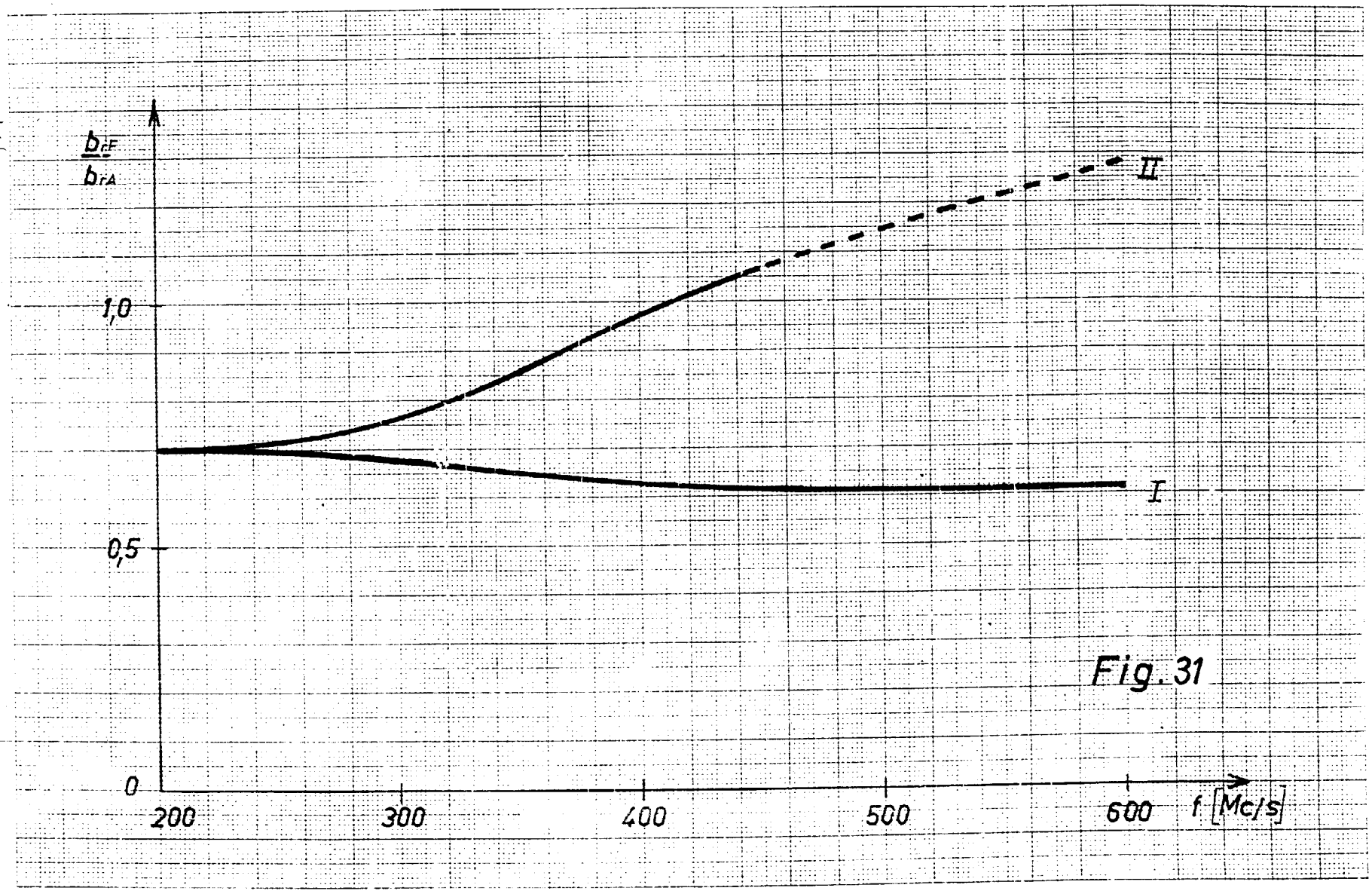

Fig. 31

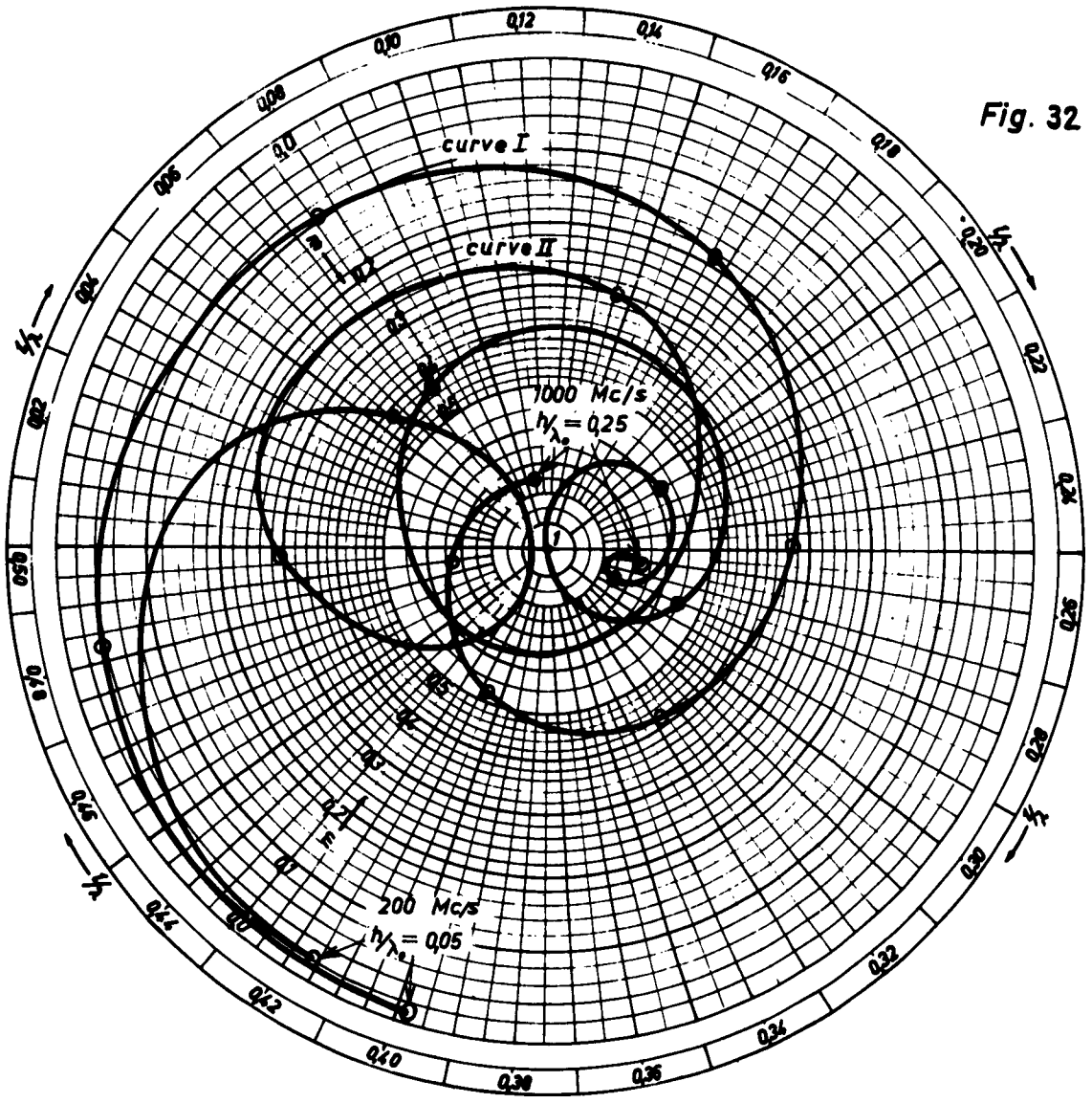

Fig. 32

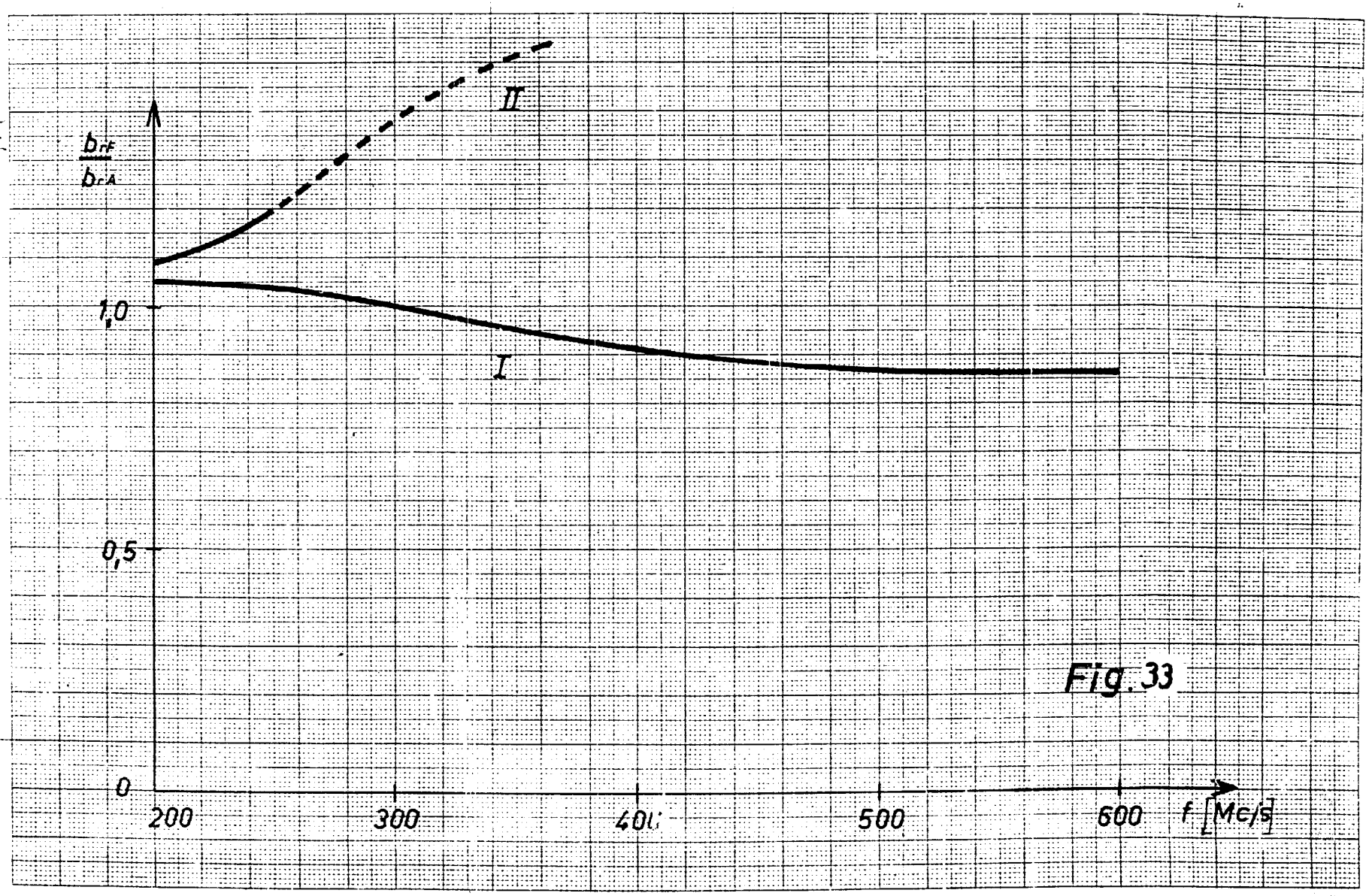

Fig. 33

Conclusions

As was shown in TR1 the practical use of a very short antenna is dependent on its bandwidth. Therefore if one wants to improve the characteristics of a very short antenna, a means must be found to increase its bandwidth. This could be possible by surrounding the radiator with dielectric material especially ferrite. First the radiator was surrounded with polystyrol and the effect of various geometric forms of the dielectric material upon the antenna behaviour was investigated. Theory and measured data has shown that a larger bandwidth is obtained when the dielectric begins at some distance away from the feeding point of the antenna than in the case of having the dielectric already begin at the feeding point. That portion of the dielectric which is in the vicinity of the feeding point of very short antennas can not bring an improvement in the radiation behaviour and thus does not result with an increase in the bandwidth. Rather, this region of the dielectric only causes an increase in the reactive power of the transmission line wave. This reactive power is undesirable since it causes a decrease in the bandwidth.

These results seem to indicate that a sphere totally filled with dielectric material may not be the most suitable shape for surrounding a dipole.

According to [13] and [14] a fundamental limit is imposed on the bandwidth of antennas by the impedance of the spherical wave function representing their radiated fields. A cosine form of the directional antenna pattern is obtained with very short antennas whose geometric height h is small compared to the wavelength regardless if the antenna is surrounded with ferrite or not. [12] Therefore only the lowest order dipole mode of these spherical wavefunctions appears. Then the impedance of the latter mode is the same for all very short antennas. Therefore a ferrite shell surrounding a very short antenna does not bring a real improvement in antenna behaviour; rather only a different transformation form of the antenna impedance results. Our impedance measurements indicate a cavity resonance of the W_1-

wave in the ferrite body. When a ferrite with very high μ_r is used, the cavity resonance is excited at very low frequencies. But this resonance does not constribute to radiation and thus has no bandwidth increasing effect because the air filled outer space region in immediate vicinity of the ferrite body can not support the W_1-wave in its propagating form. Only at very distant regions away from the antenna can W_1 again exist as a propagating wave in the air filled outer space. Thus this cavity resonance also has only a transforming effect. Since the antenna is very short all this transformations could also have been accomplished by inserting a suitable fourpole network in the feeding point of the antenna.

If the antenna is chosen to be larger than $\lambda_0/20$ then the ferrite material can also influence the impedance of the lowest order spherical wave function. This is especially true when the ferrite shell has approximately the same height as that of the antanna itself. As the antenna height is increased the wave function already has propagating wave characteristics in the air-filled outer space region near the ferrite body. Then additional radiation may be transmitted from the ferrite body into space. This additional radiation causes some enlargement of the antenna bandwidth.

Bibliography

[1] Ferromagnetic Antennas, R.New, American Electronic Lab.Inc. Colmar, Pennsylvania

[2] A Generalization of the Foster Reactance Theorem for arbitrary Impedances (Eine Verallgemeinerung des Fosterschen Reaktanztheorems auf beliebige Impedanzen), K.Fränz, Elektrische Nachrichtentechnik, Volume 20, 1943, page 113-115

[3] Research on Wideband Antenna Design, H.Meinke, Contract AF 61 (052)-41

[4] Electromagnetic Fields, E.Weber, Vol.I, page 204, New York 1950

[5] Application of Conformal Representations to Wave Fields, H.Meinke, Zeitschrift für angewandte Physik, Vol.1, (1949) pages 245-252, English translation by Liaison Office, Technical information Center, Wright-Patterson Air Force Base, Ohio under No. F-TS.9511/V

[6] A general Solution Method for Inhomogeneous Cylindrically symmetrical Wave Fields, H.Meinke, Zeitschrift für angewandte Physik, Vol.1, (1949), pages 509-516, English translation by Liaison Office, Technical information Center, Wright-Patterson Air Force Base, Ohio.

[7] The Behaviour of Electromagnetic Waves in strongly Inhomogeneous Line Components (Das Verhalten elektromagnetischer Wellen in stark inhomogenen Leitungsbauelementen), Zeitschrift für angewandte Physik, Vol.2, (1950), pages 473-478

[8] Cylinder-symmetrical Wide-band omnidirectional Radiator with High-pass Matching Characteristics (Zylindersymmetrischer Breitband Rundstrahler mit Hochpaß-Anpassung) H. Meinke, Nachrichtentechnische Zeitschrift, Vol.3, April 1960, pages 161-168

[9] Short unsymmetrical Antennas of high Efficiency and the Measurement of Antenna Efficiency, (Kurze unsymmetrische Antennen mit hohem Wirkungsgrad und die Messung des Antennenwirkungsgrades), Dissertation, Technische Hochschule, München, Institut für Hochfrequenztechnik.

[10] Contract AF 61 (052)-506
Research on Electrically Small Antennas
Technical Report No. 1 (28. Februar 1962)

[11] Contract AF 61 (052)-506
Research on Electrically Small Antennas
Technical Report No. 2 (30. November 1962)

[12] AEL Final Progress Report 1. May 1957 sect. IV B 4c
Contract No. DA - 36 - 039 SC - 73263

[13] SRI Project 2494 Technical Report 71 August 1960
AFCRL - TN - 60 - 997 sect. VB

[14] L.I. Chu : Physical limitations on Omni - Directional Antennas, I. Appl. Phys. 19, 12 (Dec. 1948)

Glossary of Symbols

A, B	Distortion factor of the coordinate system
b_r	Relative bandwidth
b_{rA}	Relative bandwidth of antenna in air
b_{rD}	Relative bandwidth of antenna in dielectric
b_{rF}	Relative bandwidth of antenna in Ferrite
β	Phase constant
C	Capacity
C^*	Capacity per unit length
C_A	Capacity of the antenna in air
C_D	Capacity of the antenna in dielectric
ε_o	Dielectric constant of free space
ε_r	Reltive dielectric constant
ε_r'	Real part of complex ε_r
ε_r''	Imaginary part of complex ε_r
E	Electric field intensity
f	Frequency
ΔF	Area element
F_n, G_n	Fourier coefficients
H	Magnetic field intensity
h	Geometrical height of the radiator
I	Current
I^*	Surface current density
K	Coupling factor
λ_o	Wavelength in air

λ_ε	Wavelength in dielectric medium
λ_0	Critical wavelength
λ^*	Wavelength in a dielectric medium with μ_r and ε_r
μ_0	Permeability of free space
μ_r	Relative permeability
μ_r'	Real part of complex μ_r
μ_r''	Imaginary part of complex μ_r
ω	Angular frequency
R_s	Radiation resistance
R_{sA}	Radiation resistance of antenna in air
R_{sD}	Radiation resistance of antenna in dielectric
R_v	Attenuation resistance
r	Radius
$\text{tg}\,\delta_\varepsilon$	Dielectric loss factor
$\text{tg}\,\delta_\mu$	Loss factor of the magnetic field
U	Voltage
W	Complex wace function
X	Antenna resistance
Δx	Coordinate difference
Δx^*	Geometrical difference between adjacent coordinate lines
Z	Impedance
Z_{Lo}	Characteristic impedance of feeding line with air
Z_L	Characteristic impedance of feeding line with dielectric
z_o	Coordinate of the outer boundary of dielectric medium
z_d	Coordinate of the inner boundary of dielectric medium
Z_A	Impedance of antenna in air
Z_D	Impedance of antenna in dielectric

List of Illustrations

Part 2: Folded dipole antenna with tunneldiode

Part 2: Folded dipole antenna with tunnel diode

Abstract:

This report deals with the effects of a combination consisting of an antenna and tunnel diodes. This is a first report explaining some fundamental rules in respect to the application of tunnel diodes with antennas; also the corresponding impedance measurement techniques are described. Part I of this treatment is primarily concerned with the stability problems involved in avoiding self-excitation phenomena within the system. Part II discusses the basic questions concerning the measurement of input impedance.

A folded unipole with a tunnel diode at the top of the radiator is studied experimentally as an example. The measurement of impedances with negative resistances by using slotted line techniques is also described. The next report will treat such combinations which are of technical interest.

I. Stability of Antenna Systems containing Tunnel Diodes

A. Negative Resistance Applications

The generation of a negative resistance, which is achieved either through an active four-terminal network with regenerative feedback or by using the mixing principles of a nonlinear reactance, requires a relatively large number of circuit components. However the tunnel diode offers a negative resistance in the form of a single component and its application requirements as a circuit element are the same as those of a positive resistance with the exception of the following three points:

a) The tunnel diode requires a bias voltage (approx. 120 mV).

b) Its regulation range is limited to a maximum of 10-20 mV caused by the descending portion of its characteristic curve.

c) The insertion of a negative resistance introduces the possibility of self-excitation of the network; in many cases this is undesirable.

Taking the requirements listed above into consideration, the TD can be used as a negative resistance element up to an upper frequency limit "f_c" which is also the case for positive resistances and has the same cause, namely: the reactive behaviour of the conductor material. (The theoretical semiconductor effect of the TD is independent of frequency up to 10^{13} cps).

The simple use of this circuit element thus provide additional degree of freedom as far as the design of the electrical networks is concerned, since the positive resistances and conductances, or the real part of impedances and admittances can be compensated for by the size of "R_n". In this respect, two application goals can be set for the use of negative resistance (excluding for the moment the use as

a self-oscillating device) and are listed below:

a) Deatenuation of a load, thus achieving an amplification effect.

b) Application of negative resistances for obtaining special impedance and admittance functions, expecially those functions having characteristic curves turning in a counter clockwise direction (influencing characteristic curves turning in a clockwise direction in respect to a wide band compensation). Amplification effect through the negative resistance in this case, is considered of no value.

   A self excitation of this current loop would disturb the operating conditions and must thus be completely avoided.

B. Network Stability

Before Networks are calculated it is normally assumed that their electrical behaviour is such that may transient excitations are of a decaying nature and after a short period of time a steady state is achieved in which the voltages and currents are then only influenced by the induced signal of the connected generators. This assumption is valid for each case of passive networks and thus need not be investigated for each individual case.

However this assumption does not necessary apply when the network contains active fourpoles with regenerative feedback and / or negative resistances. Therefore it cannot be assured that the methodes of network analysis, the complex calculation and the characteristic curve rules all fulfill the requirements for such a system. In most cases the transient oscillations of circuits incorporating negative resistances do not decay with time, rather they increase, and as a result of the non-linear limitation effects either a standing oscillation will appear or a pure exponential current increase prevents an adjustment of the operating point of the negative resistance element.

Therefore it becomes extremely desirable to associate a stability check in conjunction with the calculation of such circuits or to check the stability of an existing circuit by means of measurement. In addition it would be quite advantageous if a circuit which has been proven to be instable could be stabilized by using a suitable arrangement which does not disturb the initially preset and required circuit functions.

Both of the above mentioned problems will be treated seperately in the following text: First of all the problem of a general stability criterium check will be treated in section C - F. The stability-criterium, which is actually suitable for practical checks, is expressed at the end fo section F. Circuit recommendations which have some chance of being stable are given in section H. However in case the practical applications of them should prove to be instable outside of the operating frequency range due to stray circuit elements which are too difficult for theoretical consideration, these circuits can be restrained from self-oscillation by means of inserting a Two-Pole-Stabilizer (Section H).

C. Practical Requirements for a Stability Check

Basically it is always possible to investigate the dynamic behaviour of a circuit via a system of differential equations when the network structure and size of the individual circuit components is completely known. The transients (general solution of the homogeneous diff. eq.) as well as these currents and voltages which are caused by the connected generator (special solution of the inhomogeneous diff. eq.) by means of the complex calculation can be calculated from these diff. eqn.

The transients of interest can hardly be calculated in practice for the following two strong reasons:

1. If the network contains more than two reactive components then the solution for the characteristic equation of the n^{th} order is difficult and hardly possible in practice

2. The exact network structure nor the size of the individual components are actually unknown even for what appears to be a simple example. Experience has shown that even stray- and couple-reactances in the order of magnitude less than 1 nH and 1 pF respecively may not be neglected if the stability criterium of wide-band negative resistance circuits is to be investigated.

In respect to the first above mentioned difficulty, a way out can be found even for n^{th}-term networks in that one abandons the search for an explicit solution of the n-solutions of the characteristic equations, and rather determines if by means of a simple relationship of the function theory, whether the characteristic equation contains at least one solution (Eigen frequency) with a positive real part (an unlimited increasing transient oscillation).

This method (encircling criterium of F.Strecker [1] [2]) will be described only in short in the following since it has practically no meaning in respect to the second diffulty mentioned previously. However this method is of some value for the derivation of the suggested method of determining stability as will be shown in the following.

If the two previously mentioned difficulties are compared with one another then one comes to the conclusion that a practical and meaningful stability check definitely requires measurement of the network behaviour and network funcions. The measurements must be conducted so completely and with such a high degree of accuracy, that the above mentioned parasitic elements (1 nH, 1 pF) can be readily pinpointed in the measurement data.

These requirements are fulfilled by the impedance and admittance-functions; in reciprocal circuits these functions are superior to transformation functions due to the former's clarity in respect to their universally accepted definition as well as their reliable practical measurement. Since the

especially
ideas developed here have been developed for the use of negative resistances in linear networks, reciprocity exists without a doubt. If on the other hand one is concerned with a network in which active, non-reciprocal fourpoles are considered, then the transformation functions are incorporated as checking functions (for example the Nyauist Criterium).

The preferred functions mentioned above can be found as measured characteristic impedance- or admittance curves. In addition such curves of a practical and realizable network have a desirable advantage in that they can be constructed with great ease in the complex plane. However along with this advantage exists the fact that the characteristic curve which was found by measurement only within a limited frequency range for a network which is not completely known, can be extended for very high and very low frequencies via graphical construction since this curve is always dependent upon the driving function of the circuit element which is directly connected to the measurement terminals.

D The Encircling Criterium of Strecker

The train of thought presented in this section is concerned with a pure analytical search for the Eigen values of a complicated differential equation or of a system of coupled differential equations; however they form the basis for the following relationship between the characteristic curves of the impedance- and conductance- functions and the increasing or decaying transients of the network.

It should be noted that a stability test, no matter in which manner it is accomplished, must pertain to the completely closed network, and not only to that current loop which encompasses the negative resistance. For example, if one wishes to insert a TD into an antenna, then the network consists of: the antenna with the surrounding region and the receiver input impedance. If the latter were to be changed slightly (for example approx. 20%) the condition of matching would hardly be

altered. However as far as the stability investigation is concerned, a completely different network now exists and can for example become unstable resulting from the alteration. This critical operation behaviour of circuits containing negative resistances rests upon the fact that the desirable effect, as for example deattenuation, obtained by inserting a negative resistance, forces a circuit design which is already very close to the stability margin.

The transients (current time functions) of a purposely chosen simple example as in Fig.1 will be investigated via a system of differential equations. The following solution form is anticipated:

$$i_1 = I_{o1} e^{p_{o1} t} + I_{o2} e^{p_{o2} t} + \cdots\cdots$$

$(p_{o\mu} = \sigma_\mu + j\omega_\mu)$

This means that each mesh current: i_1, i_2 etc. consists of a sum of time-dependent current components the number of which is the same as the number of independent energy storage components within the network. As far as the stability consideration is concerned only the time dependencies are of interest, therefore only the Eigen frequencies or transient characteristics: p_{o1}, p_{o2} etc.; the initial amplitudes: I_{o1} etc. are not of interest.

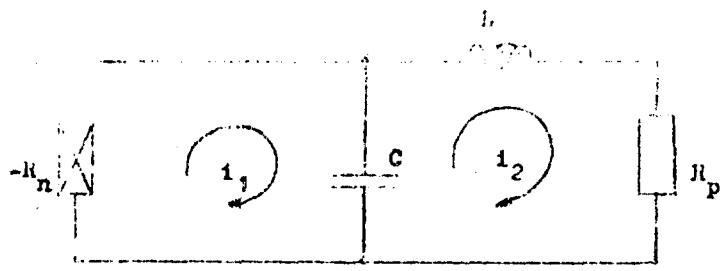

Fig.1

Example for a simple circuit including a negative resistor.

If the voltage drops are summed for the mesh currents in the clockwise direction the following is obtained:

$$\text{Mesh 1}: \quad i_1(-R_n) + \frac{1}{C}\int i_1 dt - \frac{1}{C}\int i_2 dt = 0$$

$$\text{Mesh 2}: \quad -\frac{1}{C}\int i_1 dt + \frac{1}{C}\int i_2 dt + L\frac{di_2}{dt} + i_2 R_p = 0$$

After the substitution: $i_1 = I_1 e^{p_o t}$ $i_2 = I_2 e^{p_o t}$ has been made in the equations and the latter divided through the function: $e^{p_o t}$

$$\text{Mesh 1}: \quad I_1\left(-R_n + \frac{1}{p_o C}\right) + I_2\left(-\frac{1}{p_o C}\right) = 0$$

$$\text{Mesh 2}: \quad I_1\left(-\frac{1}{p_o C}\right) + I_2\left(\frac{1}{p_o C} + p_o L + R_p\right) = 0$$

In this manner the system of homogeneous diff. eqn. is transposed to a system of algebraic equations in which p_o and the currents are unknown. The resulting equation system is one in which zero is the value to the right of the equal sign; since I_1 and I_2 should not be zero, these equations are only satisfied when the determinent of the coefficient-matrix disappears, then:

$$\Delta = \begin{vmatrix} -R_n + \frac{1}{p_o C} & -\frac{1}{p_o C} \\ \frac{1}{p_o C} & \frac{1}{p_o C} + p_o L + R_p \end{vmatrix} = 0 \qquad (1)$$

or

$$\Delta = p_o^2 R_n LC - p_o(L - R_n R_p C) - (R_p - R_n) = 0 \qquad (2)$$

The relation ship (2), is the determing equation for the n-Eigen frequencies p_{o1}, p_{o2}, $p_{o,u}$ etc. and will be called the characteristic equation. In respect to the above example a second order polynomial is obtained and only two solutions: Eigen frequencies p_{o1} and p_{o2} exist for which the polynomial can have the value zero, and pertain then only to two energy storage devices in the network.

The method of transposing the system of coupled diff. equations to a system of algebraic equations instead of setting up the characteristic equa. in the usual manner has been done intentionally here in order to be able to make use of the matrix order scheme. In this manner multi-termed networks can be investigated in a digestible manner, for example by using the many transformation rules for equivalent matrixes thus considerably simplyfying the calculation procedure for the determinent. In addition some general pure algebraic stability test methods exist, which rest upon the coefficient matrix set up in (1) (for example the determinent criterium of Hurwitz [3]). Also it is common practice to obtain the derivation of impedance and conductance functions from such mesh equations or matrixes, and in this manner the relationship between the characteristic equation and the network functions (impedance, conductance, transformation values) can be written. For an n^{th} term network a polynomial of the n^{th}-order is obtained as the characteristic equation:

$$a_n p_o^n + a_{n-1} p_o^{n-1} + \cdots\cdots a_1 p_o + a_o = 0 \qquad (3)$$

and it is now not possible to calculate explicitly the n-solutions which are the n-Eigen frequency values.

This difficulty can be bypassed in the following manner:

Actually it is not required that the numerical value of each Eigen frequency:

be known, since we are only interested in determining, if the network is stable or not and it seems to be unimportant to know exactly in what respect the corresponding network is unstable. This means that it is not required to know the exact time function with which a transient decays or increases in amplitude. Therefore it is sufficient to know, if any one of the n-solutions "p_{ou}" of the characteristic equation poses a positive real part "σ_{ou}". If this condition does exist, then the current component: $I_{ou}e^{\sigma_{ou}t}$ climbs above all limits with increasing time: however the other current components which have a negative real part in the exponent decrease towards zero with increasing time "t".

Accordingly, the initial current amplitudes "I_{ou}" are also unimportant and need not be determined here; they could have an arbitrary small value for example: they could describe the noise amplitude of the circuit component itself. The exponential increase as a function of time in reallity determines the dynamic behaviour of the circuit. It can occur that the initial transients may develop into a steady state oscillation (see Fig. 8) resulting from the non-linear behaviour of the circuit component, usually of the negative resistance itself.

In order to answer the decisive question above: "Does the characteristic equation have at least one solution with a positive real part?" The following treatment is made: The variable "$j\omega$" of the polynomial (3) is substituted by a general complex number "p" and the following characteristic function is obtained:

$$a_n p^n + a_{n-1}p^{n-1} + \cdots + a_1 p + a_o = F \qquad (4)$$

This polynomial is now considered as the transformation function transforming from the complex p-plane to the complex F-plane. Actually only the imaginary axis of the p-plane is to be transformed, thus:

$$a_n(j\omega)^n + a_{n-1}(j\omega)^{n-1} + \cdots + a_1 j\omega + a_o = F \qquad (5)$$

and a definite curve is obtained in the F-plane (see Fig. 3). Theoretically the polynomial in (5) can be decomposed to the following factors:

$$(j\omega - p_{o1})(j\omega - p_{o2}) \cdots\cdots (j\omega - p_{on}) = (F - 0) \qquad (6)$$

Each of the linear factors $(j\omega - p_{ou})$ corresponds to a vector in the p-plane which is to be considered as existing between the Eigen value p_{ou} to the movable point $j\omega$ on the imaginery axis (see fig.2). If the network is stable, which means that all Eigen frequencies lie on the left side of the p-plane, then each vector rotates about the angle $+\pi$ as ω takes on all the values between $-\infty$ and $+\infty$ in this order. The rotation angle of all the n linear factors on the left side of equation (6) must however be equal to the rotational angle of the $(F-0)$-vector on the right side of the equation.

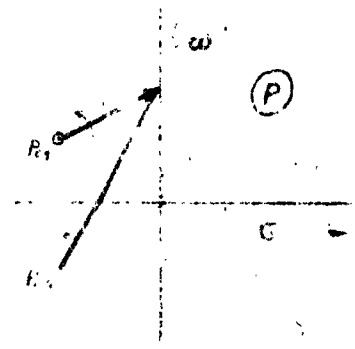

Fig.2
Zeros in the p - plane.

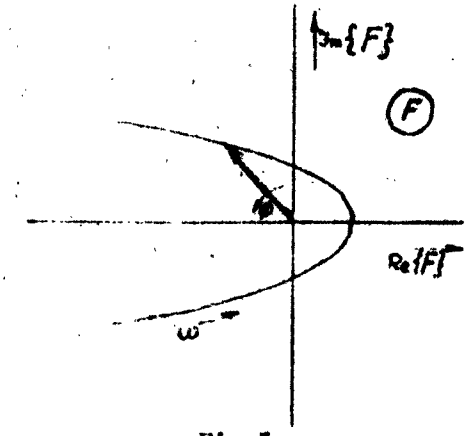

Fig.3
The plotted curve of the aiding F - Funktion.

However the actual position of the Eigen values are not known in the p-plane but the transformation of the imaginary axis of the p-plane into the curve $F(\omega)$ is available by equation (5). However since the order of the polynomial is specified by (6) and therefore also the number of the possible Eigen frequencies, or linear factors of the separation as in (6) it can now be

said: A vecotr (F-0) which exists between the origin of the F-plane to the points on the curve $F(\omega)$, will rotate about the origin with the angle $\beta = +n\cdot\pi$ if the circuit is stable, which means that all the Eigen frequencies have negative real parts (see fig.2 + 3 for n=2). However if instability exists, which means that at least one Eigen value is located in the right side of the p-plane, then one of the n possible vectors does not exist in the left side of the p-plane; thus its corresponding rotation factor $+\pi$ is missing and the rotation factor $-\pi$ of the corresponding vector causes its appearance in the right side of the p-plane (see fig.4).

Thus a single Eigen frequency having a positive real part prevents the maximum possible rotation angle of the (F-0)-vecotr $\beta_{max} = n\cdot\pi$ by the factor 2.

Therefore the results yield:

$$\begin{aligned} &\text{the circuit is stable for } \beta = n\pi \\ &\text{the circuit is unstable for } \beta < n\pi \end{aligned} \qquad (7)$$

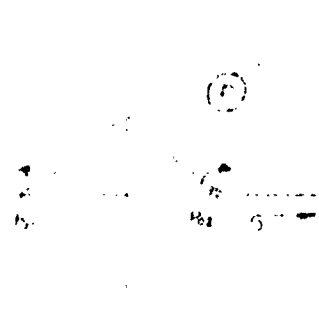

Fig.4
Zeros in the p-Plane

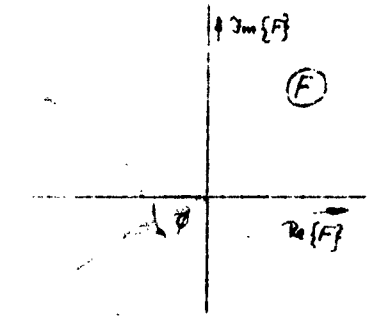

Fig.5
The plotted curve of aiding F - Funktion.

In conclusion it should once again be noted that these stability checking procedures may only then be applied when the network structure is known. The characteristic curves which are depicted in fig. 3 + 5 describe an aiding function: $F(\omega)$, which has no meaning other than being an helping function and also can not be determined by circuit measurement.

E. The Relationship between the Characteristic Equation and the Impedance or Conductance Functions of a Network

In the following it will be shown that the characteristic equation (5) is contained in each impedance and conductance function. In addition the limitations in unsing the characteristic curves of such functions in respect to the stability check, which was developed in the preceding section, will be shown.

First of all a simple network as in Fig.6 will be investigated in order to determine the relationship between the Eigen frequencies of a network and the respective impedance or conductance functions. The network of fig.6 contains a lossless parallel resonance circuit. If in the following relationship:

$$i = u \cdot Y_b \quad *)$$

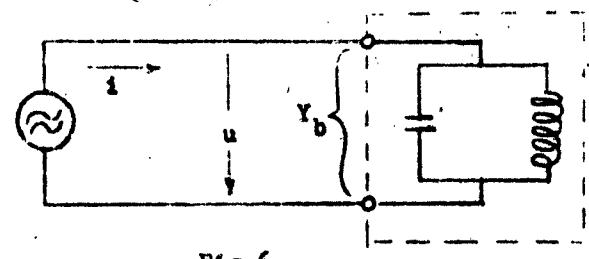

Fig.6

Example for a circuit having zeros only

a finite voltage exists at the network terminals even for an infinitely small current "i" (open ckt. terminals) then $Y_b = 0$. For the above example this condition can easily be visualized: For the Eigen frequency ω_0 a voltage can exist at the terminals of a lossless tank circuit without requiring that a current be induced into the network from without. This means that the Eigen frequencies of the network are obtained from the requirement: $Y_b = 0$. For the above example the following is valid:

$$Y_b = pC + \frac{1}{pL} = \frac{p^2LC + 1}{pL}$$

and from $Y_b = 0$ or $p^2Lc + 1 = 0$ the following is obtained:

*) the subscript "b" means that the corresponding conductance pertains to a branch of the network.

$p_o = \delta_o + j\omega_o = \frac{1}{\sqrt{LC}}$ and $\omega_o = \frac{1}{\sqrt{LC}}$

(for a lossless tank circuit: $\delta_o = 0$)

Each impedance, conductance and transformation function consists of ratio of two polynomials when considered analytically:

$$Y_b = \frac{a_n p^n + a_{n-1} p^{n-1} + \cdots\cdots a_1 p + a_o}{b_m p^m + b_{m-1} p^{m-1} + \cdots\cdots b_1 p + b_o} \qquad (9)$$

Therefore, if the Eigen frequencies can be calculated from the requirement: $Y_b = 0$, then the nummerator polynomial in (9) must be identical to the characteristic equation (3) of the circuit, as compared to the previous section where they were obtained from a system of differential equations. (For an impedance function "Z_b", the polynomial of interest is found in the denominator.) In this respect it is unimportant as to which terminals the conductance function (9) pertains since the nummerator is identical for all Y_b found in the network. Therefore when the impedance or conductance function can be presented in algebraic form as in equation (9), the characteristic equation can be recognized allowing for the use of the encircling criterium of(7).

Setting up the analytical conductance function is somewhat simplified by means of a continued fraction corresponding to an arbitrary network branch as compared to setting up the system of coupled differential equations and calculating the determinent of the coefficient matrix.

Before the encircling criterium can be applied in a merely traphical manner to characteristic curves, (actually this goal is the only one of practical interest) the meaning of the denominator polynomial of equation (9) should be given:

If a finite current is measured at the terminals of fig.7 even though the voltage is infinitely small in amplitude (input terminals of fig.7 short circuited) then in the relationship: $i = u \cdot Y_b$ of the conductance Y_b must have the value ∞ , or the denominator polynomial of equation (9) must become zero. The

Eigen frequencies are obtained from this relationship of the network which is altered in such manner: The denominator polynomial of a conductance function Y_b (or the numerator polynomial of a impedance function Z_b) is the characteristic equation for the network which is short circuited at its terminals (for Y_b or Z_b).

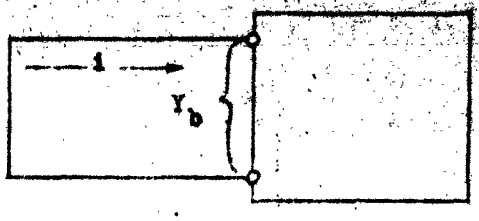

Fig.7
Example for a circuit having poles .

In order to make use of the previously mentioned stability check, the degree of the numerator polynomial must be known; this knowledge cannot be obtained from the shape of the characteristic curve. However it is known that for all the impedance, conductance and transformation functions, the numerator and denominator polynomial differ at the most by one degree , which means that they differ from one another by at most one Eigen frequency or one vector in the p-plane (see fig.2 + 4). This relationship is independent of the number of the reactance components which the network contains, thus independent of the magnitude of "m" and "n" in equation (9).

Previously it has been mentioned that the complete rotation angle of the function (3) or (4) is n $\cdot\pi$ when the variable ω passes through the values from $-\infty$ to $+\infty$ and the network is stable, which means that all the Eigen values lie in left side of the p-plane. However due to the fact that $\frac{1}{e^{j\phi}} = e^{-j\phi}$ the rotation portion of the denominator polynomial has the opposite sign as compared to the numerator polynomial and since the two polynomials can only differ in their degree by the value of one, the complete rotation of a (Y_b-0)-vector can only have the following values: $\phi = -\pi$, $\phi = 0$, or $\phi = +\pi$.

Fig.(8) shows these three possible cases; they differ from one another in that either the dregree of the numerator or denominator polynomial is larger or both have the same magnitude. The circuit differs in that the network structure directly behind

the terminals differs and the corresponding characteristic curves differ in their end points for the frequency $\omega = \pm\infty$.

At this point a limitation must be made: the example of fig.6c which is a conductance function having a higher degree in the denominator polynomial, is to be excluded in the following considerations. This particular starts with a series component whereas the conductances Y_b, which are to be considered here, are always to be measured parallel to branch. This limitation is not serious since the characteristic Y_b-curves, which serve for determining circuit stability, may correspond to any arbitrarily chosen terminal pair up to this point. Also for networks in which the structure is not completely known, a terminal can certainly be found at which a branch, namely an arbitrary parallel component as for example a parallel capacitance, exists.

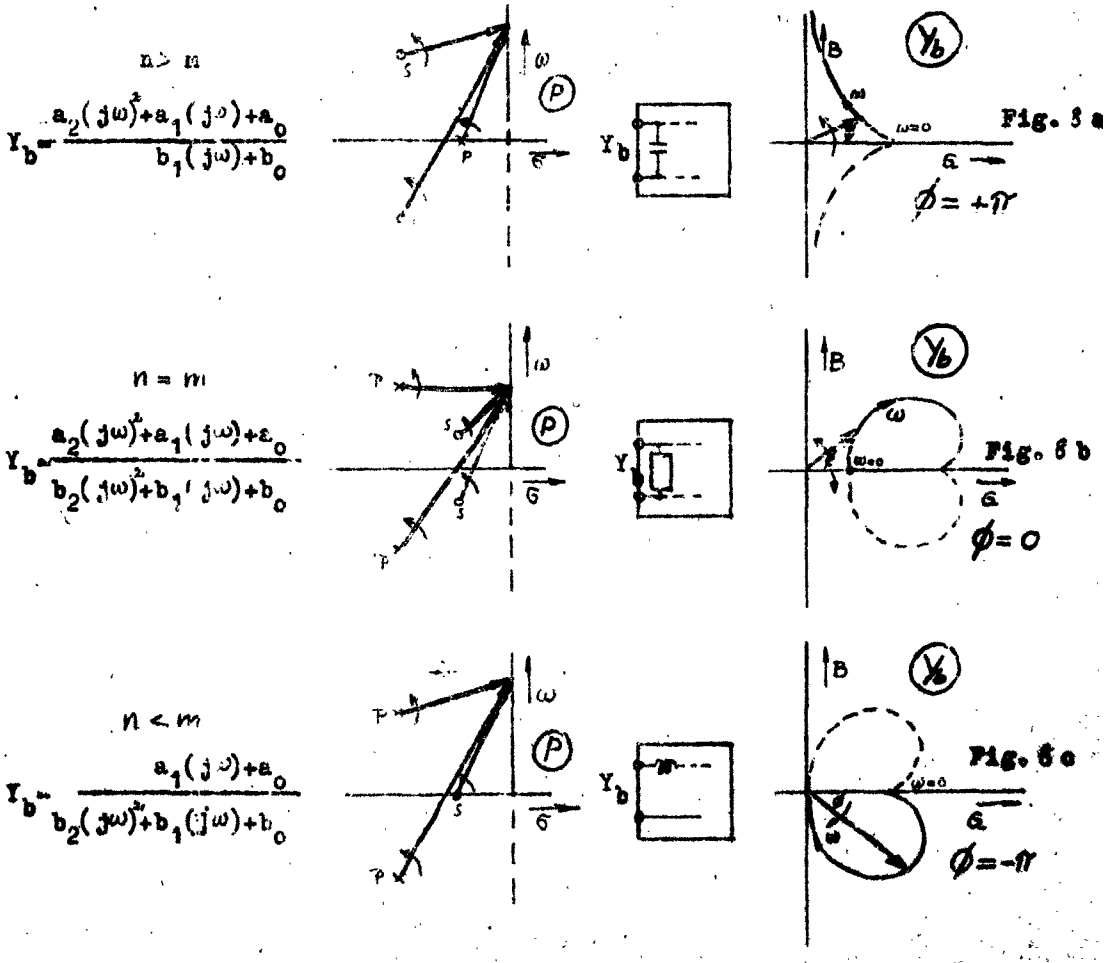

Fig.6 : Poles and zeros of a network with the corresponding admittance curves.

Therefore it can be said that the (Y_z-0)-vectot which is to be considered as existing between the origin and a movable point on the Y_b-curve, can only rotate by the angle $\phi = +\pi$ or $\phi = 0$ if the network (see fig.8) is stable, as the vector point passes along the characteristic curve for all frequencies $\omega = -\infty$ to $\omega = +\infty$ in this order.

Now is to be assumed that the network is unstable; thus the numerator of the Y_z-function possesses at least one zero in the right side of the p-plane whereas the denominator has only Eigen values (for the present consideration) in the left side of the p-plane as depicted by fig.9a + 9b. Since the vector in the right side of the p-plane gives a negative rotation component, the rotation angle sum of the passive conductance function given above, cannot be maintained. The angle ϕ of fig.9 attains the values: $\phi = -\pi$ or $\phi = -2\pi$ even for a single increasing Eigen frequency these values cannot exist for any branch-conductance Y_b of a stable network (fig.8).

$$Y_b = \frac{a_2(j\omega)^2 + a_1(j\omega) + a_o}{b_1(j\omega) + b_o}$$

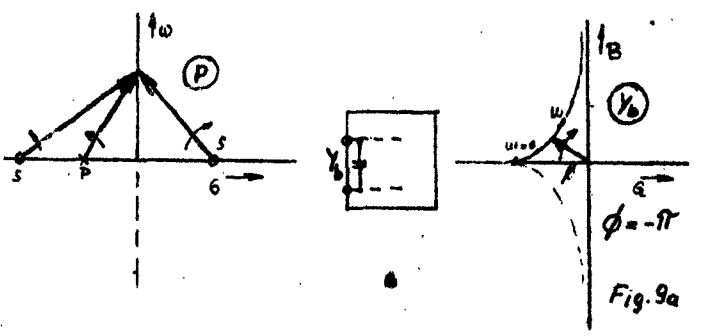

$$Y_b = \frac{a_2(j\omega)^2 + a_1(j\omega) + a_o}{b_2(j\omega)^2 + b_1(j\omega) + b_o}$$

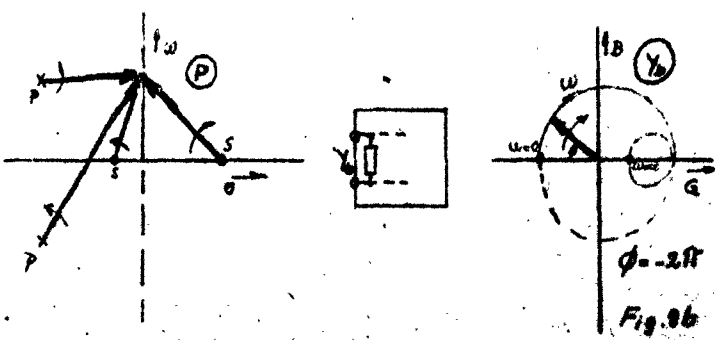

Fig.9 : Poles and zeros of a network with the corresponding admittance curves.

For the direct requirement for fig.9, namely that the circuit is stable for the condition of short circuit at the terminals of Y_b, the stability criterium can be stated in the following manner: The network is stable, if the rotation angle of the vector which is pictured as existing between the origin and an arbitrary point on the characteristic curve of an arbitrary branch conductance Y_b is not negative.

At this point it seems that an objection can be made; namely: What significance does the stability criterium have when it also requires the experimental determination of a specific stability (with short circuited terminals)? It should be reminded here that the purpose of the stability check is not only one of determining whether the particular network in question is stable, (this could also be determined via experiment) rather the principal purpose of this method seems to be the determination of definite arrangements which allow for stabilizing the network.

Since the choice of the measurement terminals is completely free for the above mentioned criterium, and no requirements of the network (for example concerning the number of the negative resistances contained therein have not been set,) it seems theoretically possible, that a terminal pair exists at which first: a short circuit does not cause instability, and second: the measurement equipment does not effect this condition (as could be caused by the imput impedance of the measurement equipment) since the measurement at an oscillating network cannot yield data which can be evaluated. Later, this general but insufficient formulation of a stability criterium will once again be referred to but dropped for the present, since the required limitations mentioned previously in this respect cannot be guaranteed when an absolutely reliable stability test is to be accomplished for a complicated circuit.

Since experience has shown, that an unstable network remains unstable for most cases even when a network branch is short circuited (normally very few branches of the network are readily available for measurement) an impedance or conductance function cannot enable a clear stability examination when these general requirements are considered.

The reason for the above statement can be obtained from the following train of thought: If the denominator of example in fig.9 had also had an Eigen value in the right side of the p-plane (unstable under the conditions of short circuited terminal pair) then the negative rotation component of the numerator polynomial would have been compensated by the corresponding component of the denominator polynomial, and the rotation angle check of the Y_b-function would have given the same result as the case for a stable circuit (fig.8).

Therefore it is quite clear that the previously developed rotation-angle-check is insuffiecient for such cases. Certainly the investigation via measurement of such network is also fruitless since, as has already previously been mentioned, the measurement of an oscillating network is of no value. However if the characteristic curve of such a circuit had been constructed in the resistance or conductance plane, then the instability could have been predicted by means of analizing the behaviour of such unusual characteristic curves. For example: if the characteristic completely remains in the right side of plane and contains only counter clockwise turning curvatures. Also the correlation of specific regions in respect to their boundary curves as obtained from conformal mapping principles can successfully lead to determination of an instability in that one determines whether the origin of the Y_b plane can be mapped into the region of the p-plane having $\sigma > 0$. Additional criterions of this nature is being intentionally ommitted here since a desirable system in this respect could not be obtained as of yet and the majority of such criterions only lead to an instability statement; however no difinite conclusion is reached as to the stability.

F Possibilities for a Clear Stability Determination

From the considerations developed in the preceding section and especially from the determination of the influence of the denominator polynomial, the following two restricted assumptions which allow for a clear and meaningful stability check via measured

or constructed impedance or admittance curves, appear to be necessary:

- The circuit contains only one negative resistance.
- The measured or geometrically constructed characteristic curves, which are used for the stability check, refer to those circuit terminals, between which the negative resistance has been inserted, (therefore no longer in an arbitrary network branch).

In this manner it is guaranteed that the denominator polynomial of the test-function Y_b can never have Eigen values in the right side of the p-plane, since the network which is short circuited at those terminals is definitely passive. The only existing negative resistance would have no effect due to the short circuit, and the statements made for fig.8 for a stable circuit in respect to the rotation angle of the (Y_b-0)-vector or the given values pertaining to an unstable circuit for fig.9 are valid. The associated requirement, that the test function must pertain to a branch of the network (in contrast to a terminal pair which would exist due to a junction separation) is without doubt fulfilled by the above requirement No.2 and retained herein.

One can summarize in the following manner:
One considers that a vector exists between the origin to the locus of the $Y_b(\omega)$ function (either measured values or geometrical construction for the only network terminals, which contain the negative resistance), when the circuit is then stable, when this vector does undergo a clockwise rotation; thus the rotation angle ϕ either has the value 0 or $+\pi$.

(For the sake of clarity, these investigations were carried through only for branch-conductance values. The same test criteriums are also valid for a branch bisection impedance (impedance between the two resulting terminals obtained by opening a network branch): thus the branch containing the negative resistance must be opened and the impedance at the two resulting new terminals must be measured. Due to the desire of obtaining practical and

and conventional measurement techniques, this test function is somewhat unsuitable. When branch-impedances $Z_b = \frac{1}{Y_b}$ are used then the sign of the given angle value changes .

Before the practical significance of the limiting assumptions is to be discussed, the above mentioned stability criterium should be transformed to a suitable form. Since the characteristic curves which are to be evaluated, exist in an unusally large frequency range, they can continuously lie further away from the point of matching (operating frequency) by spiraling about this matching point with varying radius. Therefore the presentation of curves in the Smith diagram should be set in preference to the previous presentations in the cartesian coordinate system. However a portion the impedance and conductance characteristic curves for a circuit containing a negative resistance, pass through the negative portion of the plane; the above inferred advantage (in the unity circle) of using the Smith Chart also has the large disvantage that the negative plane lies outside of the unity circle in the negative plane for the same transformation ($Y_{tr} = \frac{Y}{Y + Y_o}$ and extends to infinity.

This difficulty can be bypassed by transforming the test-function Y_b and the test point (origin). If one considers the fact that the conductance at the terminals of the negative resistance always has the form: $Y_b = Y - \frac{1}{R_n}$, then the following variation of the test vector is possible:

$$(Y_b - 0) = (Y - \frac{1}{R_n} - 0) = (Y - \frac{1}{R_n}) \quad \text{see Fig 1o}$$

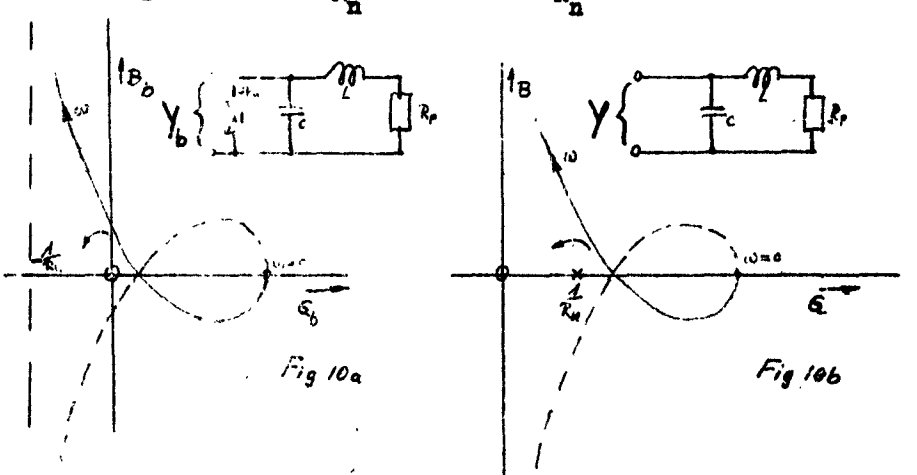

Fig.1o Transformation of the curve $Y_b(\omega)$ into the curve $Y(\omega)$ for the sake of a suitable stability test.

This means that a new conductance function Y exists, which replaces the previously used test function Y_b, or the vector which was drawn between the origin and the locus of $Y_b(\omega)$, is replaced by the new test vector, now considered to lie between the point $\frac{1}{R_n}$ to the locus of $Y(\omega)$. (fig.1o).

The new test function "Y" is that conductance, which remains at the respective terminals, when the negative resistance is removed . Therefore a pure passive conductance function remains and the corresponding characteristic curve can never exist in the negative half plane.

Therefore not only is the practical use of the Smith Chart assured, but additional practical advantages are obtained:

The self excitation of a circuit is now no longer of a disturbing nature when experimental investigations in the form of measurements are undertaken, since the circuit can only then become unstable when the negative resistance is connected. If the network contains other negative resistances, then the above criterium can be applied, (if even the first of the preset requirements is violated) if the measured characteristic curve of the test function verifies the condition, that the network is passive.

Characteristic curves of passive circuits correspond in one respect to the matching considerations of known geometric curvatures, (thus an actual measurement is superfluous in many cases) and correspond in the other respect to the firm limitations of their curvature concerning the rotation sense of a vector which is pictured as extending to such characteristic curves.

Now in consideration of the previously mentioned condition that a stable network is remarked by the fact, that the vector, which is considered as being drawn from the point $\frac{1}{R_n}$ to the points on the curve $Y(\omega)$, may not posses a clockwise rotation sense, and on the other hand, H.Wolter [4] has proven, that such a vector may not posses a counter clockwise rotation sense if the

network is passive, it can readily be concluded, that the point $\frac{1}{R_n}$ may not be encompassed by the test curve if the circuit is to be stable.

Now the impedance function can once again be introduced as the equivalent test function: if the point $\frac{1}{R_n}$ in the conductance plane is not encompassed by the characteristic curve "$y(\omega)$", then the point R_n is also not encompassed by the characteristic curve $Z(\omega)$ in the impedance plane, since in the case of reciprocal transformation the correlation of points and regions remains the same. Fig.11 shows the curves in the impedance and admittance planes for some examples of stable and unstable circuits.

Now the stability criterium can be stated in its final form:

> "If a negative resistance $-R_n$ is to be inserted into a passive network and stability is to be guaranteed, then the characteristic curve for the immittance at the foreseen terminals for tunnel diode insertion must not encompass the point $\frac{1}{R_n}$ in the conductance plane or the point R_n in the impedance plane."

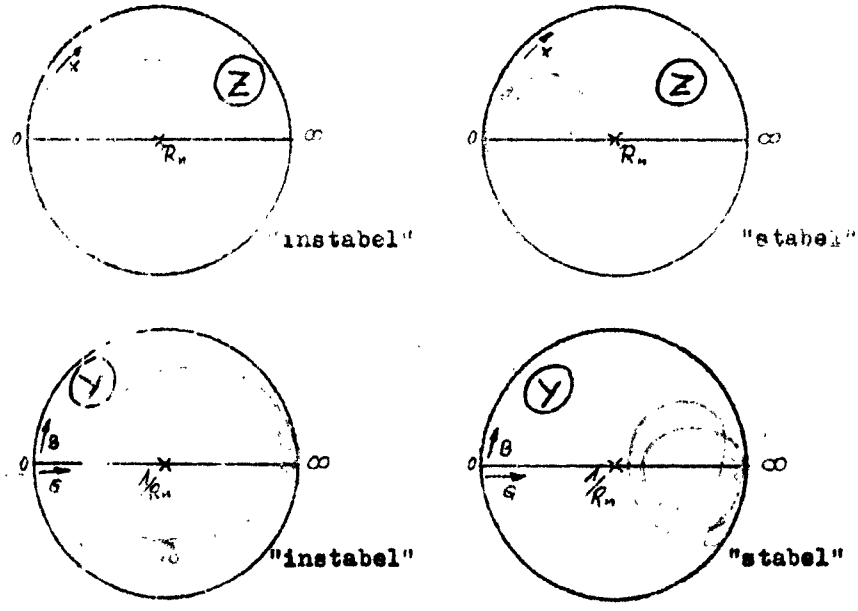

Fig.11 Stability test by impedance and admittanz curves. The right examples are stabel, the left ones are instabel.

6. Discussion of the Limitation Assumptions

It should be reminded that the reliability and clarity of the previously mentioned simple stability criterium of the measured or geometrically constructed characteristic curves was accomplished primarily by making the two following important limitations:

1. The circuit should contain only one negative resistance. (However several may be contained in the circuit, if these additional ones are always paralleled by a larger positive conductance. This condition hardly seems to be of technical interest.)

2. **The measured or geometrically constructed characteristic curves which are used for the stability consideration, must apply to those terminals of the network, between which the negative resistance is to be inserted.**

In accordance with the practical application desired, either as a two pole amplifier or as the case may be, for obtaining special impedance functions, these requirements may become difficult and some times impossible to fulfill. In the following these investigations will be conducted for the amplication behaviour of the negative resistance amplifier, since this is a completely discribebal application ge...

In respect to a low pole amplifier the first previously mentioned [illegible] for [illegible] variation since an arbitrary [illegible] is realized in one stage. Since the present state of [illegible] two pole stages differs for frequencies below the microwave range are at least equivalent in performance [illegible] as stability is concerned. In respect to the noise conditions a low noise pre-amplifier for microwaves [illegible] considered here. A corresponding two pole preamplifier [illegible] would be used to achieve a stable operating [illegible] of 10 dB. In addition it should be noted that the noise figure of the directly connected convential microwave amplifier (connected directly behind the T.D.preamp) becomes negligible as compared to the noise figure of the T.D..

The use of more than one T.D. is not necessary in this case.

If in addition the "Gain Bandwidth Product" is to be increased via series connection of several stages(having displaced tank circuit frequ..), then these stages must definitely be one-way buffered from each adjoining stage by using a non-reciprocal four pole (uniline, Gyrator). If this were not done, the end result would be a multiple parallel connection of tank circuits and T.D.s which behaves in the same manner as a single tank circuit. The non-reciprocal four poles breaks the circuit down into several component networks without reverse inpedance behaviour. Each component network, which thus only contains one T.D., fulfills the above mentioned requirements, and can therefore be clearly investigated.

The desire for inserting several T.D.s into a circuit is then always desirable, when available power of a single element (approx. 10 /uW for Ge-TDs) resulting from the minute voltage regulation region, is insufficient. (For an oscillator application this is obvious. It should be shortly mentioned here, that also for this application, which refers to an intentially unstable network, a stability is definitely worthwhile, since an undesirable sharp shift or change of frequency must be avoided.)

The direct parallel connection of several T.D.s, which fulfill the above limitations, however is without practical significance, since T.D.s having an arbitrary low resistance can be produced. However the possibility of obtaining stability becomes continuously more critical as the resistance of the TD is decreased. In this sense a series connection of low-resistance T.D.s appears to be suitable; It seems, that a negative resistance is then obtained, which has a factor n (n = number of T.D.s) larger voltage regulation range. However this arrangement of real negative resistances is not possible in principle with T.D.s, since a relatively complicated network exists already when tunnel diodes are connected in series due to the internal reactive components of the T.D. and a single negative

resistance can never be obtained in this manner. Such series circuits are basically unstable (even when the actual network consists of a simple component for example: largest possible ohmic conductance) if one expects that a suitable bias voltage distribution exists among the individual elements. In the case of individual bias voltage supplies, a series connection is basically possible and can be tested in principle by the above mentioned criterion.

In conclusion it can be noted that the T.D. practically does not fall under any limitations for a single active element when considered for the application as a low-noise small signal amplifier for microwaves (this is the most important field of application for the T.D.).

An objection to the second requirement (which pertains to checking the characteristic curve at the terminals of the negative resistance) can readily be made since these terminals are not accessible since they are located approximately 10 to 100 Å apart from one another within the semi-conductor crystal. Whereas the reactive components of the T.D. may be neglected for circuit considerations below 100 Mc, these internal reactive components such as the parasitic socket and lead reactance may not be neglected for the stability consideration. These parasitic elements as dipicted in Fig. 12 have been reduced to extremely small values via technology; however the measurement of the same can be accomplished with sufficient accuracy by using the methods [5] which was especially developed for this purpose.

Therefore the characteristic curve $Y_e(\omega)$, measured at the location of planned T.D. insertion, can be transformed to the suitable test curve $Y(\omega)$ by means of a four pole transformation, see Fig. 13.

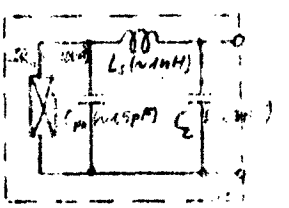

Fig.12
TD equivalent network.

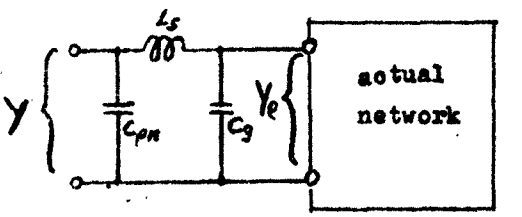

Fig.13
Transformation of the measured admittance of the actual network into the suitable test funktion Y.

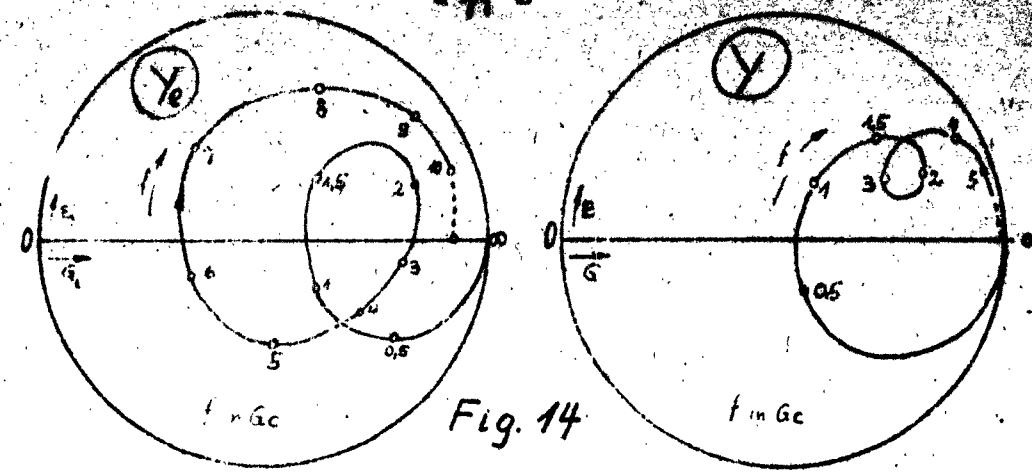

Fig. 14

Such a transformation has been accomplished in Fig. 14; the circuit is stable.

For practical applications this method has the following disadvantages: It has already been explained that the purpose of the stability test is not only that of determining whether the characteristic curve is suitable, but rather this test should also enable the determination of suitable arrangements which aid in obtaining a suitable change in the curve. The reactive components of the equivalent T.D. circuit of Fig. 12 and 13 cannot be completely freely chosen, since this can only be achieved by sorting out the T.D.s accordingly to the desired parameters. However the characteristic curve of very few circuits transformed by the equivalent reactive circuit of the T.D.

in such a way, as to yield a suitable change of the characteristic curve. The change must be accomplished in the passive network itself. However due to the four pole transformation circuit existing between the negative resistance and the passive network, it is not directly possible to determine the desirable Y_e-curve in respect to a stability consideration by observing the Y-curve.

Therefore there remains the desire to be able to make a stability consideration directly at the terminals of the actual circuit. By means of a suitable change of the test criterium this desire can be taken into account.

Until now the stability check rested upon determination and the evaluation of the relationship between the characteristic curve and the test point. If it is desired to transfer the checking relationship from the real test point $\frac{1}{R}$ or R_n to the frequency dependent input impedance $Z_n(\omega)$ of the T.D., then the new corresponding test method consists of: thoroughly investigating the relationship between the input impedance Z_e of the circuit and the characteristic impedance curve of the TD in order to determine, whether mutual curve shapes and intersection points exist.

In this respect a characteristic impedance curve (will called a boundary curve in the following) exists via imaging the impedance (or conductance) curve of the T.D. in Fig. 15. This boundary curve is the locus of all impedances which transform into the point R_n for the respective frequency parameter. The impedance curves $Z_e(\omega)$ of the circuit to be tested, may not intersect the boundary in this backward-diagram for the same frequency parameter, but may posses an arbitrary shape as a function of frequency below the boundary curve. Now in respect to the criterium expressed at the end of the preceding section, a circuit is not only then unstable when the test curve intersects the test point ,this would be the specific boundary case between stability and instability) but more generally expressed: the circuit is unstable when the test curve encompasses the test point. A necessary for an encompassment (encircling) is that the characteristic curve intersects the real axis. In the back-

ward-diagram the last requirement expressed is that the characteristic curve to be tested may not intersect any parameter curve (broken curves in Fig. 16) at a mutual frequency parameter. This is required since all points on each curve is transformed into the real axis at the respective frequency via the transformation four pole (see Fig. 13).

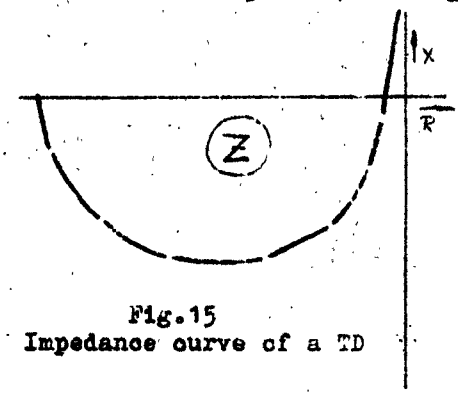

Fig.15
Impedance curve of a TD

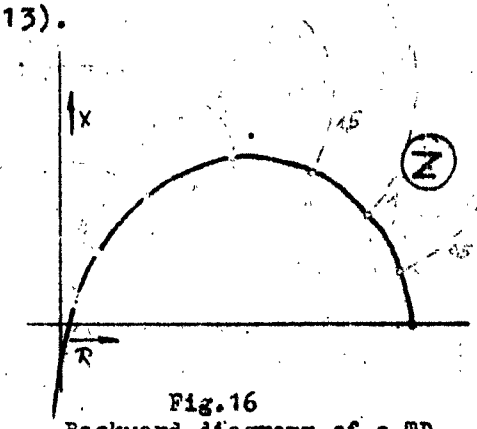

Fig.16
Backward-diagramm of a TD.

Thus the stability criterion in the backward diagram is the following:

The circuit is stable when:

1. the characteristic curve to be tested $Z_e(\omega)$ (or $Y_e(\omega)$) must remain completely below the boundary curve or
2. the characteristic curve to be tested may intersect or bound the boundary curve, but only under the condition, that no common point exists for the same frequency.

Fig. 17 a shows an example; at a mutual frequency of 1.8 Gc an intersecting point exists and the circuit is unstable. In Fig. 17b the characteristic curve has been changed in such a manner, that no frequency value common to the characteristic curve and family of parametric curves exists outside of the boundary curve.

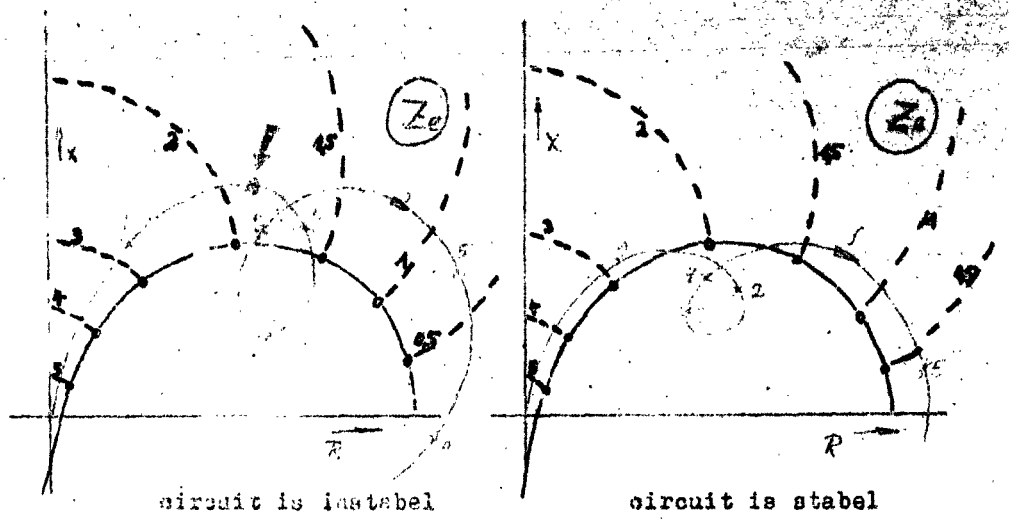

Fig.17
Stability check in the backward-diagramm.

H. Stabilization of Tunnel Diode Circuits.

Since an unstable circuit does not perform the originally design function (in this case the T.D. appears to have considerably higher negative resistance) the recognition of the stability considerations must be accepted as fundamental designing principles of a network with negative resistances.

From the fact, that the characteristic curves for the frequency $\omega = 0$ always begins at the real axis, and must also end on the real axis for the frequency $\omega = \infty$ and in addition, since the curves considered here can only follow a clockwise curvature, and finally from the knowledge of the reactance (barrier capacitance) directly adjacent to the negative resistance, an advantageous insight as to which circuits are stable in principal and which are principally unstable is achieved.

(In the following the use of the backward diagram will be avoided, since it is suitable for concrete investigations, but

is less suitable for discussing principal phenomena. The characteristic curves will once again be discussed in respect to the test point R_i).

First the so called "DC-current stability" will be observed, for example: this arises from the known requirement that the input impedance of the bias supply (Z for $\omega = 0$) must be smaller than the magnitude of the negnative resistance; Fig. 18 shows the characteristic curve. Two of its characteristics are completely sufficient for the stability consideration: it begins at $R_i > R_n$ for $\omega = 0$ and ends at the point $Z = 0$ due to the barrier capacity. These two end points of the, (in all cases) closed characteristic curves, lead without deviation towards an encircling of the poiht R_n, independent of any additional circuit characteristics, which means, independent of how many and how large the characteristic curve loops may be for the finite frequencies. The circuits is unstable for $R_i > R_n$.

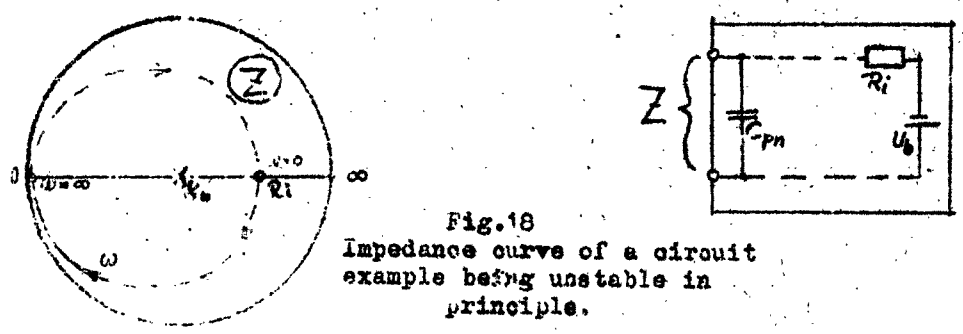

Fig.18
Impedance curve of a circuit example being unstable in principle.

As an additional example of a basically unstable circuit, the wide band matching principal via loop formation about the matching point of the impedance curve as used in high frequency circuits will be given: If a network (for instance an antenna) is to be matched to the real input impedance of the generator over a large frequency range, then the charachteristic curve of the input impedance must remain in the immediate vicinity of matching ($|Z| \sim R_i$) for each frequency in the desired band. In practice this is accomplished via matching and compensation

circuits and gives the characteristic curve of Fig. 19 a characteristic looping behaviour.

In the same manner the desired effect of the negative resistance in a passive network (deattenuation, amplification etc) is always expressed through the magnitude of the numerical relationship between the negative resistance and the magnitude of the respective parallel impedance insertion, thus through $|Z| - R_n$.

If this effect is to remain wide band in nature, then analogous to the above mentioned matching phenomena, the value $|Z|$ or the characteristic curve for $Z(\omega)$ must remain in the immediate vicinity of R_n throughout the largest possible frequency range.

(The expression "matching" is not exact as used here. In one respect the ideal situation does not at all exist when $Z = R_n$, and on the other, a negative resistance can never be matched to a positive resistance as far power transmission is concerned.)

The stability theory forbids the looping principal as depicted in Fig. 19, since the forced clockwise curving loops would encircle the test point. The characteristic curve in Fig. 20 does not contradict the stability requirement.

These pure qualitative observations already allow for recognizing the circumstance, that the desirable effect, realized by the negative resistance, can only be achieved in a narrow band region. It can also be concluded, that a complicated circuit, which tends to develop several loops, has little chance of giving a stable network when combined with a negative resistance.

Experience, resulting from practical investigations of T.D. circuits, has shown, that also those circuits which should be stable when analyzed according the stability checking procedures mentioned, actually were at first not stable when the corresponding circuit was built in practice. Characteristic curve measurement or determination of the frequency of oscillation have shown, that this instability existed considerably outside the operating frequency and did not seem to be related to the regular

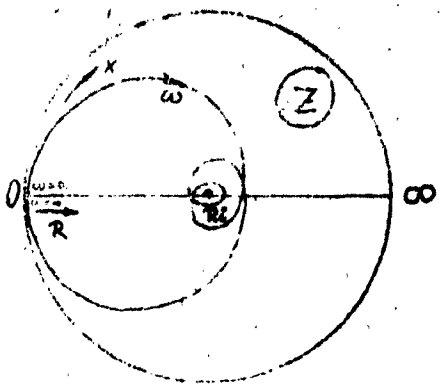

Fig.19
Impedance curve of a circuit example being unstable in principle.

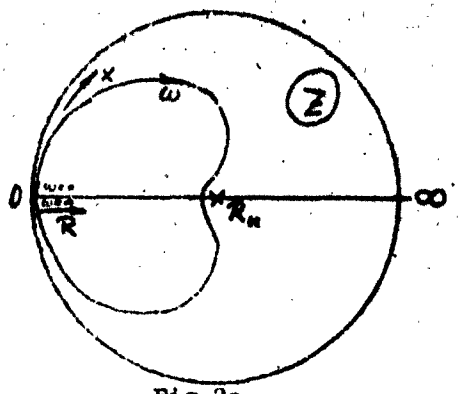

Fig.20
Impedance curve of the stable circuit.

behaviour of the inserted circuit components nor could it be removed by changing these components. This situation is also encountered in the simplest circuits; it is due to the reactance behaviour of the parasitic elements which are at first unknown for a particular circuit design and therefore could not be considered for the stability test.

If the universal application of the T.D. considers the unusual wide band behaviour of the negative resistance as a general advantage, then the disadvantage, that this wide band behaviour forces a stability check for those frequency regions in which the circuit is unknown and uninteresting, is quite evident. In practice it is hardly probable that a circuit, which has readily been adjusted for the operating frequency range by varying all incorporated components, suffices the requirements in respect to the impedance curve also for the unlimited region outside of this range.

However it is possible to influence the characteristic curve via a freely chosen supplementary circuit, in such a manner, that the stability of the network alone is valid within the operating frequency range, whereas outside the operating range the supplementary network (two pole stabilizer) specifies the stability behaviour.

The function of the supplementary network may also be included with the T.D. characteristics (this network must be inserted in the immediate vicinity of the T.D., for example at the T.D. socket) and the circuit contains a new negative resistance, which only exists within the operating frequency range; outside this range the neg.res. is compensated by a large real conductance.

Fig. 21 shows a simple example in this respect: a tank circuit of Fig. 21a is to be deattenuated by a partial coupled T.D.. In principal it is unavoidable, that the equivalent circuit of of this partial coupling (Fig. 21b) introduces a stray inductance "L_s", and thereby causes the characteristic curve pertaining to the terminals where the T.D. is to be inserted, contains an additional encirclement above the operating frequency range (3 mc) which cannot be influenced by a change of the tank circuit loading; the circuit is unstable (at approx. 150 mc).

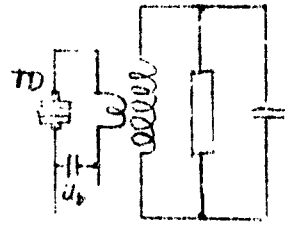

Fig.21a

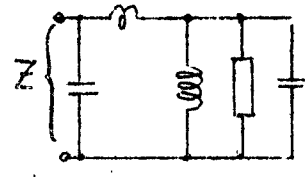

Fig.21b

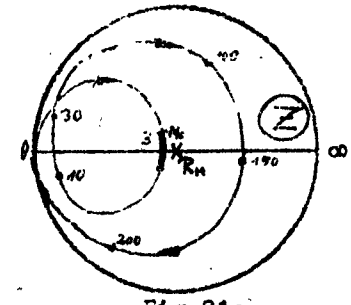

Fig.21c

Fig.21 : Stability problems at the deattenuation of a tank by a Td.

Now the task of the two-pole-stabilizer is to remove this additional encirclement without disturbing the characteristic curve within the operating frequency range. The simplest solution is obtained by using a RC-network (with the smallest possible inductance) which is connected directly parallel to the negativ resistance (Fig. 22a); the altered characteristic curve of Fig. 22b results and the circuit is now stable.

In other cases, in which the undesirable encirclement occurs at a considerably smaller frequency deviation from the operating freqnency range, an narrow band two-pole-stabilizer is used

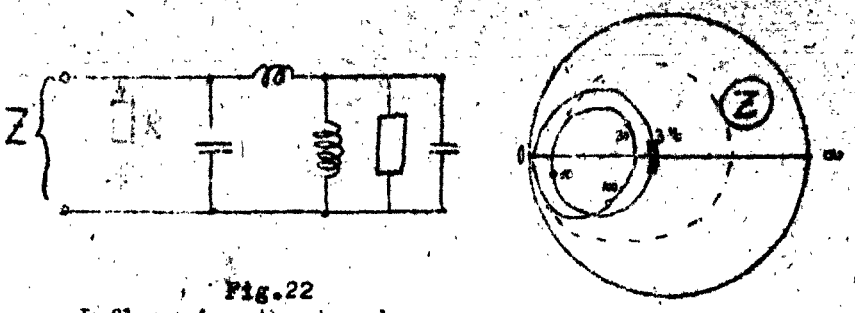

Fig.22
Influencing the impedance curve of an originally unstable circuit by a "two-pole-stabilizer".

Fig. 23b and c). The common feature of all these examples is the positive attenuating resistance. The practical design procedures are to be taken from the characteristic curve behaviour in the backward diagram.

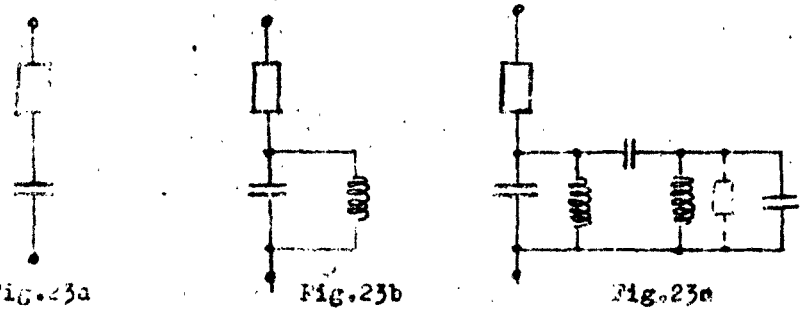

Fig.23a Fig.23b Fig.23c

For microwave applications the two-pole-stabilizer need not be inserted directly at the T.D., since the impedance behaviour along a transmission line is of a periodical occurance (for example resonator or antenna).

The primary advantage of this supplementary network is, that the stability check via characteristic curves need then only be carried for the operating frequency region where the impedance behaviour is exactly known.

II. Impedance Measurements

A. Basic Design of the Tunnel Diode Circuit

The antenna which we have investigated was chosen to have a very simple form in order insure that the preliniary investigation is as simple as possible thus yielding reliable results. According to Fig. 24 the antenna is a unipole in which one vertical conductor is connected to the conducting ground plane and the other vertical conductor is connected to the coaxial input. The Tunnel Diode is located at the highest geometrical point of the radiator: between the two conductors. The bias voltage is fed to the tunnel diode via the two perpendicular conductors.

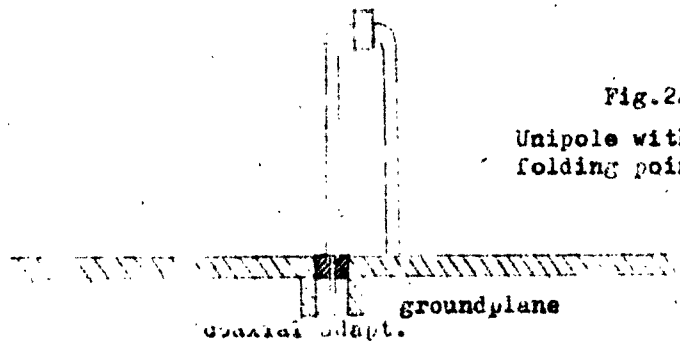

Fig.24
Unipole with TD in the folding point.

The most important requirement which is to be set on the system is that the tunnel diode is not in a state of self excitation. Due to the unavoidable reactive components of an antenna, the danger to self excitation is especially great if the dunnel diodes are combined with antennas. Two positive resistances can be connected in parallel to the T.D. (see Fig. 25) thus allowing for an adjustment of the resulting negative resistance. This arrangement is not only desirable for the measurement of the antenna feeding point impedance, but is also part of the stabilizing arrangement which is tried here. The advantage of this arrangement for adjusting the negative resistance is that the operating point remains within the linear region of the

characteristic T.D. curve. In addition an adjustable parallel capacitance was used since many cases of self oscillation could be avoided by suitable adjustment of the capacitance.

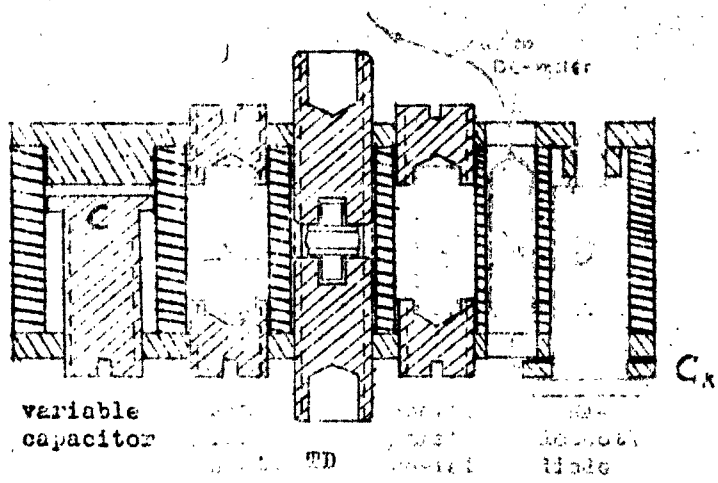

Fig.25
Tunnel diode mount in the folding point.

During the measurements the AC-voltage at the T.D. must be measured continuously for control. Therefore a diode (for detection of AC) is also connected in parallel to the T.D., which allows for measurement sensitivity of $3 \cdot (10)^{-3}$ volts. The indication obtained from this diode arrangement allows for checking the circuit stability; in case of instability, the resistance and capacitance of the stabilizing network can be varied until stability is obtained. The condition of self excitation can easily be observed in that corresponding voltage amplitude of C.1 volts or more is measured at the test diode. Thus already a slight tendency towards a self excitation can easily be observed. In addition this arrangement enables the supervision of the AC voltage which exists at the T.D. due to the impedance measurement (AC voltage is fed to the antenna for this measurement).

This voltage should not be much larger than 0.02 volts between the two terminals of the T.D., since the tunnel diode impedance changes for the case of larger voltages due to the nonlinearity of the "T.D." current.

Since the "T.D." is to be operated at high frequencies and since the T.D. mount should not radiate, the latter should be rather

small in size and should be of extremely low inductance. Fig. 25 shows the construction of the mount.

The T.D. is placed in the center threaded hole of the mount and fastened via two screws, one located in each end of hole. Two similar threaded hole fastening arrangements are located adjacent to T.D. mount for the purpose of connected R_1 and R_2 in parallel to the T.D.. These two resistances determine the attenuating or loading resistance "R" of the stabilizing. circuit. "C" is a variable capacitor. "D" is the detection diode which is used to measure the AC voltage.

One end of the diode is AC connected to the system via the capacitor "C_K". The resistance "R_m" serves as a feed-in for the DC current of the detection diode. "L" is the lead wire within the antenna conductor through which the DC current of the detection diode is acessible for measurement. The complete construction is schematically shown by Fig. 27.

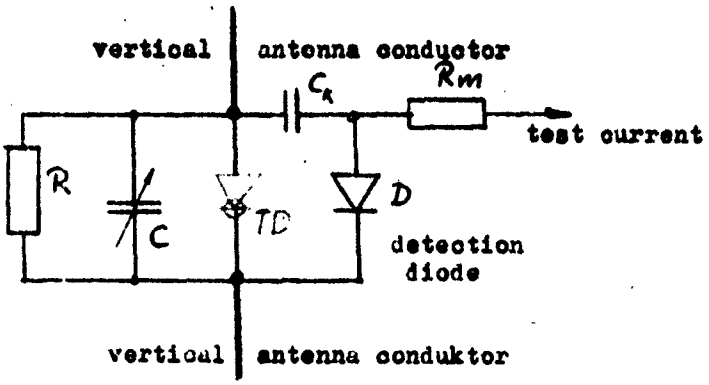

Fig.27
Circuit diagramm of the TD-mount in the folding point.

B. Measurement of Impedances containing negative resistances

The impedances were measured by using a slotted coaxial line. In accordance with Fig. 28 the line "L_s" is connected to the coaxial adapter. The slotted line is thus a part of the complete T.D. circuit and must be included in the stability consideration. Since for easy stabilization the number of resonant frequencies of the circuit must be kept as small as possible, it is appropiate to terminate the input of the slotted line with a resistance "$R = Z_0$" (characteristic impedance of the line) which is frequency independent. Then the entire line behaves as a frequency independent resistance "Z_0" at the base of the antenna and does not contain any resonances. However the stabilization of the circuit via "R" and "C" connection at the T.D. location in accordance with Section IIA must be undertaken when the slotted line is connected to the circuit.

The test signal obtained from the test generator "M" is coupled out of the line via a loosely coupled capacitive probe "P_s" which projects slightly into the slot of the line. The loose coupling insures that the stabilized impedance behaviour is not disturbed. One leg of the unipole is grounded. The other leg serves (in addition to its radiation behaviour) as the lead for the DC bias of the T.D. in that it extends as the inner conductor of the slotted line and is accessible behind the 60 ohm

termination (the outer conducter of the slotted line is AC grounded via a large capacitor "C_a" which is connected in series to the outer conductor at the dissection of the same in the vicinity of the line termination). The test voltages obtained at the slotted line are very small due to the small voltage regulation of the T.D.. The voltage curve along the slotted line is measured. Since the capacitive probe is very loosely coupled to the line the measured voltages are very small and a sensitive receiver is required.

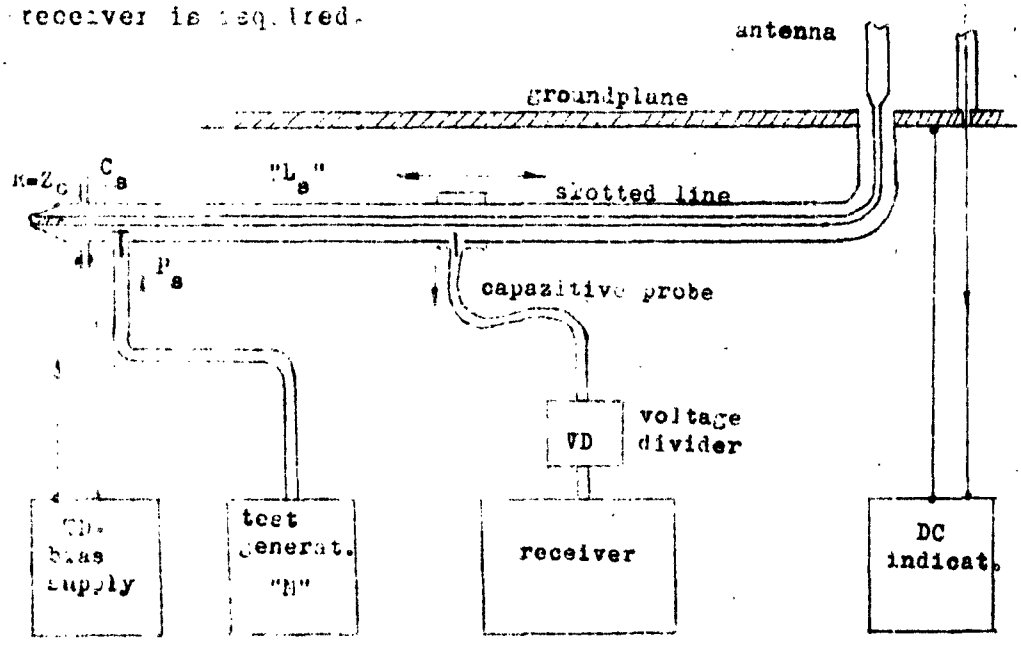

Fig.28 Test setup for impedance measurement.

Actually the measurement process consists in determining the maimum voltage "U_{max}" and the minimum voltage "U_{min}" along the line

$$VSWR = S = \frac{U_{max}}{U_{min}}$$

"S" as defined in this equation is determined by using a suitable calibrated voltage divider "VD". (In the measuring process the voltage at the receiver output is kept constant by adjusting

the VD; the attenuation of VD which has been adjusted to achieve this condition, is then recorded in each run.)

If the input impedance "Z = - R + jX" contains a negative real part "- R" then the circle diagram in the complex impedance plane must be extended in such a manner (as shown in Fig.29) that negative real parts can also be included. The diagram circles in the left side of the plane are the images of those in the right side of the plane. The VSWR values could lie on either the right hand (which contains positive resistive components), or the left hand side (which contains negative resitive components), since the measured VSWR does not give any indication as whether the real part of the impedance is negative or positive. The sign of the real part can be determined from the size of "U_{max}" of the circuit in Fig.28.

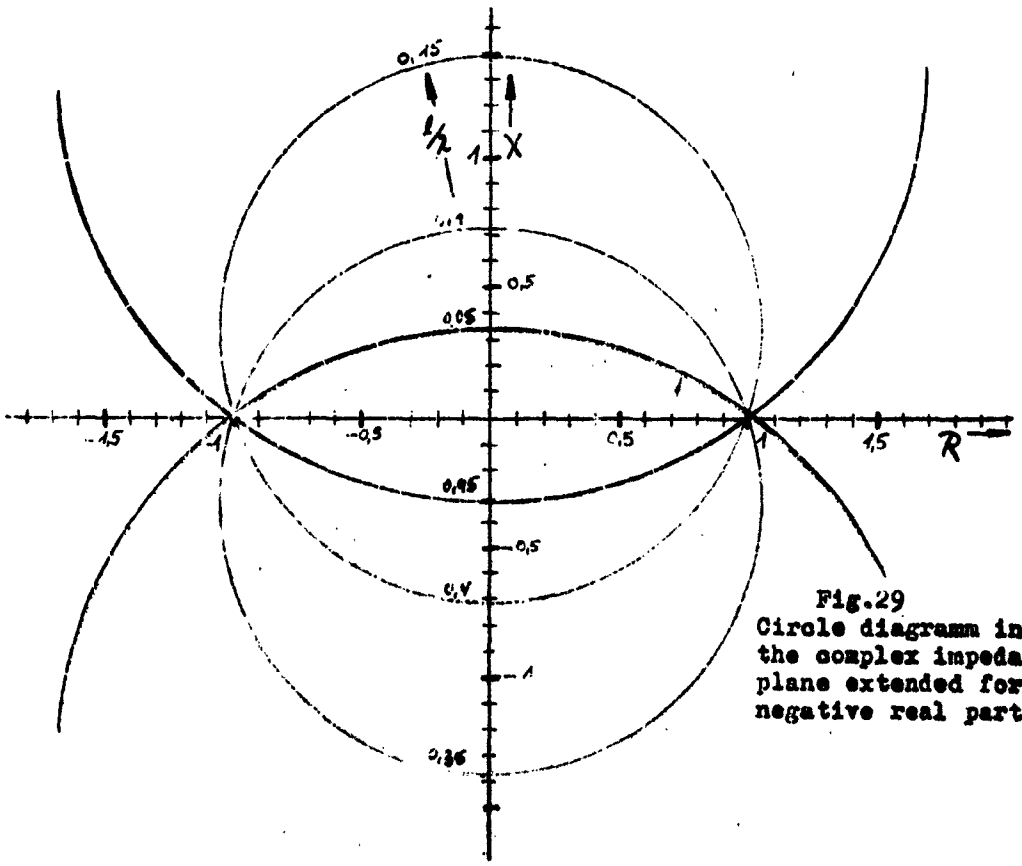

Fig.29
Circle diagramm in the complex impedance-plane extended for negative real parts.

the VD; the attenuation of VD which has been adjusted to achieve this condition, is then recorded in each run.)

If the input impedance "Z = - R + jX" contains a negative real part "- R" then the circle diagram in the complex impedance plane must be extended in such a manner (as shown in Fig.29) that negative real parts can also be included. The diagram circles in the left side of the plane are the images of those in the right side of the plane. The VSWR values could lie on either the right hand (which contains positive resistive components), or the left hand side (which contains negative resitive components), since the measured VSWR does not give any indication as whether the real part of the impedance is negative or positive. The sign of the real part can be determined from the size of "U_{max}" of the circuit in Fig.28.

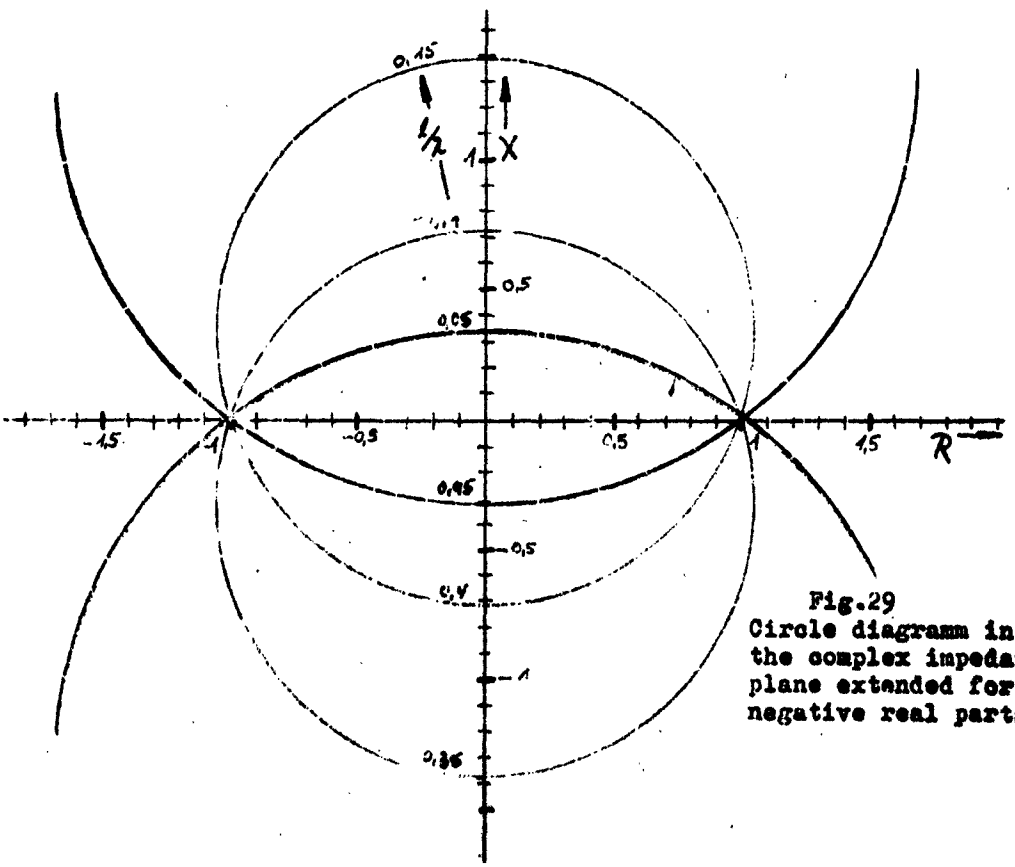

Fig.29
Circle diagramm in the complex impedance-plane extended for negative real parts.

Corresponding theory:

The generator in Fig. 28, which is loosely coupled to the line feeds the latter with a current "I" which is independent of the load (Fig. 30a). The termination "R = Z_0" at the left hand side of the line can be transformed to the location of the coupling point (see Fig. 30b) "I" and "Z_0" together form a current source. The location of a voltage maximum along the line is to be sought. Then the current source and the load "Z" which is to be measured is transformed to the location of a voltage maximum as shown in Fig. 30c (which does not change in the transformation).

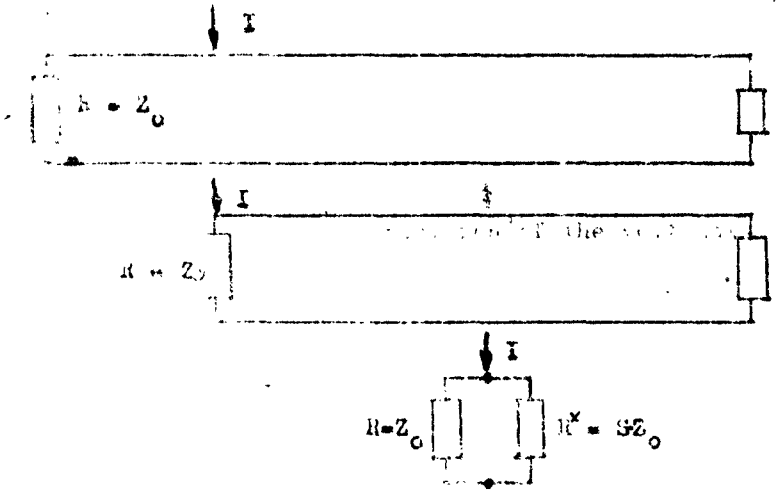

Fig.30 : Transmission line having a termination which includes a positive or a negative realpart.

As a result of this transformation, "Z" transforms to a real resistance R = S Z_L when the real part of "Z" is positive, and transforms into a negative real resistance R^x = -S·Z_L when the real part of "Z" is negative. The current "I" divides itself thus between the resistance "R" and the resistance "R^x". In this manner the maximum voltage, as described by the following equation, is obtained for Fig. 30c.

$$U_{max} = |I| \cdot Z_L \left(\frac{S}{S-1}\right) \qquad (11)$$

The sign in the denominator is the same as the sign of the real part of "Z".

At first the antenna is replaced by a matched resistance "$R = Z_o$" Then the following voltage is measured along the line since $S = 1$:

$$|U_o| = \frac{1}{2} |I| Z_o \qquad (12)$$

If the antenna is now inserted as a complex load "Z", then the following is valid if the real part of "Z" is positive:

$$U_o = U_{max} \leq 2 U_o \qquad (13)$$

If "Z" is a pure reactance then "$U_{max} = 2 U_o$". If "Z" contains a negative real part, then the following is valid:

$$U_{max} > 2 U_o \qquad (14)$$

and "U_{max}" can have an arbitrary large value. By measuring U_{max} and comparing it with U_o the sign of R^x can be found by help of (13) or (14).

C. Example of a Measurement on a Folded Dipole with T.D.

The following example has been chosen in order to explain the principles of the measurement technique and thus the example is rather simple. No particularly interesting application of a T.D. is therein described. An unsymmetrical antenna having coaxial feed-in allows for simpler measurement as compared to a symmetrical antenna. Therefore one half of a folded dipole (that portion above the conducting plane)was used.

The T.D. is located in the crest of the antenna and its associated impedance also influences the measured impedance at the feeding point. If the bias voltage of the T.D. is changed, different positive and negative values of the T.D. resistance can be obtained. Fig. 32 shows the measured antenna input impedance for various diode resistance values.

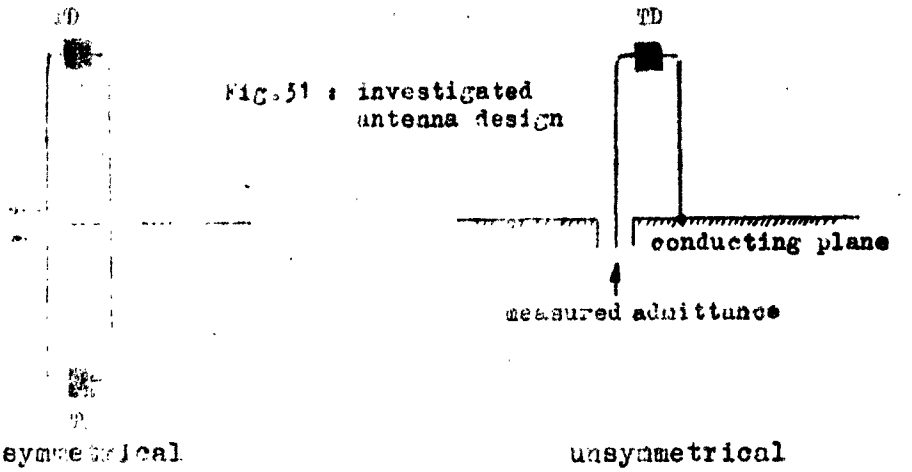

Fig.31 : investigated antenna design

Therefore cases exist in which the input admittance of the antenna contains a negative real part; in this case the antenna may operate as an amplifier. Since the curve of the input admittance contains loops in the admittance plane, a certain wide band behaviour can be obtained if the antenna is matched.

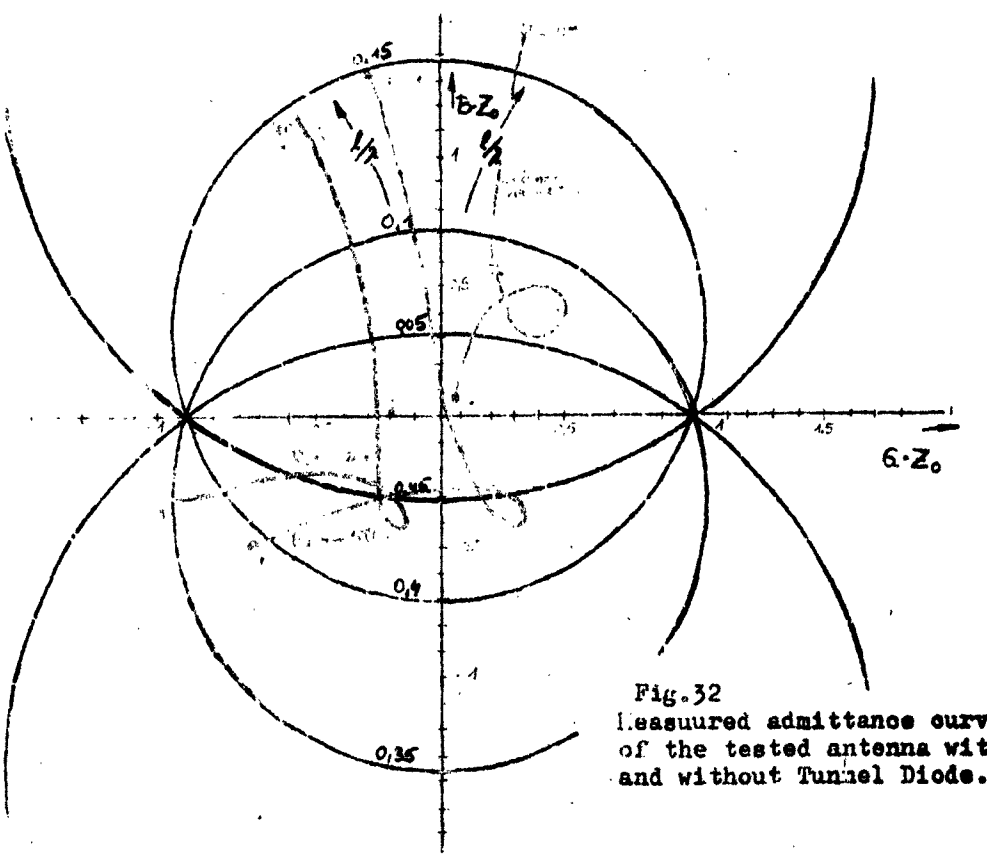

Fig.32
Measuured admittance curves of the tested antenna with and without Tunnel Diode.

Bibliography

[1] F. Strecker — " Die elektrische Selbsterregung." Hirzel Verlag Stuttgart 1947

[2] E. Görk — " Stabilitätskriterien." A.E.Ü. 4 (1950) page 89-96

[3] D. Böhne — " Impedanzmessungen an Tunneldioden im Mikrowellengebiet." Internal report of the Institut für Hochfrequenztechnik der Techn.Hochsch.München

[4] J. Steinkamp — " Impedanz einer Antenne mit Tunneldiode." Diplomarbeit at the Institut für Hochfrequenztechnik der Technischen Hochschule München.

Glossary of Symbols

p_o	Eigen value of a network.
p	Complex frequency
σ	Real part of the complex frequency
φ	Rotating angle of a vector, drawn from the origin to a curve.
Y_b	Admittance at an branch of a network. (Especially of that one, which contains the negative resistor.)
Y	Admittance at those terminals, at which the real negative resistor is to be inserted.
Y_t	Admittance at those terminals, at which the tunnel diode is to be inserted.
	Voltage standing wave ratio.
	Charakteristic impedance of a line.

Glossary of Symbols

p_o	Eigen value of a network.
p	Complex frequency
σ	Real part of the complex frequency
φ	Rotating angle of a vector, drawn from the origin to a curve.
y_b	Admittance at an branch of a network. (Especially of that one, which contains the negative resistor.)
y_-	Admittance at those terminals, at which the real negative resistor is to be inserted.
y_T	Admittance at those terminals, at which the tunnel diode is to be inserted.
	Voltage standing wave ratio.
	Characteristic impedance of a line.

List of Illustrations

Technische Hochschule
München, Institut für
Hochfrequenztechnik
30. April 1963

AF 61 (052) - 506
FR
Electronics

RESEARCH ON ELECTRICALLY SMALL ANTENNAS

Prof. Dr. H.H. Meinke

Abstract:

Part I: Antenna with Ferrite
A performance improvement of the electrically small antenna can only be obtained by achieving a bandwidth enlargement of the antenna impedance. By surrounding the antenna with ferrite of the same maximum height as

Technische Hochschule
München, Institut für
Hochfrequenztechnik
30. April 1963

AF 61 (052) - 506
FR
Electronics

RESEARCH ON ELECTRICALLY SMALL ANTENNAS
Prof. Dr. H.H. Meinke

Abstract:

Part I: Antenna with Ferrite
A performance improvement of the electrically small antenna can only be obtained by achieving a bandwidth enlargement of the antenna impedance. By surrounding the antenna with ferrite of the same maximum height as

Technische Hochschule
München, Institut für
Hochfrequenztechnik
30. April 1963

Af 61 (052) - 506
FR
Electronics

RESEARCH ON ELECTRICALLY SMALL ANTENNAS
Prof. Dr. H.H. Meinke

Abstract:

Part I: Antenna with Ferrite
A performance improvement of the electrically small antenna can only be obtained by achieving a bandwidth enlargement of the antenna impedance. By surrounding the antenna with ferrite of the same maximum height as

Technische Hochschule
München, Institut für
Hochfrequenztechnik
30. April 1963

AF 61 (052) - 506
FR
Electronics

RESEARCH ON ELECTRICALLY SMALL ANTENNAS
Prof. Dr. H.H. Meinke

Abstract:

Part I: Antenna with Ferrite
A performance improvement of the electrically small antenna can only be obtained by achieving a bandwidth enlargement of the antenna impedance. By surrounding the antenna with ferrite of the same maximum height as

the antenna a bandwidth enlargement is only possible if the geometrical height of the antenna becomes larger than about 1/20 of the wavelength in air. The outer regions of the ferrite form cause this bandwidth broadening effect.

Part II: Antenna with Tunneldiode
Stability problems and measurement of input impedance with negative resistances are discussed. A folded unipole with a tunneldiode at its top is studied experimentally.

the antenna a bandwidth enlargement is only possible if the geometrical height of the antenna becomes larger than about 1/20 of the wavelength in air. The outer regions of the ferrite form cause this bandwidth broadening effect.

Part II: Antenna with Tunneldiode
Stability problems and measurement of input impedance with negative resistances are discussed. A folded unipole with a tunneldiode at its top is studied experimentally.

the antenna a bandwidth enlargement is only possible if the geometrical height of the antenna becomes larger than about 1/20 of the wavelength in air. The outer regions of the ferrite form cause this bandwidth broadening effect.

Part II: Antenna with Tunneldiode
Stability problems and measurement of input impedance with negative resistances are discussed. A folded unipole with a tunneldiode at its top is studied experimentally.

the antenna a bandwidth enlargement is only possible if the geometrical height of the antenna becomes larger than about 1/20 of the wavelength in air. The outer regions of the ferrite form cause this bandwidth broadening effect.

Part II: Antenna with Tunneldiode
Stability problems and measurement of input impedance with negative resistances are discussed. A folded unipole with a tunneldiode at its top is studied experimentally.